A Study of the Ising Model on The Hexagonal Closed-Packed Lattice With Competing Interactions

by

Dan Simon Zimmerman

B.Sc., The Hebrew University of Jerusalem, 1980
M.Sc.,The University of British Columbia, 1982

A Thesis Submitted in Partial Fulfillment of

the Requirements for the Degree of

DOCTOR OF PHILOSOPHY

in

The Faculty of Graduate Studies

Department of Physics

We accept this thesis as conforming

to the required standard

The University of British Columbia

September 1986

In presenting this thesis in partial fulfilment of the requirements for an advanced degree at the University of British Columbia, I agree that the Library shall make it freely available for reference and study. I further agree that permission for extensive copying of this thesis for scholarly purposes may be granted by the head of my department or by his or her representatives. It is understood that copying or publication of this thesis for financial gain shall not be allowed without my written permission.

Department of Physics

The University of British Columbia
1956 Main Mall
Vancouver, Canada
V6T 1Y3

Date 18 Sep 1986

ABSTRACT

A study is made of an Ising model on the hexagonal closed-packed lattice, with ferromagnetic interactions D between nearest-neighbor spins located in adjacent layers, and antiferromagnetic interactions J between nearest-neighbor spins located in the same layer.

The ground states of the model are studied for different values of the parameter $\kappa = -J/D$. For $\kappa < 1/2$ the ground states are ferromagnetic and for $\kappa > 1/2$ the ground state spin configurations consist of stacked identical layers, such that each layer is obtained by stacking rows of alternating spins. At the point $(\kappa = 1/2, t = 0)$, where $t = T/D$, there exists a multitude of degenerate ground state spin configurations which are not stable for $\kappa \neq 1/2$.

Mean-field theory and low temperature expansions are used to study the phase diagram at low temperatures. Mean-field theory predicts that $(\kappa = 1/2, t = 0)$ is a multiphase point where an infinite sequence of modulated phases coincide. In the vicinity of the multiphase point, the mean-field phase diagram is found to be similar to the mean-field phase diagram of the three-dimensional ANNNI model near its multiphase point.

Low temperature expansions are performed to second order in x, where $x = e^{-2/t}$, around the phase boundary between the ferromagnetic and the modulated phases. In contrast to standard low temperature expansions, the complete contribution, to order x^2, is obtained by grouping the contributions from excitations which contribute to arbitrarily high orders in x. The phase boundary between the ferromagnetic and the modulated phases is found to coincide, to order x^2, with the line onto which Domany mapped a kinetic Ising model on the honeycomb lattice. This strongly suggests that the Domany line is a phase boundary in three-dimensions.

Mean-field theory shows that this Ising model contains a continuous minimum-energy surface. A renormalization group method which applies to models which

contain continuous minimum-energy surfaces is used to analyze the phase transition between the paramagnetic and the modulated phases. The calculation is performed using a Landau-Ginzburg-Wilson Hamiltonian whose minimum-energy surface consists of a hexagon and which contains fourth-order invariants due to the lattice. The calculation shows that the Hamiltonian does not contain a stable fixed point. This suggests that the paramagnetic-modulated phase transition of this Ising model is a fluctuation-induced first-order transition.

TABLE OF CONTENTS

LIST OF TABLES

LIST OF FIGURES

ACKNOWLEDGEMENT

I would like to thank my thesis advisor A. J. Berlinsky for the help, advice, and knowledge I obtained from him during my years as a graduate student.

I thank C. Kallin for collaborating in performing the low temperature expansions. I am pleased to acknowledge many helpful discussions with S. Howes. I also benefited from discussions with E. Domany, D. Mukamel, M. den Nijs, P. Palffy-Muhoray, M. Plischke, M. Shegelski and B. Sullivan.

Thanks are due to M. Choptuik for advice concerning computers and to J. Barnard for writing the macros used to 'TEX' this thesis.

I thank J. Gubernatis for sending me a copy of Ref. 9 prior to publication.

I am pleased to thank the University of British Columbia and the Natural Sciences and Engineering Research Council of Canada for financial support.

CHAPTER 1

INTRODUCTION

Obtaining exact solutions to three-dimensional models remains a challenging problem in statistical physics. In general, one-dimensional problems with short range interactions are soluble, some two-dimensional problems have been solved with great difficulty and three-dimensional problems have not been solved at all [1]. For example, calculating the thermodynamic properties of an Ising model with nearest-neighbor interactions is a trivial exercise in one dimension [2], a mathematical *tour de force* in two dimensions [3,4], and a major unsolved problem in three dimensions.

Some exact results about some three-dimensional models have been obtained by mapping soluble two-dimensional kinetic models onto surfaces in the phase diagrams of static three-dimensional models [5-8]. One method which has been used to perform such mappings involves associating the spin configurations of a two-dimensional Ising model with a discrete-time dynamics, with the spin configurations of layers in the lattice of a three-dimensional static model [6-8]. The mapping is such that spin configurations which correspond to successive time steps of the discrete-time dynamics are associated with neighboring layers in the lattice of the three-dimensional model. Having performed the mapping, exact information about the three-dimensional model is obtained using the exactly known properties of the two-dimensional model and from some partial knowledge of the properties of the three-dimensional model.

For most mappings the three-dimensional models contain many coupling constants and therefore are too complicated or not interesting enough to analyze. In contrast, recently, Domany obtained mappings of kinetic models on the honeycomb lattice onto the phase diagrams of static three-dimensional models on the hexagonal closed-packed (hcp) lattice [8]. The simplest example is the mapping of a two-dimensional kinetic Ising model, with nearest-neighbor interactions L, onto a line (referred to hereafter as the Domany line) in the phase diagram of a static model (referred to hereafter as the JD model) whose Hamiltonian is given by

$$H = -J \sum_{\{ij\}} S_i S_j - D \sum_{<ij>} S_i S_j \tag{1.01}$$

where $S_i = \pm 1$ are spins defined on the sites of the hcp lattice, shown in Fig. 1-1, $< ij >$ labels nearest-neighbor bonds between sites on adjacent layers (shown as dashed lines in Fig. 1-1) and $\{ij\}$ labels nearest-neighbor bonds between sites in the same layer (shown as solid lines in Fig. 1-1). The Domany line is given by the expressions

$$D = L \qquad \text{and} \qquad \exp(4J) = \frac{\cosh D}{\cosh 3D} \tag{1.02}$$

and therefore, for $L > 0$, which corresponds to ferromagnetic interactions, Eq. (1.02) implies that $D > 0$ and $J < 0$. Therefore, in this thesis, the JD model is only studied for the case of ferromagnetic interlayer interactions and antiferromagnetic intralayer interactions.

The mapping of the two-dimensional dynamic model onto a line in the phase diagram of the three-dimensional static model implies that along the Domany line the correlations of the JD model are related to the correlations of the two-dimensional Ising model on the honeycomb lattice [8]. On the Domany line the in-plane correlations of the static JD model are equal to the static correlations of the dynamic Ising model on the honeycomb lattice and the out-of-plane correlations

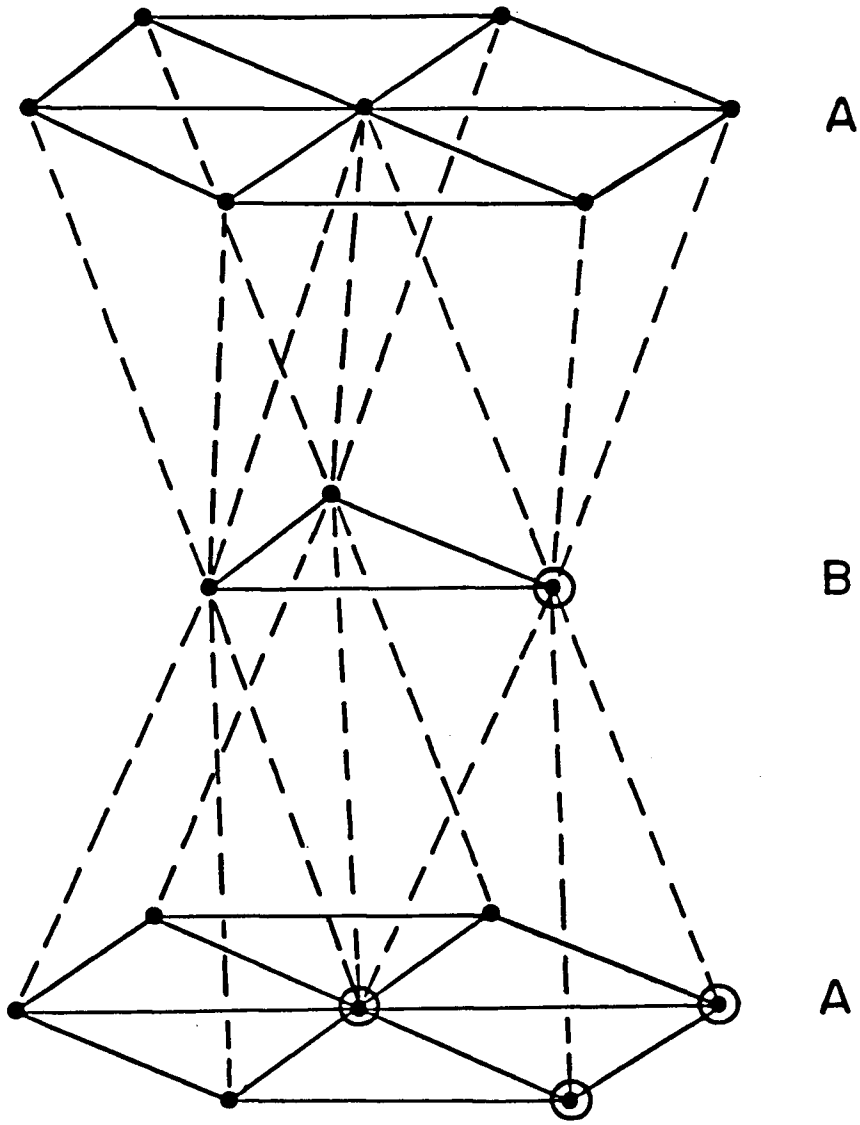

Figure 1-1 The hexagonal closed-packed lattice on which the JD model is defined. Spins located at sites which are connected by solid lines interact through antiferromagnetic interactions J, and spins connected by dashed lines interact through ferromagnetic interactios D. The two hexagonal sublattices which form the hcp lattice are labelled by A and B. The four circled sites constitute an example of the four-spin clusters described in Chapter 3.

of the static model are equal to the dynamic correlations of the dynamic model. At the critical point L_c, of the two-dimensional Ising model on the honeycomb lattice, the static and dynamic correlations diverge with different critical exponents. Therefore the point (J_c, D_c), on the Domany line, onto which L_c maps, exhibits anisotropic scaling, i.e., correlations in different directions diverge with different critical exponents.

A mean-field calculation reveals that, in addition to the paramagnetic and ferromagnetic phases, the JD model also exhibits a modulated phase and a Lifshitz point where the paramagnetic, the ferromagnetic and the modulated phases coincide [8]. Lifshitz points exhibit anisotropic scaling and therefore Domany conjectured that the point (J_c, D_c), which exhibits anisotropic scaling, is the exact location of a Lifshitz point in the phase diagram of the JD model [5,8].

A Monte Carlo simulation of the JD model, performed by Domany and Gubernatis, revealed that the Domany line and the phase boundary of the ferromagnetic phase are very close in parameter space [9]. Therefore these authors suggested that both lines might coincide. If this were the case, the Domany line would constitute the first example of an exact solution of a three-dimensional model along a whole phase boundary.

In recent years, models with competing interactions which also exhibit modulated phases have been studied extensively [10]. The best studied model is the three-dimensional Axial Next-Nearest-Neighbor Ising (ANNNI) model [11,12]. High temperature expansions [13], low temperature expansions [14], various studies based on mean-field theory [15-20], and Monte Carlo simulations [21,22] have been used to obtain information about the phase diagram of this model. These studies revealed that the three-dimensional ANNNI model exhibits a very complex phase diagram which contains a paramagnetic phase, a ferromagnetic phase, commensurate modulated phases, incommensurate modulated phases, a Lifshitz point, a multiphase point and other exotic features.

In this work methods which have been found useful in studying models with competing interactions are used to investigate the phase diagram of the JD model. A better understanding of the different features of this phase diagram is developed for the purpose of understanding the role played, in the phase diagram, by the Domany line and the special point (J_c, D_c). In particular, the low temperature region of the phase diagram is studied using mean-field theory and low temperature expansions. An asymptotic low temperature expression for the phase boundary of the ferromagnetic phase is calculated. The conjecture that the Domany line coincide with the phase boundary of the ferromagnetic phase is tested by comparing the asymptotic low temperature expression for the Domany line with the asymptotic low temperature expression for the phase boundary of the ferromagnetic phase.

In another part of this thesis, the phase transition between the paramagnetic phase and the modulated phase is studied. A linearized mean-field calculation predicts that JD model exhibits a continuous transition from the paramagnetic phase into the modulated phase. Along the order-disorder line, the modulated phase is characterized by a wave-vector which can be chosen from one or more lines in reciprocal space. Thus the model belongs to a class of models which contain an ordered phase characterized by a wave-vector which can be anywhere on a continuous surface in reciprocal space [23-28,29]. This surface is called the minimum-energy surface.

The mean-field approximation predicts that models which contain continuous minimum-energy surfaces exhibit a continuous phase transition into the modulated phase. In contrast, studies which are based on perturbation expansions and renormalization group calculations suggest that these models exhibit a first-order transition [23,27,28]. Therefore models which contain continuous minimum-energy surfaces constitute examples of models which exhibit a fluctuation-induced first-order transition, i.e., a first-order transition which is predicted to be continuous by mean-field theory [30,31].

The renormalization group calculations for models with continuous minimum-energy surfaces have been performed for cases where the minimum-energy surfaces are two symmetric polygons [27] or one square [28]. From these results it seems plausible that all models which contain a minimum-energy surface exhibit a fluctuation-induced first-order transition into the modulated phases [27]. However, due to the periodicity of the lattice, fourth-order invariants, which were not included in previous calculations for models with continuous minimum-energy surfaces, should be included in a renormalization group analysis of a Landau-Ginzburg-Wilson Hamiltonian which describes the paramagnetic-modulated phase transition of the JD model. For $-J/D = 1$ the minimum-energy surface of the JD model forms a hexagon. It follows that this phase transition can be studied using the method used by Mukamel and Hornreich to study the model where the minimum-energy surfaces consist of two polygons [27]. Therefore, in this thesis, the phase transition between the paramagnetic and the modulated phases of the JD model is studied by performing a renormalization group calculation for a model which contains a hexagonal minimum-energy surface and which includes fourth-order invariants which are due to periodicity of the lattice.

1.1 Organization of the Thesis

Chapter 2 of this thesis contains a theoretical review of topics which are relevant to this work. Basic aspects of the theory of phase transitions and critical phenomena are described. The concepts of Lifshitz points, tricritical points and Lifshitz tricritical points are introduced. Previous work on the JD model and related studies are reviewed. Finally, studies of the three-dimensional ANNNI model are also reviewed.

The results of this thesis are presented in Chapters 3 to 6. In Chapter 3 the ground states of the model are investigated. A multidegenerate point which

separates two types of ground states is found. A description is given of ground state spin configurations which are stable at the multidegenerate point.

In Chapter 4 the mean-field approximation is introduced and is used to investigate the order-disorder line. Expressions are obtained for the phase boundary between the paramagnetic and the ferromagnetic phases and for the phase boundary between the paramagnetic and the modulated phases. The low temperature region of the phase diagram is studied by solving the mean-field equations on a finite lattice. A sequence of stable phases, similar to the phases of the three-dimensional ANNNI model are found to be stable in the vicinity of the multidegenerate point. This implies that the multidegenerate point is a multiphase point.

In Chapter 5 the phase diagram of the JD model near the multiphase point is studied using low temperature expansions. The asymptotic low temperature expressions for the phase boundary of the ferromagnetic phase is calculated and is compared to the low temperature expression for the Domany line.

Chapter 6 describes the investigations of the phase transition from the paramagnetic into the modulated phases. Studies of models which exhibit continuous minimum-energy surfaces are reviewed. The JD model is shown to contain a minimum-energy surface. The Landau-Wilson-Ginzburg Hamiltonian which describes the paramagnetic-modulated transition in the JD model is described and is analyzed using a renormalization group calculation.

In Chapter 7 the results obtained in this thesis using different methods are reviewed and compared. Also these results are compared to results from other studies of the JD model.

CHAPTER 2

THEORETICAL REVIEW

In this Chapter basic concepts in the theory of phase transitions and critical phenomena are described and existing studies of the JD model and the three-dimensional ANNNI model are reviewed. In Sec. 2.1 the concepts of order parameter, critical exponents, universality of phase transitions, scaling laws, mean-field theory, Landau theory, renormalization group theory, Landau-Ginzburg-Wilson Hamiltonians and multicritical points are explained. In Sec. 2.2 Lifshitz tricritical points, which are a special kind of multicritcal point which might exist in the phase diagram of the JD model, are introduced. Section 2.3 is devoted to a review of previous work on the JD model. In Sec. 2.4 studies of the three-dimensional ANNNI model are reviewed.

2.1 Aspects of Critical Phenomena

Most discussions of critical phenomena start with a review of some physical system which exhibits a critical point [32]. However this thesis is devoted to the study of a certain type of Ising model, and therefore I chose to introduce important concepts in critical phenomena through a discussion of Ising models. The variables S_i in an Ising model are restricted to the values $+1$ or -1 and are defined on the sites $\mathbf{R}_i$ of some lattice. The energy of a given spin configuration, $\{S_i\}$, is given by

$$H_N = -\frac{1}{2}\sum_{i\neq j} J_{ij}S_iS_j - h\sum_i S_i \qquad (2.01)$$

where J_{ij} represent the coupling between the spins located on the sites i and j, h represents an external (magnetic) field and N is the number of sites in the lattice.

For appropriate values of J_{ij} and the dimensionality of the lattice, Ising models exhibit phase transitions between different phases. In order to distinguish between the different phases, one has to define suitable order parameters which depend on the phases involved in the transition. In this thesis, models which exhibit paramagnetic, ferromagnetic and modulated phases are discussed. For such models suitable order parameters, $m_{\mathbf{q}}$, are given by

$$m_{\mathbf{q}} = \left\langle \frac{1}{N} \sum_j S_j e^{i\mathbf{q}\cdot\mathbf{R}_j} \right\rangle \tag{2.02}$$

where the ensemble average of any operator A is given by

$$\langle A \rangle = \lim_{h_A \to 0} \lim_{N \to \infty} \frac{1}{Z_N} \sum_{\{S_i\}} A e^{-\beta H_N + h_A A} \tag{2.03}$$

h_A is a field which couples to A, $\sum_{\{S_i\}}$ is a sum over all possible spin configuration and the partition function Z_N is given by

$$Z_N = \sum_{\{S_i\}} e^{-\beta H_N} \tag{2.04}$$

Thus the order parameters $m_{\mathbf{q}}$ are given by the Fourier components of the site magnetizations $m_i = < S_i >$. The disordered phase, called the paramagnetic phase, is the phase where $m_{\mathbf{q}} = 0$ for all values of $\mathbf{q}$. The ferromagnetic phase is the phase where $m_0 \neq 0$ while $m_{\mathbf{q}} = 0$ for all $\mathbf{q} \neq 0$. The modulated phases correspond to the cases where $m_{\mathbf{q}} \neq 0$ for some values of $\mathbf{q}$.

Phase transitions are classified according to the manner in which the order parameter changes at the transition point. A first-order transition is one in which the order parameter changes discontinuously from its value in the disordered phase

to a different value in the ordered phase. In contrast, a continuous transition is one in which the order parameter starts changing continuously at the phase transition point. A point in the phase diagram at which a continuous transition occurs is called a critical point.

At critical points thermodynamic quantities either vanish or diverge as power laws. For example, for a transition between the ferromagnetic and the paramagnetic phases the order parameter m vanishes as $m \sim |t|^{\beta}$ as $t = (T_c - T)/T_c$ goes to zero. Also the divergences of the magnetic susceptibility and the specific heat, as the critical point is approached, are characterized by the critical exponents γ and α respectively. Another pair of important exponents, η and ν, characterize the behaviour of the two point correlation function $G(R) = \langle S_0 S_{\mathbf{R}} \rangle$. Close enough to a critical point $G(R)$ is expected to have the asymptotic form

$$G(R) - G(\infty) \sim \frac{\exp(-R/\xi)}{R^{d-2+\eta}} \tag{2.05}$$

where $\xi(t)$ is the correlation length. Near the critical point the correlation length diverges as $\xi \sim t^{-\nu}$ and thus at the critical point, $t = 0$, $G(R)$ falls as a power law which depends on the dimensionality of the system d and the critical exponent η.

A surprising aspect of phase transitions is that the critical exponents are 'universal', i.e., critical points in different physical systems and models exhibit the same critical exponents. For example, the critical exponents which characterize the critical point in a uniaxial magnetic system or in a binary mixture of fluids are equal to the critical exponents for the paramagnetic-ferromagnetic transition of an Ising model. Thus phase transitions can be classified into universality classes according to the values of critical exponents and other universal quantities.

Experimental results for real systems and calculations for models have revealed that the critical exponents are not independent quantities but are related through scaling laws. Some of these scaling laws can be derived from the so called

scaling hypothesis which states that the singular part of the free energy, i.e., the part which gives rise to the dominant power law singularities is a homogeneous function of the so called scaling variables. For example, the singular part of the free energy, f_s, for an Ising ferromagnet has the form

$$-\beta f_s(t,h) = t^{2-\alpha} Y\left(h/t^{\Delta}\right) \tag{2.06}$$

where the scaling function $Y(y)$ is a universal function of one variable and Δ, the gap exponent, is related to the exponents β and γ through the scaling law $\Delta = \beta + \gamma$. Using Eq. (2.06) to calculate the magnetization at $h = 0$, the scaling law

$$\alpha + 2\beta + \gamma = 2 \tag{2.07}$$

is obtained. The number of independent critical exponents needed to describe the rest of the exponents depends on the specific type of critical point. For example, for the paramagnetic-ferromagnetic critical point, the critical exponents $\alpha, \beta, \gamma, \eta, \nu$ can be calculated from the values of two of the exponents, the scaling law given by Eq. (2.07), and two additional scaling laws

$$d\nu = 2 - \alpha \tag{2.08}$$

$$\gamma = (2 - \eta)\nu \tag{2.09}$$

The scaling law in Eq. (2.08) is obtained from the assumption that the singular part of the free energy arises from the divergence of the correlation length. The scaling law in Eq. (2.09) follows from Eq. (2.05).

The simplest approximation which can be used to obtain qualitative information about the phase diagrams of Ising models is the mean-field approximation. The approximation consists of assuming that each spin is subject to a self-consistent

field which is due to the values of the magnetizations of the sites with which it interacts. In this way mean-field theory ignores the fluctuations in the values of the local fields. Therefore near critical points, where fluctuations are severe, mean-field theory does not provides a good description of the critical properties. In particular the mean-field values of the critical exponents differ considerably from the correct values. A derivation of mean-field theory is postponed to Sec. 4.1 of this thesis.

A closely related theory, which had an enormous impact on the development of the theory of critical phenomena, is the Landau theory. Landau assumed that the critical properties of a system can be derived from a function $f(\psi, a_i)$ which is a polynomial in powers of the order parameter ψ with coefficients a_i which depend on the thermodynamic fields. The value of the order parameter at a given point in the phase diagram is given by the the value of ψ which minimizes the function f, and the value of the free energy is given by the minimum value of f. The Landau expansion can be obtained, with the help of group theory, by examining the symmetry groups of the ordered and the disordered phases. Alternatively, the Landau expansion can be obtained from the mean-field approximation by expanding the mean-field trial free energy in powers of the order parameters. Therefore the values of the critical exponents predicted using the Landau theory are equal to the values obtained from mean-field theory.

The universality of phase transitions and the scaling laws have been succesfully explained by the renormalization group approach to critical phenomena [33]. Powerful methods based on the renormalization group approach have been found and used to calculate accurate values for the critical exponents and the scaling functions. The renormalization group approach is based on the idea that the critical properties of a system depend only on the nature of the long wave-length fluctuations. Therefore one seeks to define a renormalized Hamiltonian by integrating out, from the original Hamiltonian, the degrees of freedom which correspond to the short wave-length fluctuations. Then the critical properties of the original Hamiltonian

are obtained by studying the sequence of coupling constants which are generated by iterating the renormalization group transformations.

A renormalization group calculation begins with the definition of a transformation R_b which maps an initial Hamiltonian H into a renormalized Hamiltonian H'. The Hamiltonians are represented by points $\{t, h, \{g_i\}\}$ in a multidimensional parameter space which includes the temperature t, the magnetic field h and other possible thermodynamic fields $\{g_i\}$. The transformation R_b must satisfy the following requirements: (a) The number of degrees of freedom N is reduced to N' where $N' = N/b^d$. (b) The initial distance between degrees of freedoms is restored by rescaling vectors $x \mapsto x' = x/b$. (c) The values of the degrees of freedom are rescaled $S_x \mapsto S'_{x'} = S_x/c$ where c is a function of b. (d) The transformation must preserve the value of the partition function.

Having defined the renormalization group transformation, R_b, one looks for the fixed points H^* which satisfy $R_b H^* = H^*$. At these fixed points the correlation lengths ξ and ξ', corresponding to H and H' respectively, must satisfy $\xi = \xi'$. However, the rescaling of lengths in the renormalization group transformations implies that $\xi' = \xi/b$. It follows that at the fixed points the correlation length is either zero or infinite. For critical points the correlation length diverges, and therefore one is lead to study the fixed points where $\xi = \infty$.

The critical surface of a fixed point is defined as the collection of points in parameter space which, under successive applications of the renormalization group transformations, flow to the fixed point. The basic assumption of the renormalization group theory is that the critical point of a system is represented by a Hamiltonian which lies on the critical surface of some fixed point. Also, a system which is near a critical point is represented by a Hamiltonian which lies near a critical surface. For such a case iterating the renormalization group transformation generates a flow which initially approaches the fixed point and eventually diverges away.

Near a fixed point defined by $H^* = (t^*, h^*, \{g_i^*\})$ one can rewrite the Hamiltonian H in terms of the scaling fields $\tilde{t}$, $\tilde{h}$ and $\{\tilde{g}_i\}$, which are the eigenvectors of the linearized renormalization group transformations. Then the renormalization group transformations can be written as

$$\tilde{t}' = b^{\lambda_t}\tilde{t} \qquad \tilde{h}' = b^{\lambda_h}\tilde{h} \qquad \tilde{g}_i' = b^{\lambda_i}\tilde{g}_i \tag{2.10}$$

where b^{λ_t}, b^{λ_h} and b^{λ_i} are the eigenvalues which correspond to the eigenvectors $\tilde{t}$, $\tilde{h}$ and $\{\tilde{g}_i\}$ respectively.

A scaling field associated with an eigenvalue which is greater than one diverges under repeated applications of the renormalization group transformations. Such scaling fields are called *relevant* scaling fields with respect to the fixed point. An *irrelevant* scaling field is a scaling field which is associated with an eigenvalue which is less than one. Such a field decreases to zero under succesive iterations of the renormalization group transformations. A scaling field associated with an eigenvalue which is equal to one is called a *marginal* scaling field. The critical surface of a fixed point is obtained by fixing the values of all the relevant scaling fields to zero.

From the requirement that the partition function is preserved it follows that the free energy near a fixed point satisfies the scaling relation

$$f\left(\tilde{t}, \tilde{h}, \{\tilde{g}_i\}\right) = b^{-d} f\left(b^{\lambda_t}\tilde{t}, b^{\lambda_h}\tilde{h}, \{b^{\lambda_i}\tilde{g}_i\}\right) \tag{2.11}$$

Near an ordinary critical point there exist only two relevant scaling fields $\tilde{t}$ and $\tilde{h}$. Then setting the values of the rest of the scaling fields to zero one obtains the following asymptotic form for the free energy near a critical point

$$f(\tilde{t}, \tilde{h}) = b^{-d} f\left(b^{\lambda_t}\tilde{t}, b^{\lambda_h}\tilde{h}\right) \tag{2.12}$$

Since the rescaling factor b is arbitrary one can choose $b^{\lambda_t}\tilde{t} = 1$ and therefore from Eq. (2.12) it follows that

$$f(\tilde{t},\tilde{h}) = \tilde{t}^{d/\lambda_t} f(1,\tilde{t}^{-\lambda_h/\lambda_t}\tilde{h}) \tag{2.13}$$

Comparing Eq. (2.13) to the scaling law given by Eq. (2.06), one identifies the scaling fields $\tilde{t}$ and $\tilde{h}$ with t and h respectively and obtains the following relations for the critical exponents

$$d\lambda_t^{-1} = 2 - \alpha \qquad \text{and} \qquad \Delta = \lambda_h/\lambda_t \tag{2.14}$$

Similarly using the relation $\xi' = \xi/b$, it is easy to show that $\nu = \lambda_t^{-1}$. From this expression and from Eq. (2.14) the scaling law $d\nu = 2 - \alpha$ is obtained.

The universality of critical phenomena follows from the fact that different systems, which are described by Hamiltonians which differ only through the values of irrelevant scaling fields, lie on the same critical surface and therefore have critical behaviour which is controlled by the same fixed point.

Extensive studies have revealed that the universality of phase transitions is manifested in the fact that the universal critical properties of different models depend only on some general features of the Hamiltonian. These studies showed that the universal quantities depend on the dimensionality of the model, d, the number of components in the order parameter, n, the range of the interactions and the symmetries of the Hamiltonian [34]. The classification of phase transitions into universality classes, according to the universal properties, implies that if one is interested in calculating the critical properties of a model which is difficult to solve, one can choose to investigate soluble models which belong to the same universality class.

The Landau-Ginzburg-Wilson (LGW) Hamiltonians have been used extensively to calculate the critical properties of different universality classes [34,35]. For

each LGW Hamiltonian there exist a dimensionality d_u, called the upper critical dimensionality, such that for $d \geq d_u$ the universal critical properties are equal to the mean-field properties. One of the methods to implement the renormalization group ideas is by solving LGW Hamiltonians near their upper critical dimensionality by performing an expansion, called the ϵ expansion, in the small parameter $\epsilon = d_u - d$.

The LGW Hamiltonians contain an n component order parameter field $\sigma(\mathbf{R})$ which can have any real value and which is defined on the sites $\mathbf{R}$ of a d-dimensional lattice. The length scale for the variations in the order paramter $\sigma(\mathbf{R})$ is assumed to be large compared to the lattice spacing and therefore one can regard $\sigma(\mathbf{R})$ as a field which is defined on every point of a d-dimensional space. In reciprocal space the Fourier components, $\sigma_{\mathbf{q}}$, of the order parameter are defined for values of $\mathbf{q}$ which satisfy $0 \leq |q| \leq \Lambda$, where Λ is a cutoff of the order of the lattice constant.

For the paramagnetic-ferromagnetic critical point the LGW Hamiltonian is given in real space by

$$\beta H = \int d^d x \left[r\sigma^2 + (\nabla\sigma)^2 + u(\sigma^2)^2 \right] \tag{2.15}$$

where r and u are parameters which play the roles of fields. In momentum space the same LGW Hamiltonian is given by

$$\beta H = \int_{\mathbf{q}} \chi^{-1}(\mathbf{q}) \sigma_{\mathbf{q}} \sigma_{-\mathbf{q}} + u \int_{\mathbf{q}_1} \int_{\mathbf{q}_2} \int_{\mathbf{q}_3} (\sigma_{\mathbf{q}_1} \cdot \sigma_{\mathbf{q}_2})(\sigma_{\mathbf{q}_3} \cdot \sigma_{-\mathbf{q}_1-\mathbf{q}_2-\mathbf{q}_3}) \tag{2.16}$$

where

$$\chi^{-1}(\mathbf{q}) = r + q^2$$

and

$$\int_{\mathbf{q}} \equiv \int_{0 \leq |\mathbf{q}| \leq \Lambda} \frac{d^d q}{(2\pi)^d}$$

The partition function Z is given as a functional integral over all possible values of the fields σ

$$Z = \int d[\sigma] e^{-\beta H(\sigma)} \tag{2.17}$$

In real space the functional integral $\int d[\sigma(\mathbf{R})]$ is defined as

$$\int d[\sigma(\mathbf{R})] \equiv \prod_{\mathbf{R}} \prod_{i=1}^{n} \int_{-\infty}^{\infty} d\sigma^i(\mathbf{R}) \tag{2.18}$$

and in momentum space the functional integral $\int d[\sigma_{\mathbf{q}}]$ is defined as

$$\int d[\sigma_{\mathbf{q}}] \equiv \prod_{0 \leq |\mathbf{q}| \leq \Lambda} \prod_{i=1}^{n} \int_{-\infty}^{\infty} \int_{-\infty}^{\infty} d\left(Re\sigma_{\mathbf{q}}^i\right)\, d\left(Im\sigma_{\mathbf{q}}^i\right) \tag{2.19}$$

where from the fact that $\sigma(\mathbf{R})$ is a real field it follows that the product over wave-vectors is performed over half the points in the hypersphere $0 \leq |\mathbf{q}| \leq \Lambda$, i.e., for any pair of wave-vectors $\mathbf{q}$ and $-\mathbf{q}$ only one wave-vector is included.

Multicritical points occur when more than two scaling fields are relevant [36]. If, for example, there exist three relevant scaling fields $\tilde{t}$, $\tilde{h}$ and $\tilde{g}_3$, the fixed point is associated with a tricritical point. In order to obtain a point on the critical surface of a fixed point which describes a multicrital point, one has to choose special values for all the scaling fields which are relevant.

2.2 Lifshitz Tricritical Points

A Lifshitz tricritcal point (referred to hereafter as LTP) is a special kind of multicritical point, which might exist in the phase diagram of the JD model [9]. Therefore in this Section the concept of an LTP is introduced. In Sec. 2.2.1 aspects of the theory of tricritical points are discussed, in Sec. 2.2.2 Lifshitz points are reviewed, and in Sec. 2.2.3 the concept of an LTP is explained. The discussions of

tricritical points and Lifshitz points are mostly limited to details which are relevant to the JD model.

2.2.1 Tricritical Points

A tricritical point is defined as the end-point of a line of three-phase coexistence (a triple line) at which three coexisting phases become identical [37]. Such a point exists, for example, in the (T, H, H_s) phase diagram, shown in Fig. 2-1 of an antiferromagnetic system, where T is the temperature, H is the magnetic field and H_s is a staggered magnetic field which couples to the sublattice magnetization. For $H_s = 0$ and small values of H, there exists a line, L_λ, of continuous phase transitions from the paramagnetic phase to the antiferromagnetic phase. For higher values of the magnetic field H, one encounters a line L_T of first-order transitions into the antiferromagnetic phase. The point P, on the $H_s = 0$ plane where the first-order line, L_T, and the line of critical points, L_λ, meet is the tricritical point. The line L_T is a line where three phases: the paramagnetic and two antiferromagnetic phases with opposite sublattices magnetization coexist. Therefore the point P where the three phases become identical is a tricritical point. For small enough absolute values of H_s there exist two surfaces, called tricritical wings, of first-order transitions from the paramagnetic phase to each of the two antiferromagnetic phases. As the absolute value of H_s is increased, the tricritical wings terminate at two lines, L_+ and L_-, of critical points. Therefore the tricritical point P can also be regarded as a point where three lines (L_λ, L_+ and L_-) of critical points meet. Similarly a bicritical (tetracritical point) is a multicritical point where two (four) lines of critical points meet.

A Landau expansion which applies to a model exhibiting a tricritical point is given by

$$f = -h\psi + \frac{1}{2}a_2\psi^2 + \frac{1}{4}a_4\psi^4 + \frac{1}{6}a_6\psi^6 \qquad (2.20)$$

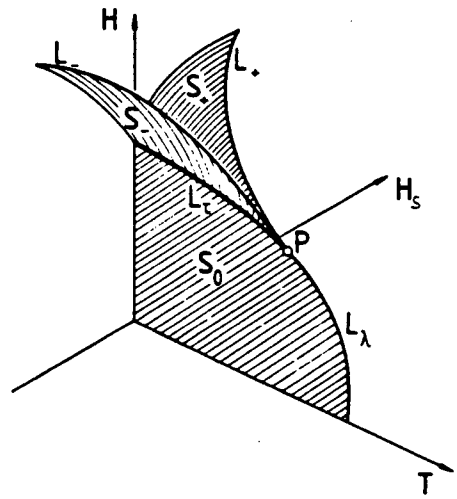

Figure 2-1 The schematic (T, H, H_s) phase diagram of an antiferromagnetic system. The temperature, the magnetic field and the staggered magnetization are given by T, H, and H_s respectively. (This figure was taken from page 4 of Ref 37.)

For $h = 0$ and $a_4 > 0$ one encounters a line of continuous transitions which occur at $a_2 = 0$ from a phase where $\psi^2 = 0$ to a phase where $\psi^2 \neq 0$. However, for $h = 0$ and $a_4 < 0$, the expansion can be regarded as a Landau expansion in ψ^2, which contains a cubic term and therefore describes a line of first-order order transitions. These two lines meet at the point $a_2 = a_4 = 0$ which is a tricritical point. The field h, which couples to the order parameter ψ, breaks the symmetry between the positive and the negative roots of ψ^2. Therefore, on the first-order line the three coexisting phases, which become identical at the tricritical point, are the phase with $\psi = 0$ and two phases with $\psi = \pm\psi_0 \neq 0$.

In order to describe the effect of spatial fluctuations on the critical properties of tricritical points one uses the following Landau-Ginzburg-Wilson Hamiltonian

$$\beta H = \int d^d x \left[-h \cdot \sigma + r\sigma^2 + (\nabla\sigma)^2 + u(\sigma^2)^2 + v(\sigma^2)^3 \right] \qquad (2.21)$$

The upper critical dimensionality of this model is equal to 3 and therefore critical exponents for tricritical points are obtained by performing an ϵ expansion around $d_u = 3$. The critical behaviour is controlled by a fixed point for which $u < 0$ and $v > 0$. The values of three scaling fields have to be set to zero in order to flow to this fixed point.

2.2.2 Lifshitz Points

A Lifshitz point is a special kind of multicritical point in a phase diagram which contains a disordered phase and two ordered phases: one characterized by a fixed equilibrium wave-vector $\mathbf{q}_0$ and the other characterized by a continuously varying wave-vector $\mathbf{q}$ [38,39]. The Lifshitz point is the point on the order-disorder line where the three phases coincide. A magnetic system, whose phase diagram is shown schematically in Fig. 2-2, serves as an example of a system which exhibits a Lifshitz point. In the vicinity of the Lifshitz point, the phase diagram contains a paramagnetic phase (P), a ferromagnetic phase (F) and a modulated phase (M). The magnetization of the modulated phase is spatially varying and is characterized by a wave-vector $\mathbf{q}$ which depends on the temperature T and the value of another thermodynamic field P.

Lifshitz points can be classified by the values of three parameters m, n and d where m is the number of spatial dimensions in which the wave-vector $\mathbf{q}$ varies, n is the number of components of the order parameter and d is the dimensionality of the system.

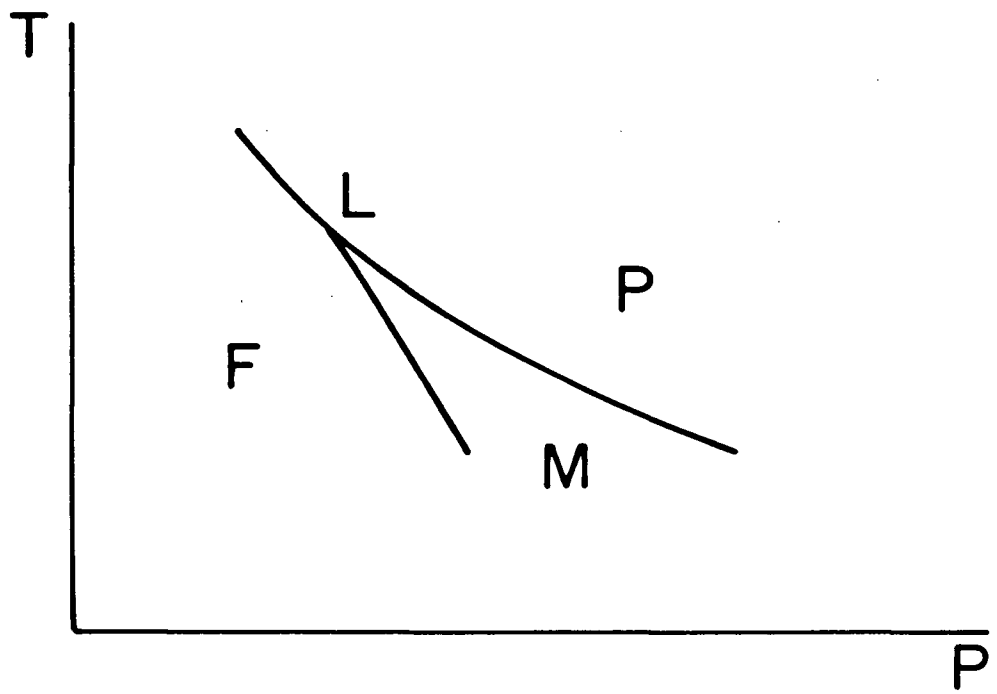

Figure 2-2 The schematic phase diagram of a magnetic system which exhibits a Lifshitz point. The Lifshitz point is the point where the paramagnetic phase, the ferromagnetic phase, and the modulated phase coincide.

A simple Landau expansion which describes an $n = 1$, Lifshitz point is given by

$$f(\psi, \mathbf{q}) = \frac{1}{2}\left[a_2 + c_1 q_\alpha^2 + q_\beta^2 + (q_\alpha^2)^2\right]\psi^2 + \frac{1}{4}a_4\psi^4 \tag{2.22}$$

where

$$q_\alpha^2 = \sum_{i=1}^{m} q_i^2 \qquad \text{and} \qquad q_\beta^2 = \sum_{i=m+1}^{d} q_i^2 \tag{2.23}$$

For $c_1 > 0$ the free energy is minimized by $q_\alpha^2 = q_\beta^2 = 0$ which corresponds to the standard continuous transition, at $a_2 = 0$, into the ferromagnetic phase. For $c_1 < 0$ the free energy is minimized by $q_\alpha^2 = -c_1/2$ and $q_\beta^2 = 0$ and thus the phase

transition occurs into a modulated phase. The point $c = 0$, $a_2 = 0$ is the Lifshitz point.

A Landau-Ginzburg-Wilson Hamiltonian which describes an (m, n, d) Lifshitz point is given by

$$\beta H = \int_{\mathbf{q}} \chi^{-1}(\mathbf{q}) \sigma_{\mathbf{q}} \sigma_{-\mathbf{q}} + u \int_{\mathbf{q}_1} \int_{\mathbf{q}_2} \int_{\mathbf{q}_3} \sigma_{\mathbf{q}_1} \sigma_{\mathbf{q}_2} \sigma_{\mathbf{q}_3} \sigma_{-\mathbf{q}_1-\mathbf{q}_2-\mathbf{q}_3} \tag{2.24}$$

where

$$\chi^{-1}(\mathbf{q}) = \left[a_2 + c_1 q_\alpha^2 + q_\beta^2 + (q_\alpha^2)^2 \right] \tag{2.25}$$

For an anisotropic Lifshitz point ($m \neq d$) the exponent ν, which describes the divergence of the correlation length ξ, is replaced by two correlation length exponents ν_{l2} and ν_{l4} and similarly the exponent η is replaced by η_{l2} and η_{l4}. The exponents with the subscript $l4$ and $l2$ describe correlations between spins which are connected by lattice vectors which lie entirely in the m and $d - m$ subspaces respectively. The rest of the exponents, which describe other divergences near a Lifshitz point, are given by the following anisotropic scaling laws

$$m\nu_{l4} + (d - m)\nu_{l2} = 2 - \alpha \tag{2.26}$$

$$\gamma = (4 - \eta_{l4})\nu_{l4} = (2 - \eta_{l2})\nu_{l2} \tag{2.27}$$

$$\alpha + 2\beta + \gamma = 2 \tag{2.28}$$

Thus for an anisotropic Lifshitz point there are three independent exponents from which the rest of the exponents can be obtained through scaling laws. In particular the mean-field values of all the exponents can be derived from the following mean-field values

$$\nu_{l2} = \frac{1}{2} \tag{2.29}$$

$$\eta_{l2} = \eta_{l4} = 0 \tag{2.30}$$

Corrections to the mean-field values of the exponents are obtained by performing an ϵ expansion from the upper critical dimensionality $d_u = 4 + m/2$. To the lowest order in $\epsilon = d_u - d$, the resulting values are

$$\eta_{l2} = \frac{n+2}{2(n+8)^2}\epsilon^2 \tag{2.31}$$

$$\eta_{l4} = -\frac{m^2+8}{6(m+2)}\eta_{l2} \tag{2.32}$$

$$\nu_{l4} = \frac{1}{2}\nu_{l2} = \frac{1}{4}\left[1 + \frac{n+2}{2(n+8)}\epsilon\right] \tag{2.33}$$

2.2.3 Lifshitz Tricritical Points

A Lifshitz tricritical point can be defined as the multicritical point in an extended parameter space where a line of tricritical points and a line of Lifshitz points intersect. Assume the following Landau expansion for a single component order parameter ψ

$$f(\psi, \mathbf{q}) = \frac{1}{2}\left[a_2 + c_1 q_\alpha^2 + q_\beta^2 + (q_\alpha^2)^2\right]\psi^2 + \frac{1}{4}a_4\psi^4 + \frac{1}{6}a_6\psi^6 \tag{2.34}$$

where q_α and q_β are given by Eq. (2.23). Assume that $a_6 > 0$ and examine the (a_2, a_4, c_1) phase diagram. From the discussion in Sec. 2.2.1 it follows that the positive c_1 axis is a line of tricritical points and similarly from the discussion in Sec. 2.2.2 it follows that the positive a_4 axis is a line of Lifshitz points. Therefore the point $(a_2 = 0, a_4 = 0, c_1 = 0)$ is a Lifshitz tricritical point.

Recently LGW Hamiltonians for an LTP have been analyzed by Aharony et al. [40] and by Dengler [41]. For the $n = 1$ case the LGW which describes an LTP is given by

$$\beta H = \frac{1}{2}\int_{\mathbf{q}} \chi^{-1}(\mathbf{q})\sigma_{\mathbf{q}}\sigma_{-\mathbf{q}} + \int_{\mathbf{q}_1}\int_{\mathbf{q}_2}\int_{\mathbf{q}_3} u(\mathbf{q}_1)\sigma_{\mathbf{q}_1}\sigma_{\mathbf{q}_2}\sigma_{\mathbf{q}_3}\sigma_{-\mathbf{q}_1-\mathbf{q}_2-\mathbf{q}_3}$$
$$+ v\int_{\mathbf{q}_1}\int_{\mathbf{q}_2}\int_{\mathbf{q}_3}\int_{\mathbf{q}_4}\int_{\mathbf{q}_5} \sigma_{\mathbf{q}_1}\sigma_{\mathbf{q}_2}\sigma_{\mathbf{q}_3}\sigma_{\mathbf{q}_4}\sigma_{\mathbf{q}_5}\sigma_{-\mathbf{q}_1-\mathbf{q}_2-\mathbf{q}_3-\mathbf{q}_4-\mathbf{q}_5} \quad (2.35)$$

where $\chi^{-1}(\mathbf{q})$ is given by Eq. (2.25) and $u(\mathbf{q}_1) = U + V\mathbf{q}_1^2$. The upper critical dimensionality for a LTP is given by $d_u = 3 + m/2$. In general one needs to fix the values of three scaling fields (four if one includes the magnetic field) in order to obtain an LTP.

2.3 Previous work on the JD model

As mentioned in the introduction, Domany has shown that a two-dimensional kinetic Ising model on the honeycomb lattice, with nearest-neighbor interactions L, and with discrete-time Glauber dynamics [42] can be mapped onto a line (the Domany line) in the phase diagram of a static three-dimensional Ising model on the hexagonal closed-packed (hcp) lattice. The Hamiltonian for the three-dimensional model (the JD model) is given by Eq. (1.01) and the Domany line is given by Eq. (1.02). One can rewritte these equations in terms of the parameter $\kappa = -J/D$, which measures the degree of competition, and the reduced temperature $t = T/D$. Then the Hamiltonian is given by

$$-\beta H = \frac{\kappa}{t}\sum_{\{ij\}} S_i S_j + \frac{1}{t}\sum_{<ij>} S_i S_j \quad (2.36)$$

and the special line is given by

$$L = \frac{1}{t} \qquad \text{and} \qquad \exp(-4\kappa/t) = \frac{\cosh 1/t}{\cosh 3/t} \quad (2.37)$$

For a ferromagnetic kinetic Ising model $L > 0$, and therefore Eq. (2.37) implies that $D > 0$ and $J < 0$. Thus one is interested in studying the JD model for the case where the interlayer interactions are ferromagnetic while the intralayer interactions are antiferromagnetic.

As a consequence of the competition between the interactions, the JD model also exhibits modulated phases. A linearized mean-field calculation showed that for $\kappa < 1/3$ the model exhibits a phase transition from the paramagnetic phase into the ferromagnetic phase [8]. However, for $\kappa > 1/3$ the transition occurs into a modulated phase characterized by wave-vectors which lie entirely in the the xy plane. Therefore for $\kappa = 1/3$, the model exhibits an $m = 2$ Lifshitz point.

The JD model is an example of a $(d+1)$-dimensional static model which contains a subspace in parameter space onto which a d-dimensional kinetic model is mapped exactly. In such cases, Domany and others have suggested that one can obtain exact results for the $(d+1)$-dimensional static model from known exact results for the d-dimensional kinetic model [5-8]. For the ferromagnetic Ising model on the honeycomb lattice, the location, L_c, of the critical point and its critical properties are known exactly [43]. Therefore Domany investigated the point (κ_c, t_c), in the phase diagram of the JD model, onto which L_c maps.

Domany argued that the special point (κ_c, t_c) exhibits anisotropic scaling. His argument is based on the fact that for this point correlations in the xy layers must correspond to the static correlations of the two-dimensinal Ising model on the honeycomb lattice, while correlations in the direction perpendicular to the layers correspond to dynamic correlations of the same model. At the critical point of the kinetic model the correlations diverge with different critical exponents and therefore it follows that (κ_c, t_c) is a critical point which exhibits anisotropic scaling. Domany predicted that the exponents $\nu_{\|}$ and $\nu_{\perp}$, which characterize the divergences of the correlation length parallel and perpendicular to the layer respectively, are given by

$\nu_{\parallel} = \nu$ and $\nu_{\perp} = z\nu$ where ν and z are the correlation length exponent and the dynamical exponent for the two-dimensional Ising model.

In a subsequent paper Domany and Gubernatis examined the possibility that one could generalize the previous conjectures and argue that the critical properties of a $(d+1)$-dimensional, $m = d$ Lifshitz point are related to the dynamical and static critical properties of a standard critical point in d-dimensions [9]. One would then expect that ν_{l4} and ν_{l2} for a $(d+1)$-dimensional Lifshitz point are equal to ν and νz of the dynamical d-dimensional kinetic critical point respectively.

However in trying to advance this generalized conjucture the following difficulties were encountered:

(a) The conjecture implies that for a Lifshitz point the mean-field values for the correlation length exponents are $\nu_{l4} = 1/2$ and $\nu_{l2} = 1$, instead of the actual known values $\nu_{l4} = 1/4$ and $\nu_{l2} = 1/2$.

(b) The upper critical dimensionality d_u for a $(d+1)$-dimensional, $m = d$ Lifshitz point is given by the solution of the equation $d_u + 1 = 4 + d_u/2$ giving $d_u = 6$, instead of the expected $d_u = 4$ for the upper critical dimensionality of a d-dimensional kinetic model.

(c) Domany found that, along the Domany line in the phase diagram of the JD model the free energy is an analytic function, implying that, at the Lifshitz point, the free energy is also an analytic function. This result requires an explanation because for most critical points the free energy is not an analytic function.

Domany and Gubernatis resolved these problems by mapping a d-dimensional time-dependent Landau-Ginzburg-Wilson Hamiltonian into the phase diagram of a $(d+1)$-dimensional static Landau-Ginzburg-Wilson model. This mapping showed that the critical point of the d-dimensional kinetic model maps not into a Lifshitz point but into a Lifshitz tricritical point in the phase diagram of the $(d+1)$-dimensional static model. The upper critical dimensionality for a d-dimensional Lif-

shitz tricritical point is given by $d_u = 3 + m/2$. Therefore for a $(d+1)$-dimensional, $m = d$, Lifshitz tricritical point the solution to the equation $d_u + 1 = 3 + d_u/2$ gives the expected $d_u = 4$ for the upper critical dimensionality of the d-dimensional kinetic model. The factor of two discrepency in the mean-field values of the correlation length exponents is explained by the fact, that for the Gaussian version of the mapping, points with 'temperature' r in the phase diagram of the dynamical model map into points with 'temperature' R in the phase diagram of the static model, such that $R = r^2$. This implies that in order to obtain the mean-field values for an LTP, one has to divide the mean-field exponents obtained from the dynamical model by a factor of two.

The problem of the analyticity of the free energy can be understood by examining more subtle details of the mapping. The time-dependent d-dimensional model contains the usual order parameter field $\sigma(\mathbf{r}, t)$ and a random gaussian noise field $\varsigma(\mathbf{r}, t)$. As part of the mapping, by formally replacing $\varsigma(\mathbf{r}, t)$ by a fermionic variable $\psi(\mathbf{r}, t)$, one obtains an effective free energy density $H_{eff}(\sigma, \psi)$ which is supersymmetric. Then the fermionic variables can be integrated out and one obtains a d-dimensional Landau-Ginburg-Wilson static model in which the supersymmetry is hidden. The analyticity of the free energy follows from the fact that the lowest eigenvalue of a supersymmetric Hamiltonian is zero [9].

These arguments suggest that, for the case of the JD model, the point (κ_c, t_c) is an $m = 2$ Lifshitz tricritical point in three-dimensions. The fact that a model which contains only two parameters, J and D, exhibits a Lifshitz tricritical point, which in general is obtained by fixing the values of three parameters, can only result from a symmetry which is not immediately apparent. Domany and Gubernatis suggested that this symmetry might be related to the hidden supersymmetry of the Landau-Ginzburg-Wilson static model.

A Monte Carlo simulation of the JD model [9] showed that the point (κ_c, t_c) separates the paramagnetic-ferromagnetic phase boundary into two regions. For

$\kappa < \kappa_c$ the transition is continuous while for $\kappa > \kappa_c$ the transition is first-order, confirming that (κ_c, t_c) is a tricritical point. The calculation also showed that the structure factor $< s(\mathbf{k})s(-\mathbf{k}) >$, where $s(\mathbf{k})$ is the Fourier transform of the order parameter, attains its maximum on a line in reciprocal space, which shrinks to zero as the Lifshitz point is approached. This is the expected behaviour for the structure factor near a Lifshitz point. Therefore the Monte Carlo simulations support the claim that (κ_c, t_c) is an $m = 2$ Lifshitz tricritical point in three-dimensions.

Another result which emerged from the Monte Carlo simulation is that the first-order part of the phase boundary of the ferromagnetic phase and the Domany line almost coincide. This suggests the possibility that, for $\kappa > \kappa_c$, the Domany line serves as the phase boundary for the ferromagnetic phase and thus that it constitutes an exact solution for a whole phase boundary in the phase diagram of a three-dimensional model.

2.4 The three-dimensional ANNNI model

In this section studies of the phase diagram of the three-dimensonal Axial Next-Nearest-Neighbor Ising model (ANNNI model), which are related to this thesis are reviewed. The ANNNI model, introduced by Elliott [11] for the purpose of describing the modulated phases of Erbium, is one of the simplest and best studied models exhibiting modulated phases. In spite of its simplicity the model exhibits an astonishingly complex phase diagram, shown in Fig. 2-3, which is not yet completely understood. In studying other models with competing interactions or models which exhibit modulated phases, one might want to use methods which were found useful in studying the ANNNI model. Also, one might want to look, in the phase diagrams of such models, for features analogous to those found in the phase diagram of the ANNNI model.

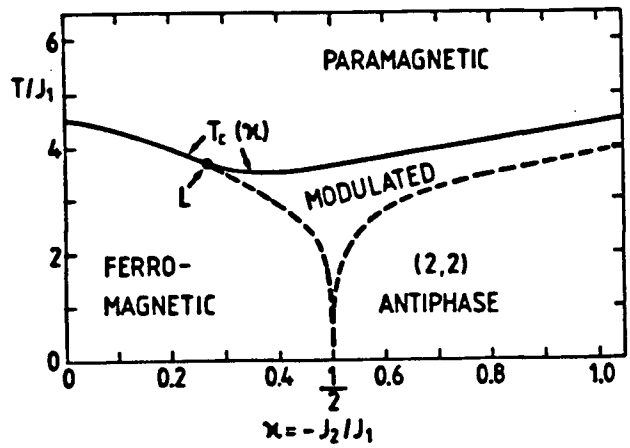

Figure 2-3 The phase diagram of the three-dimensional ANNNI model. (The figure was taken from Ref. 22)

In three dimensions the ANNNI model consists of Ising variables defined on the sites of a simple cubic lattice. Within the xy layers the spins are coupled only through nearest-neighbor ferromagnetic interactions $J_0 > 0$. However along the z-axis, the spins interact through nearest-neighbor ferromagnetic interactions $J_1 > 0$ and next-nearest-neighbor antiferromagnetic interactions $J_2 < 0$. The degree of competition between the ferromagnetic and the antiferromagnetic interactions is measured by the parameter $\kappa = -J_2/J_1$. The competing interactions stabilize modulated phases characterized by a wave-vector $\mathbf{q}$ which is parallel to the z axis axis and which depends on the temperature and on the value of κ.

At zero temperature the model is exactly soluble. For $\kappa < 1/2$ all the spins in the lattice have the same value, i.e., the ground state is ferromagnetic. For $\kappa > 1/2$ the ground state consists of bands, having two layers per band, such that in each

band all the spins have the same value and adjacent bands have spins with opposite values. These spin configurations correspond to the ground state of the $< 2 >$ phase. For $\kappa = 1/2$ the ground state is infinitely degenerate and therefore the point $(\kappa = 1/2, t = 0)$ is a multidegenerate point. At this point the ground states spin configurations consist of randomly stacked bands of alternating spins, such that each band contains at least two layers ordered ferromagnetically.

A low temperature expansion shows that a countably infinite sequence of commensurate modulated phases springs from the multiphase point and separates the ferromagnetic phase from the $< 2 >$ phase [14]. These phases, denoted by $< 2^{j-1}3 >$ for $j \geq 1$, consist of a repeated sequence of bands such that each sequence consists of $j-1$ bands having two layers per band followed by a single band having three layers. Each layer is ordered ferromagnetically and spins on adjacent bands have opposite values. Each of these phases is characterized by a wave-vector parallel to the z-axis whose magnitude is given by $q = \pi j/(2j+1)$. These values of q interpolate between the values $q = 0$ and $q = \pi/2$ which characterize the ferromagnetic and the $< 2 >$ phases respectively. These results have been obtained by extending the low temperature expansion inductively to all orders in powers of $\exp(-2\beta J_0)$ and are therefore exact results.

A variety of methods, based on mean field-theory, have been used to investigate the model [15-18]. In all these studies it was assumed that the order parameter varies only along the z-axis, and therefore one can define m_i to be the value of the order parameter for the layer labeled by i. Then the trial mean-field free energy is given by

$$F = -\frac{1}{2}\sum_i \left[4J_0 m_i^2 + J_1 m_i(m_{i+1} + m_{i-1}) + J_2 m_i(m_{i+2} + m_{i-2})\right] + T\sum_i \int_0^{m_i} \tanh^{-1} x\, dx. \tag{2.38}$$

and the mean-field equations are given by

$$T \tanh^{-1} m_i = 4J_0 m_i + J_1(m_{i+1} + m_{i-1}) + J_2(m_{i+2} + m_{i-2}) \tag{2.39}$$

The order-disorder line has been obtained by solving the linearized version of the mean-field equations. The solution reveals that for $\kappa < 1/4$ the model exhibits a transition from the paramagnetic phase into the ferromagnetic phase. For $\kappa > 1/4$ the transition occurs from the paramagnetic phase into a modulated phase and for $\kappa = 1/4$ the mean-field solution exhibits an $m = 1$ Lifshitz point.

Along the paramagnetic-modulated phase boundary the wave-vector which characterizes the modulated phase has a magnitude which is given by

$$q = \cos^{-1}(1/4\kappa) \tag{2.40}$$

thus allowing for modulated phases which are incommensurate with the lattice. Bak and Bohm have shown that the total width of the commensurate phases vanishes as $(t_c - t)^{0.5}$, and therefore, just below the order-disorder line, the phase diagram must contain incommensurate phases [15]. On the other hand, the low temperature expansions showed that at low enough temperatures the phase diagram contains only commensurate phases. Therefore the three-dimensional ANNNI model should exhibit a commensurate-incommensurate phase transition at some intermediate temperature.

The intermediate range of temperatures was studied by Selke and Duxbury [18] using a method which was first applied to the ANNNI model by Bak and Bohm [15]. The method consists of solving Eq. (2.39) numerically on a finite one-dimensional lattice with periodic boundary conditions. Their main result is that complex commensurate phases are generated out of simpler phases by structure combination processes which occur at special points called branching points. For example, for

$t < 0.66$ there exists a direct transition between the $< 23 >$ and the $< 2^2 3 >$ phases while for $t > 0.66$ one finds a new phase, the $< (23)(2^2 3) >$ phase, intervening between the $< 23 >$ and the $< 2^2 3 >$ phases. The triple point, where the $< 23 >$, the $< 2^2 3 >$ and the $< (23)(2^2 3) >$ phases coexist, is a branching point. At higher temperatures the phase $< (23)(2^2 3) >$ participates in further structure combination processes thus creating even more complex commensurate phases. In general one then expects that phases of the type $< (2^l 3)^m (2^{l+1} 3)^n >$ are generated by branching combination processes.

By solving the mean-field equations on a finite lattice, only solutions which correspond to commensurate phases can be studied. Bak and Jensen obtained solutions which correspond to incomensurate phases by representing the mean-field equations as a discrete non-linear mapping [17]. The mapping is performed by using Eq. (2.39) to calculate the four-dimensional vector V_{i+1} from the vector V_i, where $V_i = (m_{i-2}, m_{i-1}, m_i, m_{i+1})$. By iterating the mapping, different types of trajectories corresponding to the different types of phases are obtained. The paramagnetic phase is described by the fixed point $(0,0,0,0)$, the ferromagnetic phase, with the value m for the magnetization, is described by the fixed points $\pm(m,m,m,m)$, limit cycles correspond to commensurate phases and incommensurate phases are related to one-dimensional trajectories in the four-dimensional parameter phase. These calculations demonstrated the existence of a temperature, which depends on the value of κ, below which incommensurate phases disappear.

An important feature in the phase diagram of the three-dimensional ANNNI model is the uniaxial ($m = 1$) Lifshitz point located on the order-disorder line where the paramagnetic, the ferromagnetic and the modulated phases coincide. A high temperature series expansion showed that the Lifshitz point is located at $\kappa = 0.27$ [13], and therefore it is only slightly shifted from its mean-field value $\kappa = 0.25$. The knowledge of the location of the Lifshitz point facilitates Monte Carlo calculation of critical exponents for a $d = 3$, $m = 1$ Lifshitz point. These exponents

were recently calculated using the course graining of distribution function method to analyze Monte Carlo results and the values $\gamma_l = 1.40 \pm 0.06$, $\beta = 0.19 \pm 0.02$ and $\nu_{l4} = 0.33 \pm 0.03$ were obtained [22]. These values are consistent with the anisotropic scaling laws, given by Eq. (2.26)-(2.28). Also, the value of the exponent β agrees with the experimental value $\beta = 0.18 \pm 0.02$, measured for $RbCaF_3$ [44,45].

Recently, in an effort to go beyond mean-field theory, the three-dimensional ANNNI model has has been studied using the Kikuchi's cluster variation method [19] and the Kirkwood approximation [20]. The phase diagrams which have been obtained are in qualitative agreement with the mean-field phase diagram and are expected to be much more accurate. As expected, the phase transitions from the paramagnetic phase into the ferromagnetic and into the modulated phases occur at temperatures which are lower than the transition temperatures obtained using the mean-field approximation. Also the fraction of the ordered region which is occupied by the highly modulated phases is smaller than in mean-field theory. This suggests that the highly modulated phases are more likely to be washed out by fluctuations. The phase transitions from the paramagnetic phase into the ferromagnetic or the modulated phases are continuous while transitions between modulated phases are first-order.

CHAPTER 3

THE GROUND STATES OF THE JD MODEL

Any atempt to investigate the low temperature phases of a model must begin with a study of its ground states. The spin configurations for the different possible ground states are those which minimize the energy, given by Eq. (1.01).

The calculation of the energy of a given spin configuration is simplified by the observation that all the bonds connecting the sites of the hexagonal closed-packed lattice can be divided into clusters such that each bond belongs to a single cluster. This follows from the fact that the bonds in each triangular layer of the hcp lattice can be divided into triangles and each lattice site of the hcp lattice is centered above one of these triangles. Therefore the bonds of the hcp lattice can be divided into clusters such that each cluster contains three bonds connecting three sites which form a triangle in a layer and three additional bonds which connect each of these sites to the site located above the center of the triangle. Each of these four-spin-clusters forms a tetrahedron which points in the direction perpendicular to the layers and whose base is parallel to the layers. The triangles, i.e, the bases of the tetrahedrons, which belong to the A sublattice and the triangles which belong to the B sublattice point in opposite directions. In Fig. 1-1, the four circles show the four lattice sites of one of the four-spin clusters.

The energy of a given spin configuration can be calculated by summing the contributions to the energy from each of the four-spin clusters. The minimum possible energy is obtained when the contribution from each of the four-spin clusters

is minimized. In the following, the ground state energies and the ground state spin configurations will be obtained. First, a condition which depends on the value of κ will be imposed on the allowed spin configurations in each of the four-spin clusters. This condition follows from the requirement that the energy of each four-spin cluster be minimized. Next, the spin configurations of the hcp lattice which are consistent with this condition will be described.

The contribution E_c to the energy from a given four-spin cluster is given by

$$E_c = -J\left(\sigma_1\sigma_2 + \sigma_2\sigma_3 + \sigma_3\sigma_1\right) - D\left(\sigma_1 + \sigma_2 + \sigma_3\right)S_1 \tag{3.01}$$

where σ_1, σ_2 and σ_3 are the spin variables which form the triangle and S_1 is the spin variable located above the center of the triangle. In order to minimize E_c, the value of S_1 must be given by

$$S_1 = \mathrm{sgn}\left(\sigma_1 + \sigma_2 + \sigma_3\right) \tag{3.02}$$

i.e., the value of the spin above the center of the triangle is equal to the value of the majority of the spins in the triangle. There exist two basic types of four-spin clusters which satisfy this 'majority rule':

(a) Type I: All the spins in the triangle have the same sign. The contribution to the total energy from such a cluster is given by $-(3J + 3D)$.

(b) Type II: There are two spins in the triangle having a given sign while the third spin has the opposite sign. The contribution to the total energy from such a cluster is $-(-J + D)$.

The energy per spin of a spin configuration which contains a fraction l of type I clusters and a fraction $1 - l$ of type II clusters is given by

$$E(l) = -2l(2J + D) - D + J \tag{3.03}$$

For $2J + D > 0$, i.e., for $\kappa < 1/2$ the energy $E(l)$ is minimized by $l = 1$ implying that all the four-spin clusters are of type I. Similarly, for $\kappa > 1/2$ the energy per spin $E(l)$ is minimized by $l = 0$ and all the four-spin clusters are of type II.

For $\kappa = 1/2$ the two types of clusters contribute equally to the energy and therefore one can obtain an infinite number of degenerate spin configurations consisting of combinations of clusters of type I and clusters of type II. Therefore the point $\kappa = 1/2$, $t = 0$ is a highly degenerate point. If some of these degenerate spin configurations serve as ground states of different phases this multidegenerate point will be a multiphase point.

In order to obtain the ground state configurations for $\kappa \geq 1/2$ ($\kappa \leq 1/2$) one has to find the spin configurations which are consistent with the requirement that all the four-spin clusters are of type I (type II). For $\kappa < 1/2$ there exist only two possible spin configurations which are consistent with the requirement that all the four-spin clusters are of type I. One configuration consists of all the spins having the value $+1$ and the second configuration consists of all the spins having the value -1. These spin configurations are the ground states of the ferromagnetic phase (referred hereafter as the $< F >$ phase). The ground state energy per spin of the $< F >$ phase is given by $-3J - 3D$.

For $\kappa > 1/2$ there exist many possible spin configurations which are consistent with the requirement that all the four-spin clusters are of type II. From the fact that each triangle in the bases of the four-spin clusters contains two spins having a given sign and a third spin having the opposite sign, it follows that each layer of the hcp lattice is a ground state of the antiferromagnetic Ising model on the triangular lattice [46]. From the condition that all the spins in the lattice satisfy the majority rule it follows that, for $\kappa < 1/2$, only ground states of the antiferromagnetic Ising model on the triangular lattice which upon using the 'majority rule' generate another ground state, can be stacked to obtain the ground states of the JD model. Most of the ground states of the antiferromagnetic Ising model do not satisfy this

requirement. A careful examination shows that, for $\kappa \geq 1/2$ only ground states which contain parallel rows of alternating spins can be used to obtain the desired ground states of the JD model.

The ground states of the JD model which are generated in these way have the property that all the layers of the hcp lattice are identical. This implies that each of the two hexagonal sublattices of the hcp lattice is ordered ferromagnetically in the direction perpendicular to the layers and that both sublattices are identical.

The requirement that only ground states of the two-dimensional Ising antiferromagnet which contain parallel rows of alternating spins can be stacked to obtain the ground states of the JD model still allows for a multitude of degenerate ground states. This degeneracy is due to the fact that the parallel rows which form the layers can be stacked randomly. The number of possible ground states of this type is $\exp\left(\alpha N^{1/3}\right)$ where $\alpha = \ln 2$ and therefore for $\kappa > 1/2$ the entropy per spin of the grounds states of the JD model is zero. This raises the likelihood that these spin configurations constitute the ground states of a phase which possesses long range order. Assuming that this is the case, a phase whose ground state spin configurations have the property that all the four-spin clusters are of type II will be referred hereafter as the $< AF >$ phase.

At $\kappa = 1/2$ spin configurations which contain mixtures of type I and type II clusters are degenerate with the spin configurations which correspond to the $< F >$ and $< AF >$ phases. For $\kappa > 1/2$ $(\kappa < 1/2)$ these spin configurations have higher energies than the energies of the spin configurations which correspond to the ground states of the $< F >$ $(< AF >)$ phase. Therefore ground state spin configurations which contain mixtures of type I and type II clusters are only stable at the point $\kappa = 1/2$.

There exist many possible spin configurations which are degenerate at the multidegenerate point and which contain mixtures of type I and type II clusters.

The simplest type consist of spin configurations which are uniaxial, i.e., these configurations contain a direction in the layer where all the spins have the same sign. It follows that the spin configuration of a single layer can be described by specifying the spin configuration of a single row which is not the row where all the spins have the same value. Then from the condition that all the four-spin clusters must satisfy the majority rule, it follows that all the layers of the hcp lattice must have identical spin configurations. As an example, Fig. 3-1 shows the spin configuration of parts of two layers which are stacked to form the ground state of a phase called the $< 3 >$ phase. This notation follows from the fact that the row which characterizes the phase, shown in Fig. 3-2a, contains a periodic sequence of spins such that each three spins have a given value and are followed by three other spins which have the opposite value.

In this way, the uniaxial spin configurations which are degenerate at the multidegenerate point can be described by the spin configuration of a single row. The notation $< n_1, n_2, \cdots, n_k >$ will be used to describe the periodic spin configuration of a row which contains n_i spin variables, $i = 1, \cdots, k$ having a given value, followed by n_{i+1} variables, having the opposite value. For the purpose of obtaining a spin configuration which is repeated periodically, periodic boundary conditions are imposed, i.e., the last n_k variables are followed by n_1 variables having the opposite values. For the cases where $n_i = n_{i+1} = \cdots = n_r$ the notation $< n_1, \cdots, n_i^r, \cdots, n_k >$ is used. For example $< 2^3 1 >$ stands for $< 2221 >$.

Next , spin configurations which play an important role in the following sections are described:

(I) The $< n >$ phases for $n \geq 3$. In each layer of an $< n >$ phase one finds rows of spins which contain n spins having a given value followed by n spins having the opposite value. The $< 3 >$ phase is an example of one of these phases. The $< F >$ phase can be identified with the $n = \infty$ phase.

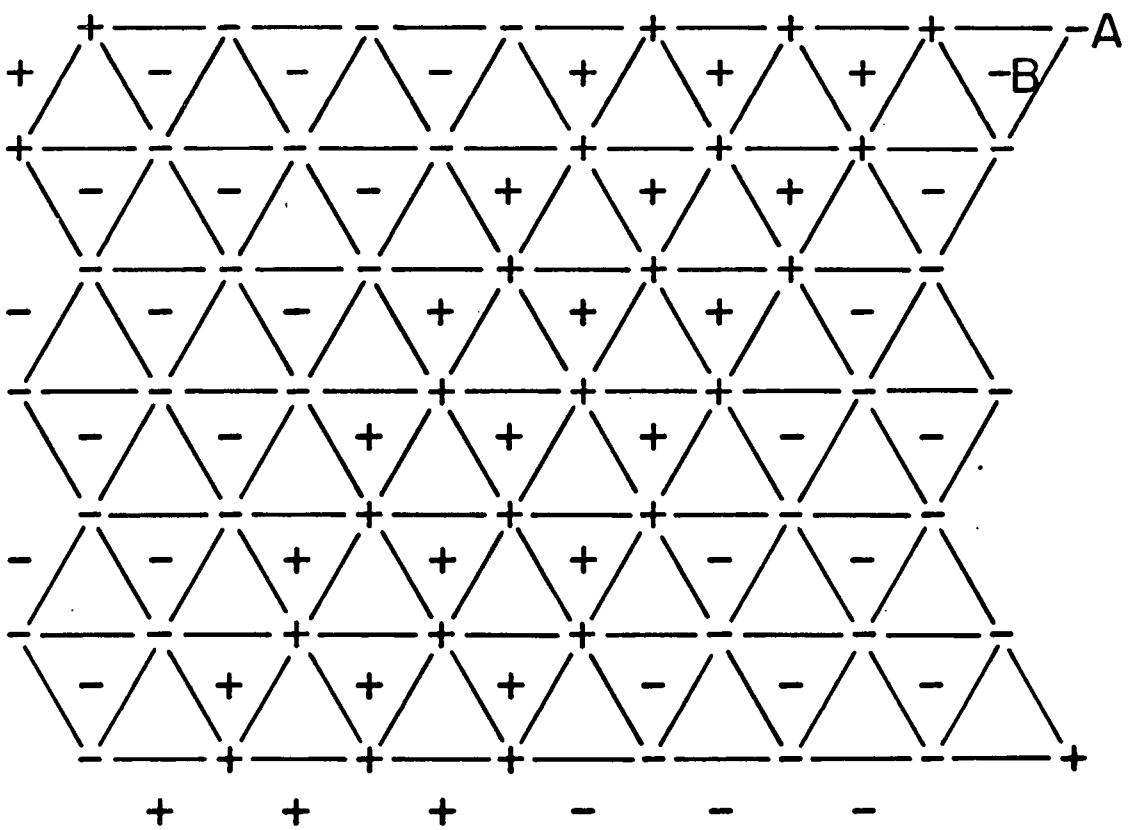

Figure 3-1 The spin configuration of parts of two layers in the ground state of the $< 3 >$ phase. The spin configuration of all the hcp lattice is obtained by stacking the layers labelled by A and B to give the spin configuration of the hexagonal sublattices A and B respectively.

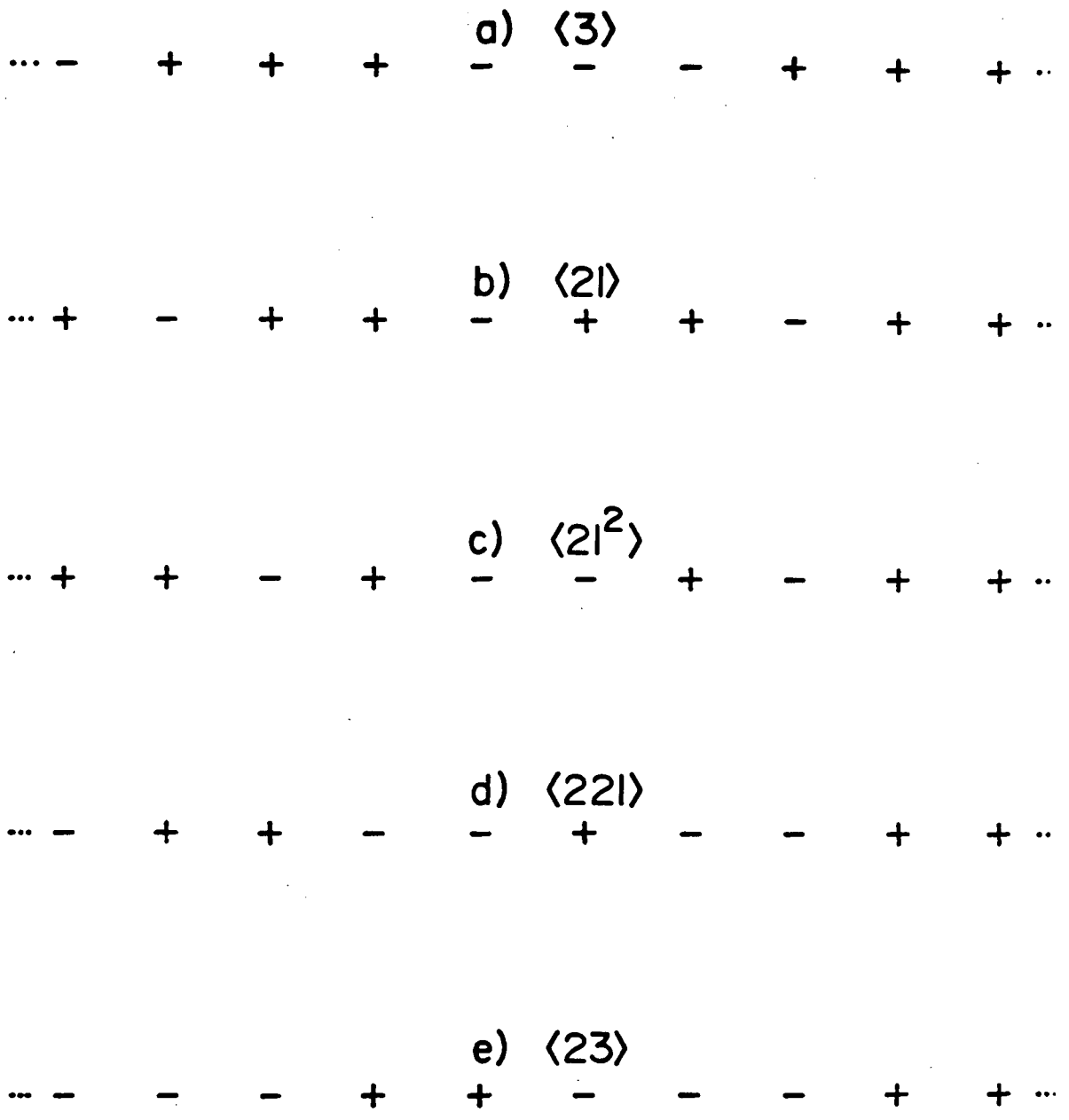

Figure 3-2 The spin configurations of parts of rows in the ground states of various phases. The layers in the spin configuration of these phases are obtained by stacking these rows uniformly.

(II) The $< 21^j >$ phases for $j = 0, 1 \cdots$. In each layer of a $< 21^j >$ phase one finds rows which contain j alternating spins between pairs of spins having the same value. Figures 3-3b and 3-3c show parts of the rows which are used to construct the layers of the $< 21 >$ and $< 21^2 >$ phases respectively. The $< 21^\infty >$ phase is one of the possible ground states of the $< AF >$ phase.

Each of the spin configurations described above might correspond to the ground state of some commensurate modulated phase. Therefore one would like to associate wave-vectors with each of these phases. A possible choice of wavevectors is obtained by calculating the Fourier components of the modulation along the rows. In this way one associates a set of amplitudes and wavevectors with each spin configuration. If one wishes, for the sake of simplicity and at the risk of losing information, one can associate only one wave-vector with a spin configuration. A natural choice is the wavevector which maximizes $a_q^2 + b_q^2$, where a_q and b_q are the amplitudes for the cos and sin Fourier components respectively. In this way the spin configurations $< n >$, are associated with the wave-vector $q = 2\pi/2n$ and the spin configurations $< 21^j >$ are associated with $q = 2\pi(j+1)/2(j+2)$.

In addition to the uniaxial phases, it is also possible to find other spin configurations which are degenerate at the multidegenerate point. These configurations are described by wave-vectors which are not parallel to an in-plane row of spins, i.e., these configurations are not uniaxial. In the following chapters of this thesis, the low temperature phase diagram of the JD model is studied for the purpose of determining which of the spin configurations which are degenerate at the multiphase point are stabilized at non-zero temperature. These studies strongly suggest that only the uniaxial spin configurations are stabilized in the vicinity of the multidegenerate point. This suggestion follows from the fact that all the spin configurations which are not uniaxial and which were tested were found not to be stable in the vicinity of the multiphase point. Therefore this Chapter does not contain descriptions of

spin configurations which are not uniaxial and which are degenerate only at the multiphase point.

CHAPTER 4

MEAN-FIELD THEORY FOR THE *JD* MODEL

Mean-field theory is considered to be the simplest approximation which can be used to obtain qualitative information about the phase diagram of a many body system. The mean-field approximation is expected to yield a correct description of the phase diagram for cases in which spatial fluctuations are small. In three dimensions fluctuations are less severe than in one or two dimensions, and therefore the mean-field approximation is expected to be a reliable tool for investigating the general features of the phase diagrams of three-dimensional models. Near critical points, where fluctuations diverge, mean-field theory does not describe the critical properties properly.

In Sec. 4.1 the mean-field approximation for a general Ising model is derived. In Sec. 4.2 mean-field theory is applied to the *JD* model. In Sec. 4.3 the linearized version of the theory is used to obtain information about the order-disorder line. Some of the results described in this Section were already published by Domany and are repeated here for the sake of completness [8]. In Sec. 4.4 the phase diagram near the possible multiphase point is studied by solving the mean-field equations on a finite lattice numerically.

4.1 Mean-field theory for an Ising model

The mean-field approximation can be derived using several different methods. In this work the derivation given by Schick in Ref. 47 is used. Let the Gibbs free energy $G(T,h)$ be defined by

$$e^{-\beta G(T,h)} = \sum_{\{S_i\}} e^{-\beta H} \tag{4.01}$$

where the Hamiltonian for the model, H, is given by Eq. (2.01) and let w be a function of the variables $\{S_i\}$, defined as

$$w = e^{\beta G} e^{-\beta H} \tag{4.02}$$

By taking the ln of both sides of Eq. (4.02), multiplying by w, and taking the sum over all posible spin configurations $\{S_i\}$, one obtains the following exact expression

$$G = \sum_{\{S_i\}} (wH + Tw \ln w) \tag{4.03}$$

for the Gibbs free energy G in terms of w.

Let $G(\tilde{w})$ be the functional

$$G(\tilde{w}) = \sum_{\{S_i\}} (\tilde{w}H + T\tilde{w} \ln \tilde{w}) \tag{4.04}$$

where $\tilde{w}$ is any function of the variables $\{S_i\}$. The exact Gibbs free energy is given by $G = G(w)$. Schultz has shown that for any function $\tilde{w}$, the functional $G(\tilde{w})$ satisfies $G(\tilde{w}) \geq G(w)$ where equality is obtained for $\tilde{w}$ equal to the exact function w [48]. Therefore one can derive approximations for G variationally by

choosing functions $\tilde{w}$ which depend on some parameters and then minimizing the functional $G(\tilde{w})$ with respect to these parameters.

The mean-field approximation, like the Hartree approximation in quantum mechanics, is obtained by choosing $\tilde{w}$ to be a product of functions which depend on the value of one spin

$$\tilde{w} = \prod_i \frac{e^{-\beta h_i S_i}}{2cosh(\beta h_i)} \tag{4.05}$$

and choosing the variational parameters $\{m_i\}$ to be given by

$$m_i = \sum_{\{S_i\}} \tilde{w} S_i = \tanh \beta h_i. \tag{4.06}$$

Then using Eq. (4.05) and Eq. (4.06) one obtains

$$G(T, h; \{m_i\}) = -\sum_{<ij>} J_{ij} m_i m_j + T \sum_i \int_0^{m_i} \tanh^{-1} x \, dx - h \sum_i m_i \tag{4.07}$$

for the trial Gibbs free energy. The mean-field approximation to the Gibbs free energy is obtained by minimizing Eq. (4.07) with respect to the variational parameters $\{m_i\}$. The values of $\{m_i\}$ are obtained by solving the mean-field equations

$$m_i = \tanh \beta \left(\sum_j J_{ij} m_j + h \right) \tag{4.08}$$

which are derived by extremizing Eq. (4.07) with respect to $\{m_i\}$.

4.2 Mean-field theory for the JD model

For the purpose of applying mean-field theory to the JD model it is useful to regard the hcp lattice as a hexagonal lattice with two sites per unit cell. Let (x, y, z)

be a coordinate system in which the z axis is perpendicular to the triangular layers of the hcp lattice. Let

$$\mathbf{a}_1 = (1,0,0) \qquad \mathbf{a}_2 = \left(-\frac{1}{2}, \frac{\sqrt{3}}{2}, 0\right) \qquad \mathbf{a}_3 = (0,0,1)$$

be the primitive lattice vectors spanning the hexagonal lattice and let $(0,0,0)$ and $(1/2, \sqrt{3}/2, 1/2)$ be the positions of the two sites in the unit cell. Then the Hamiltonian for the JD model can be rewritten as follows

$$H = -\frac{J}{2}\sum_{R,i} S^a_{\mathbf{R}} S^a_{\mathbf{R}+\alpha_i} - \frac{J}{2}\sum_{R',i} S^b_{\mathbf{R}'} S^b_{\mathbf{R}'+\alpha_i} - D\sum_{R,i} S^a_{\mathbf{R}} S^b_{\mathbf{R}+\beta_i} \tag{4.09}$$

where $S^a_{\mathbf{R}}$ and $S^b_{\mathbf{R}'}$ are the site variables at the positions $\mathbf{R}$ and $\mathbf{R}'$ of sublattices a and b respectively. The vectors α_i, for $i = 1, \cdots, 6$, are the lattice vectors connecting a spin to its six in-plane nearest-neighbors and β_i, for $i = 1, \cdots, 6$, are the lattice vectors connecting a spin to its six out-of-plane nearest-neighbors. The vectors α_i are given by

$$\begin{aligned} \alpha_1 &= \left(\frac{1}{2}, \frac{\sqrt{3}}{2}, 0\right) & \alpha_4 &= -\alpha_1 \\ \alpha_2 &= (1,0,0) & \alpha_5 &= -\alpha_2 \\ \alpha_3 &= \left(\frac{1}{2}, \frac{-\sqrt{3}}{2}, 0\right) & \alpha_6 &= -\alpha_3 \end{aligned} \tag{4.10}$$

and the vectors β_i are given by

$$\begin{aligned} \beta_1 &= \left(\frac{1}{2}, \frac{1}{2\sqrt{3}}, \frac{1}{2}\right) & \beta_4 &= \left(\frac{1}{2}, \frac{1}{2\sqrt{3}}, -\frac{1}{2}\right) \\ \beta_2 &= \left(-\frac{1}{2}, \frac{1}{2\sqrt{3}}, \frac{1}{2}\right) & \beta_5 &= \left(-\frac{1}{2}, \frac{1}{2\sqrt{3}}, -\frac{1}{2}\right) \\ \beta_3 &= \left(0, -\frac{1}{\sqrt{3}}, \frac{1}{2}\right) & \beta_6 &= \left(0, -\frac{1}{\sqrt{3}}, -\frac{1}{2}\right) \end{aligned} \tag{4.11}$$

Using the mean-field approximation, described in the previous section, the following expression for the trial Helmholtz free energy is obtained

$$F = -\frac{J}{2}\sum_{R,i} m^a_{\mathbf{R}} m^a_{\mathbf{R}+\alpha_i} - \frac{J}{2}\sum_{R',i} m^b_{\mathbf{R}'} m^b_{\mathbf{R}'+\alpha_i} - D\sum_{R,i} m^a_{\mathbf{R}} m^b_{\mathbf{R}+\beta_i}$$
$$+ T\left(\sum_i \int_0^{m^a_{\mathbf{R}}} \tanh^{-1} x\, dx + \sum_i \int_0^{m^b_{\mathbf{R}'}} \tanh^{-1} x\, dx\right) \qquad (4.12)$$

where $m^a_{\mathbf{R}}$ and $m^b_{\mathbf{R}'}$ are the mean-field values for the ensemble average of $S^a_{\mathbf{R}}$ and $S^b_{\mathbf{R}'}$ respectively. The values of $m^a_{\mathbf{R}}$ and $m^b_{\mathbf{R}'}$ are obtained by solving the following mean-field equations

$$m^a_{\mathbf{R}} = \tanh\left(\beta J\sum_i m^a_{\mathbf{R}+\alpha_i} + \beta D\sum_i m^b_{\mathbf{R}+\beta_i}\right)$$
$$m^a_{\mathbf{R}} = \tanh\left(\beta J\sum_i m^a_{\mathbf{R}+\alpha_i} + \beta D\sum_i m^a_{\mathbf{R}+\beta_i}\right) \qquad (4.13)$$

which are derived by extremizing Eq. (4.12) with respect to $m^a_{\mathbf{R}}$ and $m^b_{\mathbf{R}'}$. For finite lattices, Eq. (4.13) are a set of $2N$ coupled equations with $2N$ unknowns which, in general, admits more than one solution. The mean-field free energy and the mean-field approximation to the Helmholtz free energy is given by the minimum value of the trial free energy.

4.3 The order-disorder line

In the vicinity of the phase transition line from the disordered phase (the paramagnetic phase) to the ordered phases (the ferromagnetic and the modulated phases) the values of $m^a_{\mathbf{R}}$ and $m^b_{\mathbf{R}'}$ are expected to be small and therefore one can solve the mean-field theory by expanding the expression for the trial free energy in

powers of $m^a_{\mathbf{R}}$ and $m^b_{\mathbf{R}'}$. Thus from Eq. (4.12) one obtains the following Landau expansion

$$f = f_0 + f_2 + \sum_{n=2}^{\infty} f_{2n}$$

where

$$f \equiv \frac{1}{2N} F_{2N}\left(T, \{m^a_{\mathbf{R}}\}, \{m^b_{\mathbf{R}'}\}\right)$$

is the trial free energy per spin and

$$f_0 = -T \ln 2$$

$$f_2 = \frac{T}{2}\sum_{\mathbf{R}} (m^a_{\mathbf{R}})^2 + \frac{T}{2}\sum_{\mathbf{R}'} (m^a_{\mathbf{R}'})^2$$
$$- \frac{J}{2}\sum_{R,i} m^a_{\mathbf{R}} m^a_{\mathbf{R}+\alpha_i} - \frac{J}{2}\sum_{R',i} m^b_{\mathbf{R}'} m^b_{\mathbf{R}'+\alpha_i} - D\sum_{R,i} m^a_{\mathbf{R}} m^b_{\mathbf{R}+\beta_i}$$

$$f_{2n} = \frac{T}{2n(2n-1)}\left[\sum_{\mathbf{R}} (m^a_{\mathbf{R}})^{2n} + \sum_{R'} \left(m^b_{\mathbf{R}'}\right)^{2n}\right] \tag{4.14}$$

For high enough temperatures the entropy terms in f_2 (the terms multiplying T) are greater than the interaction terms (the terms multiplying J and D) and therefore f_2 is positive. Then the trial free energy is minimized by the paramagnetic solution $m^a_{\mathbf{R}} = 0$ and $m^b_{\mathbf{R}'} = 0$ for all values of R and R'. For small enough values of T, f_2 is negative and the trial free energy is minimized by solutions which describe ordered phases. In order to find the order-disorder line, which occurs when f_2 vanishes, it is useful to write f_2 in terms of the order parameters $m^a_{\mathbf{q}}$ and $m^b_{\mathbf{q}}$ which are given by the Fourier components of the magnetization

$$m^a_{\mathbf{q}} = \frac{1}{N}\sum_{\mathbf{R}} m^a_{\mathbf{R}} e^{i\mathbf{q}\cdot\mathbf{R}} \tag{4.15}$$

and

$$m_{\mathbf{q}}^{b} = \frac{1}{N}\sum_{\mathbf{R}'} m_{\mathbf{R}'}^{b} e^{i\mathbf{q}\cdot\mathbf{R}'} \tag{4.16}$$

Then one obtains

$$f_2 = \frac{1}{4}\sum_{\mathbf{q}} \begin{pmatrix} m_{\mathbf{q}}^{a} & m_{\mathbf{q}}^{b} \end{pmatrix} \begin{pmatrix} T + 2J(\mathbf{q}) & D(-\mathbf{q}) \\ D(\mathbf{q}) & T + 2J(\mathbf{q}) \end{pmatrix} \begin{pmatrix} m_{-\mathbf{q}}^{a} \\ m_{-\mathbf{q}}^{b} \end{pmatrix} \tag{4.17}$$

where

$$J(\mathbf{q}) = -\frac{J}{2}\sum_{i} e^{i\mathbf{q}\cdot\alpha_i} \qquad \text{and} \qquad D(\mathbf{q}) = -D\sum_{i} e^{i\mathbf{q}\cdot\beta_i}. \tag{4.18}$$

The expression for f_2 is diagonalized by defining new order parameters $\psi_{\mathbf{q}}^{+}$ and $\psi_{\mathbf{q}}^{-}$ which are given by

$$\begin{pmatrix} \psi_{\mathbf{q}}^{+} \\ \psi_{\mathbf{q}}^{-} \end{pmatrix} = \frac{1}{2}\begin{pmatrix} 1 & \frac{D(\mathbf{q})}{\sqrt{D(\mathbf{q})D(-\mathbf{q})}} \\ 1 & -\frac{D(\mathbf{q})}{\sqrt{D(\mathbf{q})D(-\mathbf{q})}} \end{pmatrix} \begin{pmatrix} m_{\mathbf{q}}^{a} \\ m_{\mathbf{q}}^{b} \end{pmatrix} \tag{4.19}$$

Then in terms of the new order parameters f_2 is given by

$$f_2 = \frac{1}{2}\sum_{\mathbf{q}} A_{+}(\mathbf{q})\,\psi_{\mathbf{q}}^{+}\psi_{\mathbf{q}}^{+} + A_{-}(\mathbf{q})\,\psi_{\mathbf{q}}^{-}\psi_{\mathbf{q}}^{-}$$

where

$$A_{\pm} = T + 2J(\mathbf{q}) \pm \sqrt{D(\mathbf{q})\,D(-\mathbf{q})} \tag{4.20}$$

The phase transition temperature T_c and the wave vectors $\mathbf{q}$, which characterize the ordered phases on the order- disorder line are given by the values of T and q for which $A_{+}(\mathbf{q})$ or $A_{-}(\mathbf{q})$ vanish at the highest possible T. In this case $A_{+}(\mathbf{q}) \geq A_{-}(\mathbf{q})$ and therefore the transition occurs when $A_{-}(\mathbf{q}) = 0$. Using Eq. (4.09) and Eq. (4.10) one obtains

$$T_c = \max\{2J\Delta - 2D\cos\frac{q_z}{2}\sqrt{3 + 2\Delta}\} \tag{4.21}$$

where

$$\Delta = \left(2\cos\frac{q_x}{2}\cos\frac{\sqrt{3}q_y}{2} + \cos q_x \right) \tag{4.22}$$

For all values of κ, the right hand side of Eq. (4.21) is maximized by $q_z = 0$ which implies uniform order in the direction parallel to the layers. Therefore from mean-field theory, it follows that the ordered phases of the JD model can be described by first describing the spin configuration of a given layer. Then, the spin configuration of the hexagonal sublattices is obtained by stacking the triangular layers uniformly.

For $0 \leq \kappa \leq 1/3$, the right-hand side of Eq. (4.21) is maximized by $q_x = q_y = 0$ implying a transition from the paramagnetic phase into the ferromagnetic phase and the transition temperature is given by $t_c = 6 - 6\kappa$.

For $1/3 < \kappa < \infty$ the transition occurs into a modulated phase which is characterized by a continuously varying wave-vector given by $(q_x, q_y, q_z = 0)$ where q_x and q_y are given by the solutions of the equation $\kappa^{-2} = \Delta$ and the transition temperature is given by $t_c = 3\kappa + \kappa^{-1}$.

These results can also be deduced by expanding $A_-(\mathbf{q})$ in powers $\mathbf{q}$. Thus one obtains, for small values of $\mathbf{q}$

$$f_2 = \frac{1}{2}\sum_{\mathbf{q}} \left[T - 6J - 6D + \frac{1}{2}(3J + D)q^2 - \frac{1}{96}\left(D + 9J \right) q^4 + \frac{3D}{8}q_z^2 \right] \psi_{\mathbf{q}}^- \psi_{-\mathbf{q}}^- \tag{4.23}$$

where $q^2 = q_x^2 + q_y^2$. For $0 \leq \kappa \leq 1/3$ the coefficient multiplying q^2 is positive and therefore f_2 is minimized by the ferromagnetic solution $q_x = q_y = 0$ and $q_z = 0$. For $0 < \kappa < 1/3$, $3J + D$ is negative and therefore f_2 is minimized by

$$q^2 = 24\frac{3\kappa - 1}{9\kappa - 1} \qquad \text{and} \qquad q_z = 0 \tag{4.24}$$

and thus the JD model exhibits a transition into a modulated phase. The point $(\kappa = 1/3, t = 4)$, on the order-disorder line, where the coefficient multiplying q^2 vanishes, is an $m = 2$ Lifshitz point in three dimensions.

The limit $\kappa = \infty$, in which the JD model reduces to the antiferromagnetic Ising model on a set of decoupled triangular lattices, can be obtained by fixing the value of J to a constant and allowing the interlayer coupling D to tend to zero. Then mean-field theory and similar approximations [49] predict a transition into an ordered phase characterized by the wave-vectors $(\pm\frac{4\pi}{3}, 0, 0)$ at $T_c = -3J$. However, the exact solution to the antiferromagnetic Ising model on the triangular lattice shows that for $t \neq 0$ the model is disordered [46].

4.4 The phase diagram near the multiphase point

The mean-field phase diagram of the JD model near the multidegenerate point is obtained by solving the mean-field equations using a numerical iterative procedure similar to the one used by Bak and Bohm to investigate the three-dimensional ANNNI model [15].

For any given point (κ, t) in the phase diagram, one seeks to find solutions to the mean-field equations, which correspond to different phases characterized by different wave-vectors q. One assigns initial values $\{m_i^a\}$ and $\{m_i^b\}$ to the sites of a $2xNxN$ hcp lattice, with periodic boundary conditions, where 2 is the number of layers and N is either equal or is a multiple of the periodicity of the required phase. From the initial spin configuration a subsequent configuration is obtained by substituting the values of $\{m_i^a\}$ and $\{m_i^b\}$ in the left-hand-side of the mean-field equations. This new spin configuration is then used to generate a subsequent spin configuration and the procedure is repeated until a self-consistent solution is found. As the initial values for the spin configuration one uses either a sinusoidal configuration with the required periodicity or another solution which corresponds to the same phase and which has been previously obtained for a nearby point in the

phase diagram. For each solution to the mean-field equations the trial free energy is calculated using Eq. 4.13 and the stable phase is obtained by finding the solution which minimizes the trial free energy.

The resulting phase diagram near the multidegenerate point is shown in Fig. 4-1. For a given value of t and for increasing values of κ, one first encounters the $< F >$ phase followed by the $< 21^j >$ phases, such that phases with higher values of j appear for larger values of κ, and then the $< AF >$ become stable. The width of the $< 21^j >$ phases becomes exceedingly small as j is increased and therefore the number of $< 21^j >$ phases which are observed is limited by the numerical precision used in solving the mean-field equations. It follows that the multidegenerate point is a multiphase point. An example of the results for the phase boundaries is shown in Table 4-1.

Table 4-1

The mean-field phase boundaries for t=0.5 and t=0.8

Boundary	$t = 0.5$	$t = 0.8$
$< F > - < 2 >$	−0.498	−0.489
$< 2 > - < 21 >$	−0.5015	−0.506
$< 21 > - < 21^2 >$	−0.50215861	−0.514109
$< 21^2 > - < 21^3 >$	−0.502158709726	−0.514179115
$< 21^3 > - < 21^4 >$	−0.502158709777	−0.514179526

From the numerical results the following asymptotic expressions for the phase boundaries between the $< F >$,$< 2 >$,$< 21 >$,$< 21^2 >$ and $< 21^3 >$ phases were obtained

$$\kappa(F,2) = \frac{1}{2} - \frac{t}{4}x + Ax^2 + O(x^3)$$

$$\kappa(2,21) = \frac{1}{2} + \frac{t}{4}x + Bx^2 + O(x^3)$$

$$\kappa(21,21^2) = \frac{1}{2} + \frac{t}{4}x + Cx^2 + O(x^3)$$

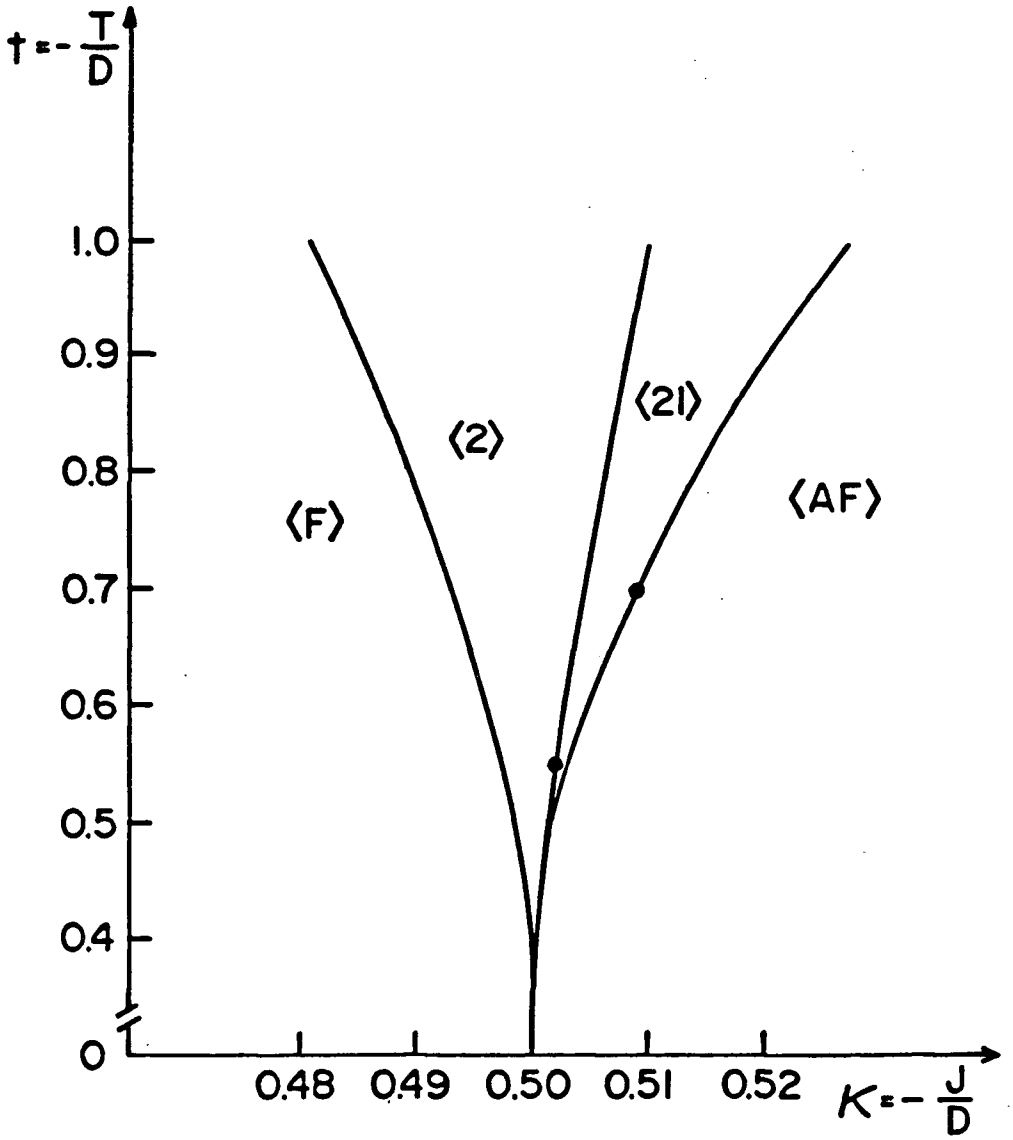

Figure 4-1 The mean-field phase diagram near the multiphase point. The $< 21^j >$ phases, for $j \geq 2$, which are stable between the $< 21 >$ and the $< AF >$ phases, are not shown because their region of stability is not noticeable on the scale of the figure. The dots on the phase boundaries are the branching points where the phases $< 2^2 1 >$ and $< 2^3 1 >$ become stable. These phases are too narrow to be noticeable on the scale of the figure.

$$\kappa(21^2, 21^3) = \kappa(21, 21^2) + O(x^3) \tag{4.25}$$

where $x = \exp(-2/t)$ and A, B, and C are constants. From these expressions it follows that the widths of the $< 2 >$ and $< 21 >$ phases decreases with temperature as $\exp(-2/t)$ and $\exp(-4/t)$ respectively. The width of the $< 21 >$ phase decreases as x^3 and therefore to order x^2 the phase boundary between the $< 21 >$ and the $< 21^2 >$ is given by the same expression as the phase boundary between the $< 21^2 >$ and the $< 21^3 >$. These results suggest that in mean-field theory the width of the $< 21^j >$ phases decrease as x^{j+1} as the temperature goes to zero.

These results, for the low temperature phases of the JD model are similar to the results obtained for the three-dimensional ANNNI model near its multiphase point [14,15]. This similarity suggests the need to investigate whether other features of the three-dimensional ANNNI model exist in the mean-field phase diagram of the JD model. In particular the mean-field phase diagram of the three-dimensional ANNNI model contains phases which are not stable near the multiphase point but which become stable as the temperature is increased [18]. Therefore the phase diagram of the JD model has been searched for phases which are stabilized at finite temperatures.

As in the case of the ANNNI model for $\kappa > 1/2$ one finds branching points, (κ_b, t_b), where new phases, which are not stable for $t < t_b$, become stable, for $t > t_b$, through a structure combination branching process. For example, the point $(0.50219(1), 0.5228(1))$ is a branching point for the phase $< 221 >$. Similarly one finds that the phase $< (21)(21^2) >$ emerges from a branching point at $(0.50091(1), 0.704(1))$. These two branching points are shown as dots in Fig. 4-1 but the phases $< 21^2 >$ and $< (21)(21^2) >$ are too narrow to be noticeable on the scale of the figure.

Structure combination branching processes can also occour through phases which have already been created through the same mechanism at a lower temperature. For example, the phase $< 2^3 1 >$ which evolves from the phases $< 2 >$ and $< 2^2 1 >$ is stable at $t = 1.0$ and therefore has emerged from some branching point at a lower temperarure. In this way more and more commensurate phases are generated as the temperature is increased. In general one can, therefore, expect that the mean-field phase diagram of the JD model contains branching points where phases of the type $< (21^j)^m (21^{j+1})^l >$ appear as a consequence of structure combination branching processes.

For $\kappa < 1/2$ and low enough temperatures mean-field theory predicts a direct transition from the $< F >$ phase to the $< 2 >$ phase and therefore the rest of the $< n >$ phases are not stable. However as the temperature is increased one finds transitions from the $< F >$ phase into other phases. Fig. 4-2 shows part of the phase boundary between the $< F >$ phase and the modulated phases. For values of t such that $t < 2.9779(1)$ one finds direct transitions into the $< 2 >$ phase while for $t > 3.0304$ (but close enough to 3.0304) one encounters a transition into the $< 3 >$ phase. For $2.9779(1) < t < 3.0304(1)$ the transition occur into one of the $< 2^j 3 >$ for $j = 1, 2, \cdots$ where phases with larger values of j appear successively as t is decreased.

These results indicate that at low enough temperature there exists a one to one correspondence between the phases of the three-dimensinal ANNNI model and the phases of the JD model, a phase $< n_1, n_2, \cdots, n_j >$ in the phase diagram of the JD model corresponds to the phase $< n_1 + 1, n_2 + 1, \cdots, n_j + 1 >$ in the phase diagram of the ANNNI model.

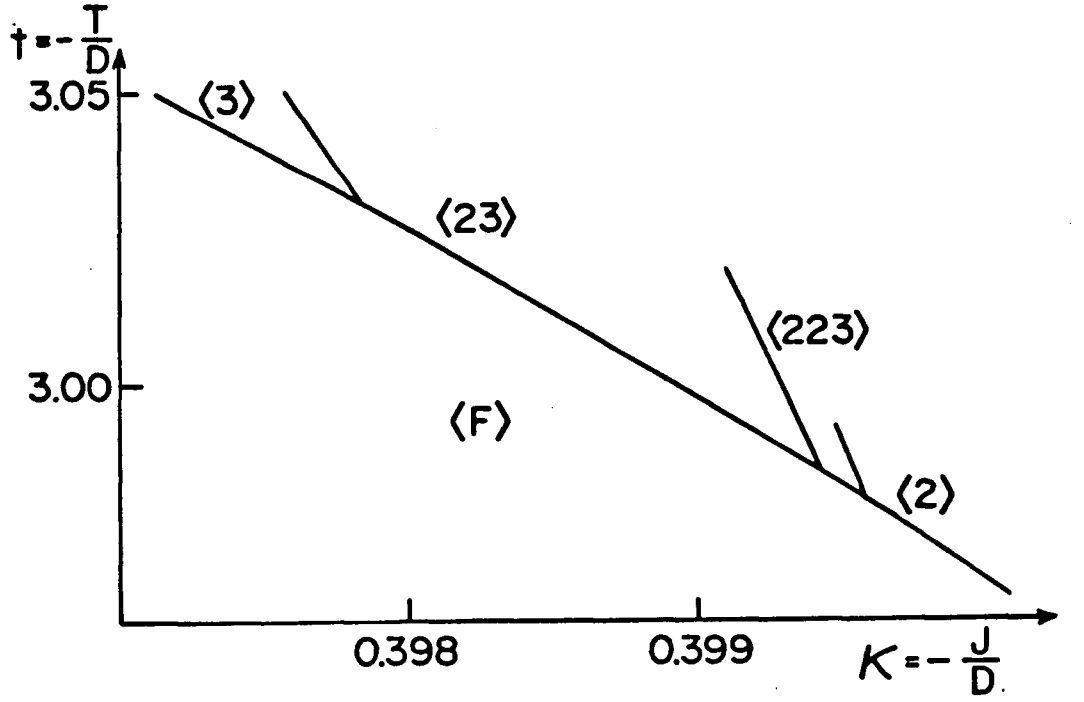

Figure 4-2 The region of the ferromagnetic-modulated phase boundary where the $< 3 >$ phase becomes stable. The phases $< 2^j 3 >$, for $j \geq 1$, are stable between the $< 2 >$ and the $< 3 >$ phases. For $j \geq 3$, these phases appear in a narrow range between the $< 2 >$ and the $< 2^2 3 >$ phases.

CHAPTER 5

LOW TEMPERATURE EXPANSIONS FOR THE JD MODEL

Low temperature expansions have been proven to be useful for calculating the properties of models which exhibit a multiphase point at zero temperature [14]. In this Chapter low order low temperature expansions are used to investigate the JD model near its multiphase point. In this thesis a low temperature expansion for the free energy $-\beta f(s)$ of each possible ground state s has not been performed. Instead, the low temperature expansions are calculated for the ground states of phases which are found to be stable, at low temperatures, by the mean-field approximation. These phases are likely to be the stable phases in the vicinity of the multiphase point. This choice is also motivated by the fact that in other models analogous uniaxial ground states are found to be the stable phases near multiphase points [10,14].

In Sec. 5.1 the method used to generate the low temperature expansions is introduced. Section 5.2 describes the calculation of the low temperature expansions to order x for the $< F >$, the $< n >$, the $< 2 >$ and the $< 21^j >$ phases. In Sec. 5.3 the excitations which contribute to order x^2 to the free energy of the $< 2 >$ and the $< n >$ phases are described and their contribution to the free energy of the $< n >$ phases is calculated. In Sec. 5.4 the phase boundary between the $< F >$ phase and the modulated phases is calculated and is compared to the asymptotic low temperature expression for the Domany line. In Sec. 5.5 the stability of the $< 21^j >$ phases, for $j \geq 1$, is investigated by calculating, to order x^2, the low

temperature expansion for the free energy of these phases. Section 5.6 concludes the Chapter.

5.1 Low temperature expansions

In this work the low temperature expansion for the free energy of a given phase is obtained by calculating the contributions to the partition function from the low energy excitations of the model above the ground state of the given phase [50].

Let $NE_h(s)$ be the ground state energy of a configuration of spins containing N spins where h is the magnetic field and s denotes one of the ground states of the model. Let $F_i(N)$ be a polynomial in N which gives the contributions to the partition function $Z_N(s)$ from low energy excitations obtained from the ground state by overturning i spins. Then $Z_N(s)$ is given by

$$Z_N(s) = e^{-\beta E_h(s)N}\left[1 + \sum_i F_i(N)\mu^i\right] \tag{5.01}$$

where $\mu = e^{-\beta h}$. Let the free energy of the phase be given by

$$-\beta f(s) = -\beta E_h(s) + \sum_i g_i \mu^i \tag{5.02}$$

From Eqs. (5.01) and (5.02) it follows that in the thermodynamic limit

$$\exp\left(N\sum_i g_i\mu^i\right) = 1 + \sum_i F_i(N)\mu^i \tag{5.03}$$

By formally expanding the left hand side of Eq. (5.03) in powers of N and by equating terms having equal powers of μ one obtains that g_i is given by

$$g_i = \left. \frac{\partial F_i(N)}{\partial N} \right|_{N=0} \tag{5.04}$$

i.e., g_i is equal to the coefficient multiplying the linear term in $F_i(N)$.

Therefore in order to obtain a low temperature expansion in terms of some small expansion parameter x, one has to identify the excitations which contribute to the partition function to a given order in x. For each of these excitations, one obtains the contribution to g_i by calculating the contribution to $F_i(N)$ and then extracting the coefficient multiplying the term linear in N.

In this way one calculates a free energy $f(s)$ for each possible ground state s. The free energy f, at a given point in the phase diagram, is given by the minimum value of $f(s)$ and the stable phase is the phase whose ground states yield the minimum of $f(s)$ [51].

5.2 Expansions for the JD model to order x

In this Section low temperature expansions are used to examine the stability of the $< 21^j >$, for $j \geq 0$, and the $< n >$ phases. The low temperature expansions are generated, as described in Sec. 5.1, by calculating the contributions to the free energy of each possible phase from the ground state and from excitations above the ground state. The free energy of a given phase is given by

$$-\beta f(s) = -\beta E_0(s) + \sum_i \left. \frac{\partial F_i(N,x,y)}{\partial N} \right|_{N=0} \tag{5.05}$$

where $E_0(s)$ is the ground state energy of the phase, $x = \exp(-2/t)$, $y = \exp(-4\delta/t)$, $\delta = 1/2 - \kappa$, and $F_i(N,x,y)$ is the contribution to the partition function, for a lattice

containing N spins, from excitations above the ground state which are obtained by overturning i spins.

For the purpose of identifying the clusters of spins which have to be overturned in order to contribute to the expansion to a given order in the expansion parameter x, it is useful to characterize different spins in the spin configuration of the ground states according to the number of in-plane and out-of-plane nearest-neighbors which have the same value as the spin. Table 5-1 shows four different types of spins. For each type of spin, the number of out-of-plane and in-plane nearest neighbors which have the same value as the value of the spin is given by L_o and L_i respectively. The energy above the ground state for a spin configuration obtained from the ground state by overturning the spin is given by ΔE.

Table 5-1

The four types of spins in the spin configurations of the ground states. The number of out-of-plane and in-plane nearest-neighbors with signs equal to the sign of the spin are given by L_O and L_I respectively. The energy of the excitation obtained by overturning the spin is given by ΔE.

Type	L_O	L_I	ΔE	$e^{-\beta\Delta E}$
F	6	6	$12J+12D$	x^3y^3
A	6	4	$4J+12D$	x^5y
B	4	4	$4J+4D$	xy
AF	4	2	$-4J+4D$	x^3y^{-1}

The spin configurations of the ground states of the $< F >$ phase contain only spins of type F while the ground states of the $< AF >$ phase contain only spins of type AF. The $< n >$ phases contain spins of type A, B, and F, while the $< 21^j >$ phases contain spins of type A, B, and AF. The fraction of spins of type A, B, and F in the spin configuration of a ground state of one of the $< n >$ phases is given by $1/n$, $1/n$, and $1-2/n$ respectively, while the fraction of spins of type A, B, and AF

for the $< 21^j >$ phases is $1/(j+2)$, $1/(j+2)$, and $j/(j+2)$ respectively. Figure 5-1 shows the types of spins in the ground state of the $< 3 >$ phase.

The ground state energies of the $< F >$, $< n >$, $< 21^j >$ and the $< AF >$ phases are given by

$$-\beta E_0 (< F >) = \frac{3}{2t} + \frac{3\delta}{t} \tag{5.06}$$

$$-\beta E_0 (< n >) = \frac{3}{2t} + \frac{3\delta}{t} - \frac{4\delta}{nt} \tag{5.07}$$

$$-\beta E_0 \left(< 21^j >\right) = \frac{3}{2t} + \frac{\delta}{t} - \frac{2j\delta}{(j+2)t} \tag{5.08}$$

$$-\beta E_0 (< AF >) = \frac{3}{2t} - \frac{\delta}{t} \tag{5.09}$$

To the lowest order in x, the only contribution to the free energy comes from overturning a single type B spin. The $< F >$ and the $< AF >$ phases do not contain type B spins and therefore this type of excitation only contributes to the free energy of the $< 21^j >$ and $< n >$ phases. To the lowest order in x, the free energies of different phases are given by

$$-\beta f (< F >) = \frac{3}{2t} + \frac{3\delta}{t} \tag{5.10}$$

$$-\beta f (< n >) = \frac{3}{2t} + \frac{3\delta}{t} - \frac{4\delta}{nt} + \frac{xy}{n} \tag{5.11}$$

$$-\beta f \left(< 21^j >\right) = \frac{3}{2t} + \frac{\delta}{t} - \frac{2j\delta}{(j+2)t} + \frac{xy}{(j+2)} \tag{5.12}$$

$$-\beta f (< AF >) = \frac{3}{2t} - \frac{\delta}{t} \tag{5.13}$$

Equating the free energies of the $< F >$ and the $< n >$ phases one obtains the equation

$$x \exp\left(\frac{-4\delta_c}{t}\right) = \frac{4\delta_c}{t} \tag{5.14}$$

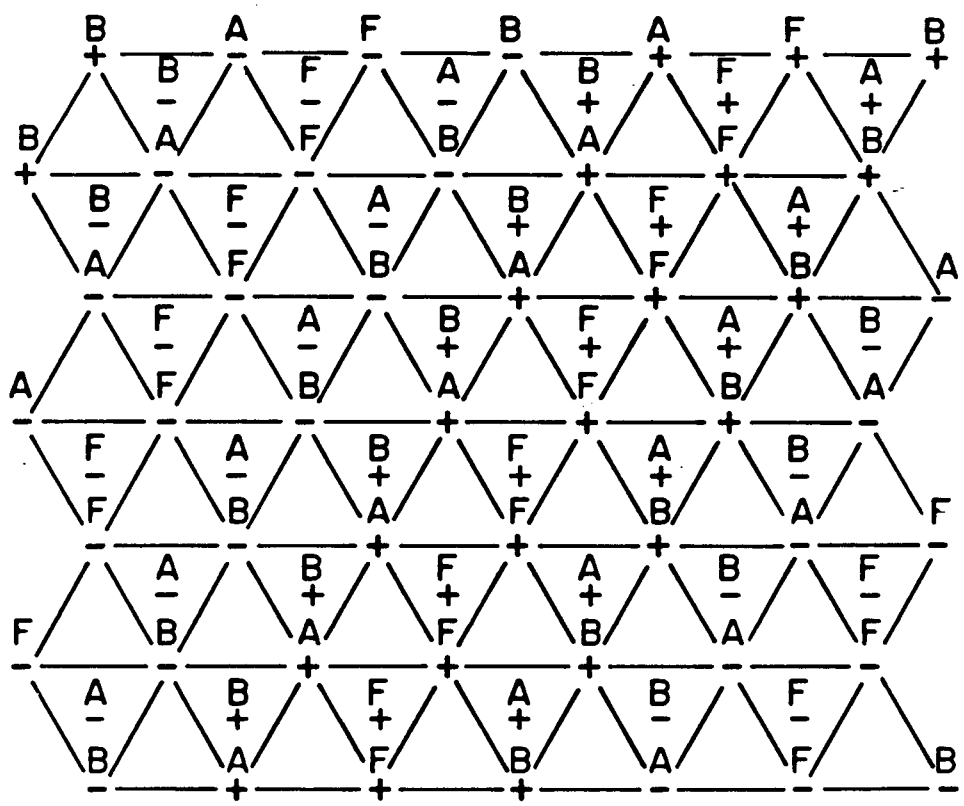

Figure 5-1 The different types of spins in the ground state spin configuration of the $< 3 >$ phase. The spin configuration contains rows of spins of type A, followed by rows of spins of type B and F.

or equivalently $y = e^{-x\gamma} \approx 1 - x$, for the possible phase boundary between the $< F >$ and the $< n >$ phases. Then, using Eq. (5.14) one can rewrite Eqs. (5.10) to (5.13) in the following form:

$$\beta f\,(< n >) = \beta f\,(< F >) + \frac{4}{nt}(\delta - \delta_c) \tag{5.15}$$

$$\beta f\left(< 21^j >\right) = \beta f\,(< 2 >) + \frac{2j}{t(j+2)}(\delta + \delta_c) \tag{5.16}$$

$$\beta f\,(< AF >) = \beta f\left(< 21^j >\right) + \frac{4}{t(j+2)}(\delta + \delta_c) \tag{5.17}$$

These equations imply that for $\delta < \delta_c$ the $< F >$ phase is the most stable phase, for $-\delta_c < \delta < \delta_c$ the $< 2 >$ phase is the stable phase, and for $\delta < -\delta_c$ the stable phase is the $< AF >$ phase.

Therefore, to the lowest order in x, one finds that the stable phases are the $< F >$, the $< 2 >$, and the $< AF >$ phases. The phase boundary $\kappa(F, 2)$ between the $< 2 >$ phase and the $< F >$ phase, and the phase boundary $\kappa(2, AF)$, between the $< 2 >$ phase and the $< AF >$ phase are obtained by solving Eq. (5.14). To the lowest order in x one obtains

$$\kappa(F, 2) = \frac{1}{2} - \frac{tx}{4} \tag{5.18}$$

$$\kappa(2, AF) = \frac{1}{2} + \frac{tx}{4} \tag{5.19}$$

Along the line described by Eq (5.18), the $< n >$ phases have the same free energy as the $< F >$ and the $< 2 >$ phases. Therefore, to first-order in x, one cannot establish the stability of the $< n >$ phases as intermediate phases between the $< F >$ and the $< 2 >$ phases. Similarly, one also deduces that along the line described by Eq. (5.19), the $< 21^j >$ phases, for $j \geq 1$, have the same free energy

as the $< 2 >$ and the $< AF >$ phases and therefore the stability of these phases cannot be determined.

In order to decide whether the $< n >$ phases and the $< 21^j >$ phases, for $j \geq 1$, have regions of stability near the multiphase point one has to extend the previous calculations beyond the lowest order in x. Therefore, in the following, the low temperature expansion is extended to include all terms which contribute to the free energy to order x^2.

5.3 Expansion to order x^2 for the $< n >$ phases

The low temperature expansion, performed to order x, showed that along the phase boundary between the $< F >$ and the $< 2 >$ phases, the $< n >$ phases have the same free energy as the $< F >$ and the $< 2 >$ phases. Therefore if one wishes to calculate the phase boundary between the $< F >$ phase and the modulated phases one has to calculate the free energy of the $< F >$, the $< 2 >$ and the $< n >$ phases to order x^2. For most models such a calculation only requires finding the excitations which directly contribute to order x^2. In contrast, for the JD model, the calculation to order x^2 is significantly more complex, due to the fact that certain type of excitations, which contribute to the free energy terms proportional to arbitrary powers of x, can be grouped together to give a total contribution which is of order x^2 along the phase boundary between the $< F >$ and the $< 2 >$ phase. In the following, the excitations and groups of excitations which contribute to the free energy to order x^2 are described and their contribution is calculated. In Sec. 5.3.1 the different types of excitations which contribute to order x^2 are described and classified. In Sec. 5.3.2 the contribution from one class of excitations is described in detail for the purpose of elucidating the method which is used in Sec. 5.3.3 to calculate the contribution from all the excitations which contribute to order x^2.

5.3.1 Groups of excitations which contribute to order x^2

The simplest excitation which contributes to the low temperature expansion of the free energy to order x^2 is obtained by overturning two spins of type B which are not nearest-neighbors. For the $< n >$ phases, there are $N(N-5)/2n$ possible ways to choose two spins of type B out of the spin configurations of the ground states of the $< n >$ phases. Each spin of type B contributes a factor xy to the free energy (see Table 1) and therefore the contribution from this excitation to the free energy of the $< n >$ phases is given by

$$-\frac{5}{2n}e^{-\beta(8J+8D)} = -\frac{5}{2n}x^2y^2 \tag{5.20}$$

A more complicated excitation is obtained by overturning the clusters of spins shown in Fig 5-2. Each of these clusters contains i spins of type A which belong to one of the two hexagonal sublattices and spins of type B which belong to the other sublattice. The solid lines in Fig. 5-2 represent out-of-planes bonds connecting type A spins to type B spins. The dashed lines represent in-plane bonds connecting type B spins. A cluster of this type which contains i spins of type A will be referred as a chain of length i.

The contribution to the free energy from a chain of length i is proportional to $x^3y^3y^{2i-1}$ and therefore is manifestly of higher order than x^2. However, the total contribution obtained by summing over all the possible values of i is given by

$$x^3y^3\sum_{i=1}^{\infty}y^{2i-2} = x^3y^3\frac{1}{1-y^2} \tag{5.21}$$

and therefore along the phase boundary of the $< F >$ phase, given by $y = 1 - x$, the contribution to the free energy from these excitations is of order x^2. Thus in

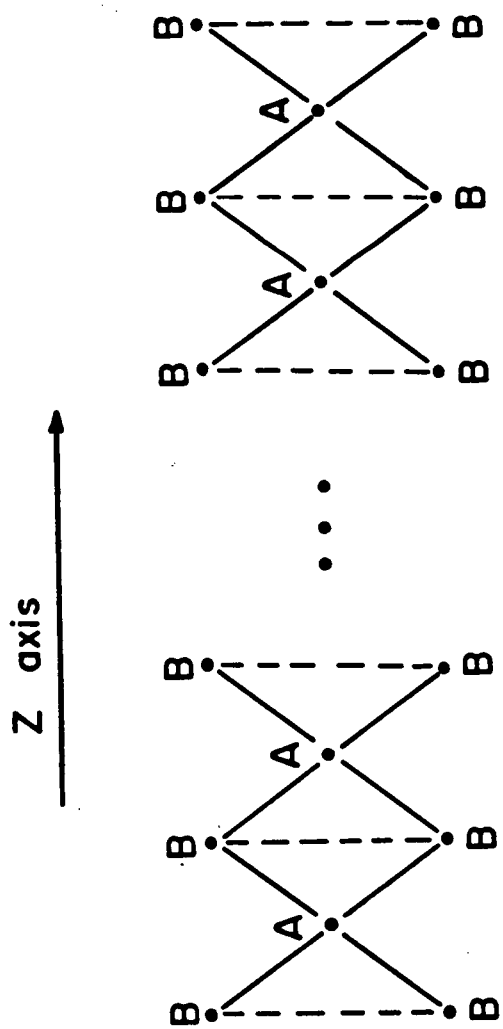

Figure 5-2 A chain of spins. All type A spins lie on a row parallel to the z axis in one of the sublattices, and are connected to type B spins in the other sublattice.

spite of the fact that each chain contributes to the free energy to order x^3, the total contribution from all the chains is proportional to x^2.

For values of $y \geq 1$, i.e., for $\kappa \geq 1/2$, the sum over i is divergent. In the following, it is shown that by grouping this divergent contribution with contributions from other types of excitations, which are described below, finite expressions for the free energy of the different phases are obtained.

The excitations which cancel the divergence consist of the chains described above and k additional isolated spins of type B, i.e., spins of type B which are not nearest-neighbors one to the other and which are not nearest-neighbors to any of the spins in the chain. The excitations which contain only a single chain correspond to the $k = 0$ case. Each of these excitations contribute terms to the free energies of the different phases which are proportional to $x^3y^3\,(xy)^k\,y^{2i-1}$. However, as in the previous case, the total contribution obtained by summing over all possible values of i is of order x^2.

This result can be demonstrated by examining the case of $k = 1$. For this case, there are $\frac{1}{n}N(N-8-6i)$ ways to choose a chain and a single B spin from the spins in the ground states of the $< n >$ phases. Therefore the total contribution from these excitations to the free energy of the $< n >$ phase is proportional to

$$-6x^4y^4\sum_{i=1}^{\infty} iy^{2i-1} - 8x^4y^4\sum_{i=1}^{\infty} y^{2i-1} \tag{5.22}$$

For the first term, the sum over i gives $(1-y^2)^{-2}$ and therefore along the phase boundary of the $< F >$ phase, where $y = 1 - x$, this sum is proportional to x^{-2}. In this way, the first term in Eq. (5.22) is of order x^2. The second term is of order x^3 and therefore will be ignored.

For the case of excitations which include k spins of type B, the number of ways to choose a chain of length i and k isolated spins of type B is given by

$$\frac{N}{n}\frac{1}{k!}\prod_{j=1}^{k}(N - c_j - \alpha i) \tag{5.23}$$

where c_j are constants and for the case of the $< n >$ and the $< 2 >$ phases $\alpha = 6$ and $\alpha = 8$ respectively. The constants c_j multiply terms in the free energy which are of order higher than x^2 and therefore do not have to be computed. For example, as already mentioned, $c_1 = 8$ multiplies the second term in Eq. (5.22) which is of order x^3. The contribution to the free energy of the $< n >$ phase, obtained by extracting the coefficient multiplying N in Eq. (5.23), is given by

$$\frac{1}{nk!}(-\alpha i)^k (xy)^{k+3} y^{2i-2} \tag{5.24}$$

The total contribution from all possible excitations of this type is given by

$$\frac{9}{n}x^3y^3\sum_{i=1}^{\infty}\sum_{k=0}^{\infty}\frac{1}{k!}(-\alpha xyi)^k y^{2i-2} = \frac{9}{n}x^3y^3\sum_{i=1}^{\infty}e^{-\alpha xyi}y^{2i-2}$$
$$= \frac{9}{n}x^3y^3\frac{1}{e^{\alpha xy} - y^2} \tag{5.25}$$

The factor of 9 in this equation is due to the fact that for each chain there exist eight additional chains which contribute to the free energy to the same order in x and y. Four of these chains are obtained from the original chain by omitting one of the spins of type B from one of the edges of the chain. The other four chains are obtained from the original chain by omitting two spins of type B, one from each edge.

A comparison between the sum over i in Eq. (5.25) and the sum in Eq. (5.21), shows that including the contributions from excitations which consist of a chain and isolated spins of type B results in y^2 being replaced by $y^2e^{-\alpha xy}$. From the values of

α for the different phases and from the expressions for the phase boundaries given by Eq. (5.18) and Eq. (5.19), it follows that for the domain where the modulated phases are stable the quantity $y^2 e^{-\alpha xy}$ is less than one and therefore the geometric series in Eq. (5.25) converges. Thus grouping the contributions from the excitations which contain a chain with excitations which also include isolated B spins cures the divergence found for $y \geq 1$ in Eq. (5.21).

An inspection of Eq. (5.22) and Eq. (5.25) shows that contributions to the free energy which are of order x^{3+k} can be summed to give a total contribution to the free energy which is of the order of x^2 if the sum also includes k powers of i. In the following, more complex excitations which also contribute to order x^2 are described. These additional excitations are obtained by modifying the excitations discussed above so that the sums include additional powers of xi.

One type of such an excitation is obtained by adding to the excitations already discussed a single spin of type F which is an out-of-plane nearest-neighbor to one of the A spins in the chain. Such an inclusion multiplies the contribution to the free energy by a factor of xy. This can be understood from the fact that once the chain is overturned, the F spins which are attached to the A spins become B spins. Then if overturned these spins contribute to the free energy as if they were originally spins of type B, i.e., they contribute one power of xy. The extra power of i, needed to compensate for the extra power of x, follows from the fact that the F spin can be located at i positions along the chain.

In the same spirit, adding l spins of type F multiplies the contribution to the free energy from the chain by x^l. These l powers of x are compensated by l powers of i which originate from the fact that there are $i^l/l! + O(i^{l-1})$ ways to choose the l spins of type F. The total contribution, to order x^2, to the free energy from excitations which are obtained by overturning clusters which contain a chain

of length i, k isolated spins of type B, and l spins of type F is given by

$$\frac{9}{n}x^3y^3\sum_{i=1}^{\infty}\sum_{k=0}^{\infty}\sum_{l=0}^{\infty}\frac{1}{k!l!}\left(-\alpha xyi\right)^k\left(xy\right)^l y^{2i-2}=\frac{9}{n}x^3y^3\frac{1}{e^{(\alpha-1)xy}-y^2} \tag{5.26}$$

From Eq. (5.25) and Eq. (5.26) it follows that taking into account excitations which are obtained by overturning clusters which include spins of type F amounts to changing α to $\alpha-1$. This result can be understood from the fact that once the main cluster is overturned, the F spins become B spins and therefore each of the spins of type A, in the chain, excludes one less spin of type B.

Another contribution to order x^2 is obtained by grouping excitations which contain more than one chain such that in each chain there exist spins of type A which are nearest-neighbors to some of the spins of type A in the neighboring chain. The inclusion of each additional chain multiplies the contribution to the free energy from the cluster by a factor of x^2. These extra powers of x are compensated by summing over the variables which describe the length of the additional chain.

As an example consider the case shown in Fig. 5-3 of a cluster which consists of a short chain of length j and a long chain of length i. The contribution to the free energy from such a cluster is proportional to x^5y^{2i+1}. This contribution contain two more factors of x than the contribution from one chain of length i. For a given value of i, the total contribution to the free energy from all possible values of j is proportional to

$$\sum_{j=1}^{i-1}\left(i-j-1\right)x^5y^{2i+1}=\frac{1}{2}i^2x^5y^{2i+1}+O(i)x^5y^{2i+1} \tag{5.27}$$

Thus the two powers of i, in the first term in the right-hand side, compensate the two additional powers of x and the contribution to the free energy from these excitations is also of order x^2.

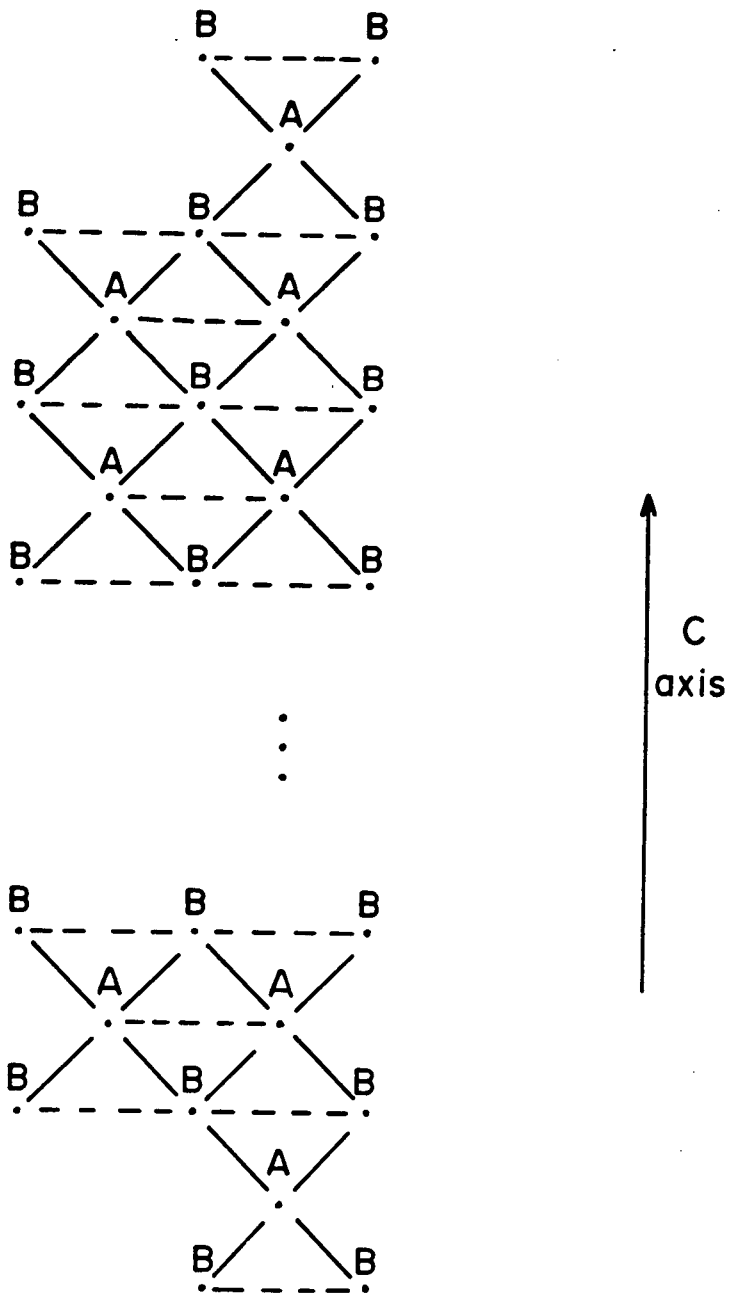

Figure 5-3 An example of an excitation which consist of two chains.

As for the case of excitations which contain one chain, additional excitations which when grouped together also contribute to the free energy to order x^2, can be obtained by adding to excitations which contain an arbitrary number of chains, isolated spins of type B and adding spins of type F which are attached to the chains. A detailed description of the calculation of the contribution to the free energy from excitations which include more than one chain, is postponed to later in this section.

The last type of excitation which also contributes to order x^2 can be obtained by modifying excitations which contain more than two chains. For these cases, once the chains are overturned, the spins of type A which contain two in-plane nearest-neighbors in two neighboring chains turn into spins of type B. Thus, as in the case of the excitations which are obtained by overturning F spins, additional excitations which also contribute to order x^2 can be obtained by not overturning an arbitrary number of spins of type A, provided that these spins contain two in-plane nearest-neighbors which are part of the cluster. Also, as for the case of excitations which include F spins, the contribution from excitations which include A spins which are not overturned is taken into account by subtracting 1 from the number of spins of type B which are excluded by the spin of type A which is not overturned.

From all the previous considerations it follows that a complete calculation , to order x^2, of the free energy of the different phases must include contributions from a variety of different types of excitations. In order to keep track of the different contributions, the excitations will be grouped into classes such that each class contains all the excitations which include the same number of chains. The excitations in a given class differ from one another according to the lengths of the chains, the distribution of isolated B spins, the number of the F spins which are attached to the A spins, and the number of A spins which are not overturned.

5.3.2 The contribution from the class of three chains

In this subsection, the calculation of the contribution of order x^2 to the free

energy of the $< n >$ phases, from all the excitations which belong to the class of three chains, will be explained in detail. This calculation is the simplest example which includes all the features which have to be considered in a calculation of the contribution from an arbitrary class.

The calculation of the contribution to the free energy from a given class is facilitated by classifying the excitations which belong to the class into subclasses. Each subclass contains all the excitations whose clusters have the same distributions of widths, where the width of a cluster, at a given position, is equal to the number of spins of type A which are encountered as the cluster is scanned in a direction parallel to the layers, i.e., along a row of spins of type A. A section of width l_k and length i_k is a part of a cluster in which there exist i_k consecutive positions where the width of the cluster is l_k.

The class of three chains contains two subclasses. The first subclass contains all the excitations containing clusters which have two sections of width 1, two sections of width 2, and a single section of width 3. Figure 5-4 shows an example of a cluster of chains which belongs to excitations which correspond to this subclass. The second subclass contains all the excitations whose chains contain three sections of width 1 and two sections of width 2. Figure 5-5 shows an example of a cluster of chains which corresponds to excitations which belong to this subclass. In general, the notation $1^{l_1}2^{l_2}\ldots k^{l_k}$ will be used to describe a subclass of excitations whose clusters include l_j sections of width j, where $j = 1, \cdots k$. Using this notation, the subclasses of the class which contain three chains are denoted by $1^2 2^2 3^1$ and $1^3 2^2$.

The total contribution, to order x^2, to the free energy of the $< n >$ phases from the excitations which belong to the subclass $1^2 2^2 3^1$ is given by

$$\frac{1}{n} 3^2 2^4 C(3;2,2,1) x^7 y \sum_{i_1=1}^{\infty}\sum_{i_2=1}^{\infty}\sum_{i_3=1}^{\infty}\sum_{i_4=1}^{\infty}\sum_{i_5=1}^{\infty} y^{2(i_1+i_2+i_3+i_4+i_5)} e^{Axy} e^{Bxy} \qquad (5.28)$$

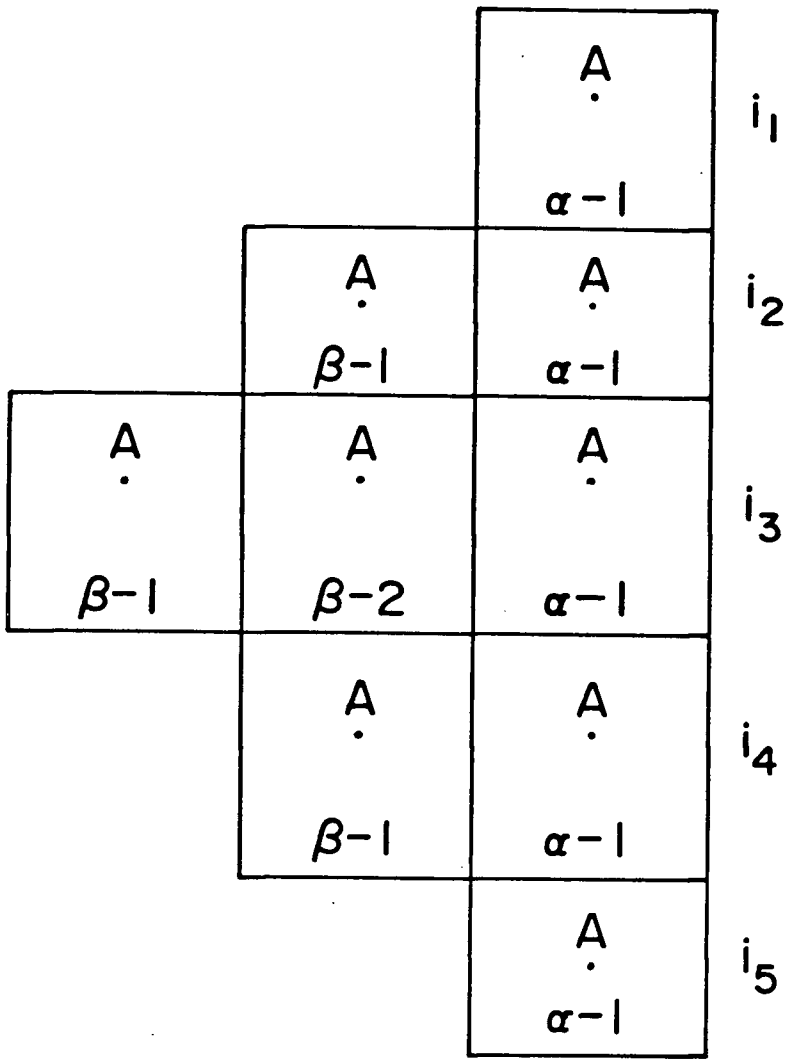

Figure 5-4 An example of a excitation which includes three chains and which belongs to the subclass $1^2 2^2 3$. The dots represent some of the A spins in the cluster. The variables $i_1, \cdots, i_5$ are the lengths of the sections. The contributions from the different segments to the exponentials are shown in each segment.

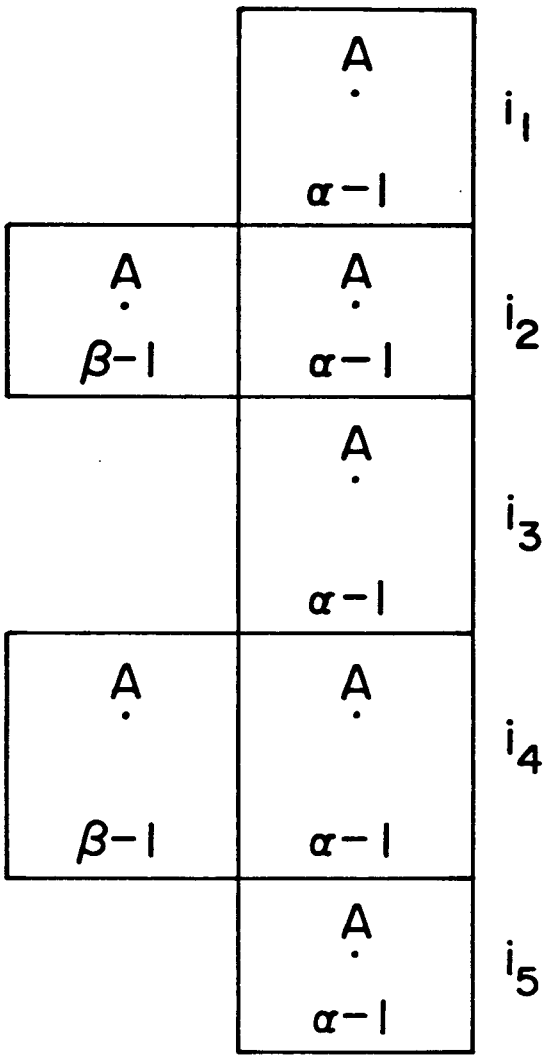

Figure 5-5 An example of an excitation in the subclass $1^3 2^2$ of the class of three chains.

where $i_1, \cdots, i_5$ are the lengths of the sections of the clusters and

$$A = -(\alpha - 1)(i_1 + i_2 + i_3 + i_4 + i_5) - (\beta - 1)(i_2 + i_3 + i_4) - (\beta - 1)i_3 \qquad (5.29)$$

$$B = -(\beta - 2)i_3 \qquad (5.30)$$

and for the $< n >$ phases $\alpha = 6$ and $\beta = 2$.

In the following, the different considerations which led to these expressions are explained. The powers of x and y follow from a calculation of the energy of an excitation which only includes a cluster of chains with lengths which are described by the variables $i_1, \cdots, i_5$. For each cluster, the exponentials result from the sums over all the other possible excitations which include the cluster. The exponentials which contain α and β result from the sums over all the different isolated spins of type B. The value of α is the number of spins of type B which are excluded, i.e., which cannot be one of the isolated B spins, per each spin of type A which is located in a segment of a chain which forms one border of a section. The value of β is the additional number of excluded spins of type B, per spin of type A, in each additional segment of the section. The number one which is subtracted from each α and β results from the sums over all excitations which include F spins. The additional one, which is subtracted from each β which correspond to segments of chains which do not form any of the two borders of the section, results from the excitations which are obtained by not overturning spins of type A.

In this way, each segment of a chain in each section of the cluster, is associated with an exponential whose argument is the length of the section multiplied by a number which depends on the location of the segment of the chain in the section. In Fig. 5-4 and Fig. 5-5 these numbers are shown for the different segments of the chains in the different sections. For each section, one segment of a chain which is on the border of the section is assigned the number $\alpha - 1$. The segment of a chain

on the second border of the section is assigned the number $\beta - 1$. All the segments of chains in the interior of the sections are assigned the values $\beta - 2$.

The coefficient $3^2 2^4$ results from the different possible ways of terminating the chains. Each of the two exterior ends of the chains can be terminated in three possible ways. One way consists of including both spins of type B which are attached to the last A spin in the chain. The other two ways correspond to the cases where one of the B spins is omitted. Each of the four interior ends of the chains can be terminated in two ways. A single B spin which is attached to the end of the chain can be included or omitted.

The coefficient $C(3;2,2,1)$ is equal to the number of different possible clusters which belong to the subclass $1^2 2^2 3^1$ in the class of three chains. In general, $C(m;l_1,\cdots,l_k)$ is equal to the number of clusters in the subclass $1^{l_1} 2^{l_2} \cdots k^{l_k}$ of the class of excitations which contain m chains.

Evaluating the sum in Eq. (5.28) one obtains

$$\frac{9 \cdot 2^8}{n} x^7 \left[B(\alpha - 1)\right]^2 \left[B(\alpha + \beta - 2)\right]^2 B(\alpha + 2\beta - 4) \tag{5.31}$$

where

$$B(u) = \frac{1}{e^{uxy} - y^2} \tag{5.32}$$

The contribution to the free energy, to order x^2, is obtained by substituting $y = 1 - x$ in Eq. (5.31) and is given by

$$\frac{9 \cdot 2^8}{n} \frac{1}{(2 + \alpha - 1)^2} \frac{1}{(2 + \alpha + \beta - 2)^2} \frac{1}{(2 + \alpha + 2\beta - 4)} x^2 = \frac{9}{n} \frac{1}{2 \cdot 7^2} x^2 \tag{5.33}$$

where the number 2 in each denominator follows from the expansion of y^2 and the rest of the terms in the denominators follow from the expansions of the exponentials.

Similarly the contribution to the free energy, to order x^2, from the subclass $1^3 2^2$ is given by

$$\frac{9 \cdot 2^8}{n} \frac{1}{(2+\alpha-1)^3} \frac{1}{(2+\alpha+\beta-2)^2} x^2 = \frac{9}{n} \frac{2^2}{7^3} x^2 \tag{5.34}$$

Therefore the total contribution from the class of three chains is given by

$$\frac{9}{n} \left(\frac{2}{7}\right)^2 \left(\frac{1}{7} + \frac{1}{8}\right) x^2 \tag{5.35}$$

5.3.3 The contribution to order x^2 for the $< n >$ phases

In this subsection, the total contribution to the free energy of the $< n >$ phases, which is of order x^2, is calculated. This contribution includes the contribution from overturning two isolated spins of type B and the contribution from excitations which contain chains. The calculation for these excitations is performed by calculating the contribution from a given subclass and then summing over all possible subclasses and all possible classes.

Let $1^{l_1} 2^{l_2} \cdots k^{l_k}$ be a subclass in the class of m chains. The contribution, to order x^2, from the excitations in this subclass is given by

$$\frac{9}{n} 4^{(m-1)} C(m; l_1, \cdots, l_k) \, [B(u_1)]^{l_1} \, [B(u_2)]^{l_2} \prod_{i=3}^{k} [B(u_i)]^{l_i} \, x^2$$

where $B(u)$ is defined in Eq. (5.32) and

$$u_1 = \alpha - 1$$

$$u_2 = \alpha + \beta - 2$$

$$u_i = \alpha + \beta - 2 + (i-2)(\beta - 2) \tag{5.36}$$

These expressions are derived using the same considerations which were used in the previous subsection to calculate the contribution from the subclasses of the class of three chains. The argument u_1 in $B(u_1)$ originates from the single segment of chain in the l_1 sections which have width 1. The argument u_2 in $B(u_2)$ is the sum of $\alpha - 1$ and $\beta - 1$ which are the contributions from the first and the second segments of the l_2 sections whose width is 2. The arguments in the rest of the B functions are obtained by summing the contributions, $\alpha - 1$ and $\beta - 1$, which originate from the exterior segments and the contribution $\beta - 2$ which originates from the $i - 2$ interior segments of a section whose width is i. The factors $3^2 2^{2(m-1)}$ correspond to the three possible ways to terminate each of the two exterior ends of chains and the two possible ways to terminate each of the interior ends.

Substituting $y = 1 - x$ in Eq. (5.36), one obtains that the contribution, to order x^2, from this subclass is given by

$$\frac{9}{n} 4^{(m-1)} C(m; l_1, \cdots, l_k) \frac{1}{(1+\alpha)^{l_1}} \prod_{i=2}^{k} \frac{1}{[\alpha + \beta + (i-2)(\beta-2)]^{l_i}} x^2 \tag{5.37}$$

For the case of the $< n >$ phases $\alpha = 6$ and $\beta = 2$ and therefore Eq. (5.37) gives

$$\frac{9}{n} 4^{(m-1)} C(m; l_1, \cdots, l_k) \frac{1}{7^{l_1}} \frac{1}{8^{l_2 + l_3 + \cdots + l_k}} = \frac{9}{n} \frac{2}{16^m} \left(\frac{8}{7}\right)^{l_1} C(m; l_1, \cdots, l_k) \tag{5.38}$$

where the last equality follows from the relation

$$\sum_{i=1}^{k} l_i = 2m - 1 \tag{5.39}$$

The total contribution from all the subclasses which contain l_1 sections of width 1 is given by

$$\frac{9}{n} \frac{2}{16^m} \left(\frac{8}{7}\right)^{l_1} D(m; l_1) x^2 \tag{5.40}$$

where

$$D(m;l_1) = \sum_{l_2,\cdots,l_k} C(m;l_1,l_2,\cdots,l_k) \tag{5.41}$$

is equal to the number of clusters in the class of m chains such that the cluster contains l_1 sections of width 1 and is given by

$$D(m;l_1) = 4^{m-1}\frac{(2m-l_1-2)!}{(m-1)!(m-l_1)!}(l_1-1) \tag{5.42}$$

The total contribution from all subclasses and all classes is given by $N_n x^2/n$ where

$$N_n = \frac{9}{7} + \frac{9}{2}\sum_{m=2}^{\infty}\sum_{l_1=2}^{m}\frac{1}{4^m}\left(\frac{8}{7}\right)^{l_1}\frac{(2m-l_1-2)!}{(m-1)!(m-l_1)!}(l_1-1) \tag{5.43}$$

where the first term is the contribution from the class of one chain, the first sum in the second term is a sum over all the rest of the classes and the second sum is a sum over all possible values of l_1 in a given class. The second term in Eq. (5.43) is equal to 12/7 (see Appendix A) and therefore $N_n = 3$.

The total contribution to the free energy of the $< n >$ phases is given by

$$-\frac{5}{2n}x^2 + \frac{3}{n}x^2 = \frac{1}{2n}x^2 \tag{5.44}$$

where the first term is the contribution from overturning two spins of type B and the second term is the contribution from all the other excitations. The free energy of the $< n >$ phase, along the line $y = 1 - x$, is given by adding the contribution which is to order x^2 to the expression in Eq. (5.11). Thus the free energies of the $< n >$ phases are given by

$$-\beta f\,(< n >) = \frac{3}{2t} + \frac{3\delta}{t} - \frac{4\delta}{nt} + \frac{xy}{n} + \frac{x^2}{2n} + O\left(x^3\right) \tag{5.45}$$

5.4 The phase boundary for the $< F >$ phase

From the calculations in the previous section it follows that in the vicinity of the phase boundary of the ferromagnetic phase, the free energy of the $< F >$ phase and the free energy of the $< n >$ phases are given by Eq. (5.10) and Eq. (5.45). The contribution to order x^2 to the free energy of the $< 2 >$ phase is obtained by performing a calculation similar to that described in Sec. 5.3. The contribution from each subclass is given by Eq. (5.37) where $\alpha = 9$ and $\beta = 4$. Let the total contribution from all the subclasses be given by $N_2 x^2/2$. From the fact that the values of α and β for the $< N >$ phases $(\alpha = 6, \beta = 2)$ are smaller than the corresponding values for the $< 2 >$ phase $(\alpha = 9, \beta = 4)$, it follows that $N_2 < N_n = 3$. This implies that the $< n >$ phases are stable in a region of the phase diagram between the $< F >$ and the $< 2 >$ phases. Therefore, in order to obtain an expression, to order x^2, for the paramagnetic-modulated phase boundary one has to calculate the phase boundary between the $< F >$ and the $< n >$ phases.

The phase boundary between the $< F >$ phase and the $< n >$ phases is obtained by equating the free energy of the $< F >$ and the free energies of the $< n >$ phases. From Eq. (5.10) and Eq. (5.45) it follows that this phase boundary is independent of n and is given by

$$\kappa\,(F, n) = \frac{1}{2} - \delta_c \tag{5.46}$$

where

$$\delta_c = x - \frac{1}{2}x^2 \tag{5.47}$$

Subtituting Eq. (5.47) and Eq. (5.10) into Eq. (5.45) it follows that

$$-\beta f\,(< n >) = -\beta f\,(< F >) + \frac{4}{nt}\,(\delta_c - \delta) \tag{5.48}$$

This equation implies that for $\delta > \delta_c$, the $< F >$ phase is the stable phase and for $\delta < \delta_c$ the $< 3 >$ phase is the stable phase. The phase boundary between the $< F >$ phase and the $< 3 >$ phase is given by

$$\kappa(F,3) = \frac{1}{2} - \frac{1}{4}tx + \frac{1}{8}tx^2 + O(x^3) \tag{5.49}$$

Along this phase boundary, the $< n >$ phases, for $n \geq 4$, have the same free energy as the $< F >$ and the $< 3 >$ phases. Therefore in order to further resolve these phases, one has to calculate expressions for the free energies and for the phase boundaries to higher order in x. The phase boundary between the $< F >$ phase and the rest of the $< n >$ phases is expected to differ from the phase boundary between the $< F >$ phase and the $< 3 >$ phase only in order x^3.

Having calculated the phase boundary between the ferromagnetic and the modulated phases, one can compare the expressions for the phase boundary and the Domany line. For small values of t, an expansion of Eq.(2.37) shows that the Domany line terminates at the multiphase point and that in its vicinity it is given by

$$\kappa_D = \frac{1}{2} - \frac{1}{4}tx + \frac{1}{8}tx^2 + O\left(x^3\right) \tag{5.50}$$

From Eq (5.49) and Eq (5.50) it follows that the asymptotic low temperature expansion for the Domany line and the phase boundary for the ferromagnetic phase agree in the first three leading terms.

The phase boundary between the $< 3 >$ phase and the $< 2 >$ phase is obtained by equating the free energy of the $< 3 >$ phase, given by substituting $n = 3$ in Eq. (5.45), and the free energy of the $< 2 >$ phase given by

$$-\beta f(< 2 >) = \frac{3}{2t} + \frac{\delta}{t} + \frac{xy}{n} - \frac{5}{4}x^2 + \frac{N_2}{2}x^2 + O\left(x^3\right) \tag{5.51}$$

This phase boundary is given by

$$\kappa(3,2) = \frac{1}{2} - \frac{t}{4}x + \frac{t}{4}\left(\frac{19}{2} - 3N_2\right)x^2 \tag{5.52}$$

An exact evaluation of N_2 has not been performed in this thesis. However summing the contribution to N_2 from the six first classes reveals that the sum is rapidly convergent and that N_2 is given by $N_2 = 1.040$.

5.5 Expansion to order x^2 for the $< 21^j >$ phases

The calculations in Sec. 5.2 show that, to order x, the JD model exhibits a transition from the $< 2 >$ phase into the $< AF >$ phase, and that the $< 21^j >$ phases, for $j \geq 1$, are found to coexist with the $< 2 >$ and the $< AF >$ phase along their phase boundary which is given by $y = 1 + x$. Therefore, as for the case of the $< n >$ phases, the stability of the $< 21^j >$ phases has to be determined by calculating to higher order in x the free energies of the $< 2 >$, the $< 21^j >$ and the $< AF >$ phases.

A calculation to order x^2 of the free energies of the $< 21^j >$ phases is performed using the method described in Sec. 5.3. The excitations which contribute to order x^2, along the line $y = 1 + x$, are similar to the excitations described for the $< n >$ phases in Sec. 5.3.1. The only difference results from the fact that the $< 21^j >$ phases do not contain spins of type F and the $< n >$ phases do not contain spins of type $< AF >$. Therefore, for the $< 21^j >$ phases, the excitations which are analogous to the excitations of the $< n >$ phases which contain spins of type F, contain spins of type AF. However the calculation to order x^2 of free energy of the $< 21^j >$ phases is identical to the same calculation for the $< n >$phases. The only difference in the final expressions for the contribution to the free energy to order x^2 results from the fact that for the $< n >$ phases these contributions were evaluated

along the line $y = 1 - x$ whereas for the $< 21^j >$ phases the evaluation is along the line $y = 1 + x$.

In Appendix A it is shown that the double sum which gives the contribution to order x^2 to the free energy of the $< 21^j >$ phases is divergent. This divergence suggests that the $< 21^j >$ phases are not stable phases.

5.6 Conclusions

In this Chapter the stability of the $< n >$ and the $< 21^j >$ phases was investigated by performing a low temperature expansion about these ground states. To order x, the $< 2 >$ phase was found to be stable in a region of the phase diagram whose width is of order x. The $< n >$ phases were found to be stable only on the $< F >$-$< 2 >$ phase boundary and similarly the $< 21^j >$ phases, for $j \geq 1$, were found to be stable only on the $< 2 >$-$< AF >$ phase boundary. To order x^2, the calculation showed that the $< 3 >$ phase has a region of stability of width x^2 between the $< F >$ and the $< 2 >$ phase while the $< n >$ phases, for $n \geq 4$, are stable only on the $< F >$-$< 3 >$ phase boundary. To order x^2 the contribution to the free energy of the $< 21^j >$ phases was found to be divergent. This suggests that the $< 21^j >$ phases are not stable phases.

The phase boundary between the ferromagnetic and the modulated phases was calculated to order x^2 and was found to coincide with the low temperature asymptotic expansion of the Domany line. This result strongly suggests that the Domany line is the phase boundary of the ferromagnetic phase.

CHAPTER 6

THE PARAMAGNETIC-MODULATED TRANSITION

In this Chapter the possibility that the JD model exhibits a fluctuation-induced first-order transition between the paramagnetic and the modulated phases is examined. In Sec. 6.1 studies which suggest that models with continuous minimum-energy surfaces exhibit a fluctuation-induced first-order transition are reviewed. In Sec. 6.2 it is shown that the JD model contains minimum-energy surfaces. In Sec. 6.3 the Landau-Ginzburg-Wilson (LGW) Hamiltonian which is used to describe the paramagnetic-modulated phase transition of the JD model is described and in Sec. 6.4 this LGW Hamiltonian is analyzed using an ϵ expansion. Section 6.5 concludes the Chapter.

6.1 Models with continuous minimum-energy surfaces

For most models the quadratic term in the LGW Hamiltonian attains its minimum on a point or on a set of discrete points in reciprocal space. For example, the LGW Hamiltonian which describes the paramagnetic-ferromagnetic phase transition, Eq. (2.16), attains a minimum at the point $q = 0$. In contrast, models with continuous minimum-energy surfaces are models in which the quadratic term in the LGW Hamiltonian attains its minimum on one or more continuous surfaces in reciprocal space. Such models have been introduced to describe phase transitions

from a disordered phase into an ordered modulated phase characterized by a wave-vector $\mathbf{q}$ which can be any wave-vector chosen from the continuous minimum-energy surfaces [23].

The nematic to smectic-C transition in liquid crystals is an example of a phase transition which is described by an LGW Hamiltonian whose minimum-energy surface consists of two continuous surfaces in reciprocal space [52]. The nematic phase is a phase where anisotropic molecules are, on average, aligned with their long axes parallel to a given direction denoted by a unit vector $\hat{n}$ [53]. The smectic-C phase is a phase which contains nematic order, also characterized by a unit vector $\hat{n}$, and a one-dimensional density wave characterized by a wave-vector $\mathbf{q_0} = (\pm q_{0z}, \mathbf{q}_{0\perp})$ where q_{0z} is the component of $\mathbf{q_0}$ in the direction of $\hat{n}$, and $\mathbf{q}_{0\perp}$ is the component of $\mathbf{q_0}$ in the direction perpendicular to $\hat{n}$ [53]. Therefore the wave-vector $\mathbf{q_0}$ can be any of the wave-vectors lying on two rings in reciprocal space and the LGW Hamiltonian which describes the nematic to smectic-C phase transition contains minimum-energy surfaces consisting of these two rings.

For the cases where the LGW Hamiltonian does not contain cubic terms, mean-field theory predicts that the models exhibit continuous phase transitions into the modulated phase. However, Brazovskii, using perturbation theory, argued that, due to the existence of the minimum-energy surface the phase transition is first-order [23]. Thus these are examples of models which exhibit a fluctuation-induced first-order phase transition, i.e., a first-order phase transition for which mean-field theory predicts a continuous transition. The nematic to smectic-C transition has been analyzed, using the arguments of Brazovskii, by Swift and Leitner [24,26] who predicted a first-order phase transition, in agreement with experiments [54].

Brazovskii's arguments are based on perturbation theory and therefore cannot be regarded as rigorous near the phase transition point. Therefore Mukamel and Hornreich performed a renormalization group calculation for a model in which the minimum-energy surfaces consist of two squares, instead of the two rings which

occur for the nematic to smectic-C phase transition [27]. They obtained recursion relations for the renormalization group transformations which do not contain a stable fixed point. This suggests that, for dimensionalities which are lower than the upper critical dimensionality $d_u = 5$, the two square model exhibits a fluctuation-induced first-order phase transition [30]. Mukamel and Hornreich also extended their calculations to models where the continuous minimum-energy surfaces consist of two symmetric polygons with an arbitrary number of edges. For these models the recursion relations also do not contain a stable fixed point. Ling et al. performed a similar calculation for an n-component model in which the minimun-energy surface is a square [28]. They also found that for finite n and $d < 5$ the model does not contain a stable fixed point. These results for different models with a continuous minimum energy surface, the perturbative arguments of Brazovskii and the experimental results for the nematic to smectic-C transiton suggest that models which contain continuous minimum-energy surfaces exhibits a first-order transition for dimensionalities below the upper critical dimensionality. The precise shape of the constant-energy surface does not appear to play a role in determining the order of the phase transition [27].

6.2 The minimum energy surface for the JD model

In Chap. 4 it was shown that for values of $\kappa > 1/3$ mean-field theory predicts that the JD model should exhibits a continuous transition from the paramagnetic phase into a modulated phase characterized by a wave vector $\mathbf{q} = (q_x, q_y, 0)$ where q_x and q_y satisfy the equation

$$\kappa^{-2} = 2\cos\frac{q_x}{2}\cos\frac{\sqrt{3}q_y}{2} + \cos q_x \qquad (6.01)$$

For a given value of $1/3 < \kappa < \infty$ the solutions to Eq. (6.01) consist of one or two lines in reciprocal space. These lines constitute the minimum-energy surfaces

of the JD model. Therefore the transition between the paramagnetic phase and the modulated phase might be a first-order transition of the type described in the previous section.

For a general value of κ the lines of constant energy do not form a simple polygon. However, for the value $\kappa = 1$, the solutions to Eq. (6.01) form a hexagon in reciprocal space. The hexagon, shown in Fig. 6-1 is given by the lines

$$q_x = \pm\pi$$

$$q_x + \sqrt{3}q_y = \pm 2\pi$$

$$q_x - \sqrt{3}q_y = \pm 2\pi$$

For this case one can use the method of Mukamel and Hornreich and perform a renormalization group calculation for a model whose minimum-energy surface is a hexagon. Such calculation differs from the calculation of Mukamel and Hornreich in two ways. First, Mukamel and Hornreich used two symmetric polygons to approximate the two rings which constitute the minimum-energy surfaces for the nematic to smectic-C phase transition, while for the JD model one needs only one hexagon. Also, and more significantly, in the case of the JD model, as a consequence of the periodicity of the lattice, wave-vectors are defined modulo reciprocal lattice vectors, and therefore one has to include additional fourth-order invariants in the Hamiltonian. Such terms were not included by Mukamel and Hornreich because they sought to describe a transition between two liquid phases.

Therefore, in the following, an LGW Hamiltonian which contains a hexagonal minimum-energy surface and fourth-order invariants due to the lattice is analyzed. This LGW Hamiltonian is assumed to describe the phase transition betwen the paramagnetic and the modulated phase of the JD model.

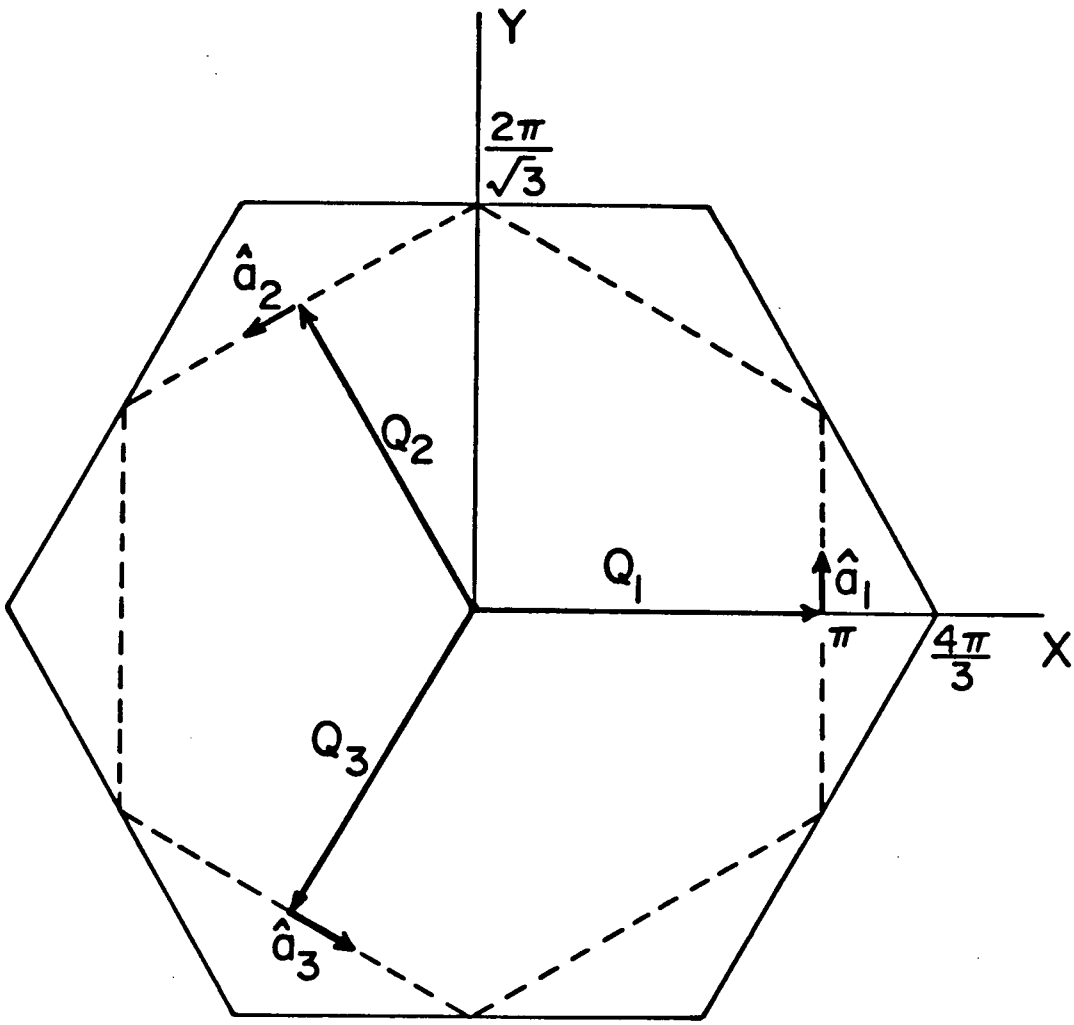

Figure 6-1 The minimum energy surface for $\kappa = 1$. The solid line is the boundary of the first BZ of a triangular lattice. The dashed line is the minimum energy surface for $\kappa = 1$.

6.3 The LGW Hamiltonian

In this Section the LGW Hamiltonian is described. The LGW Hamiltonian is constructed, in the usual way, in terms of the Fourier components of the order parameter which lie near the critical modes. Let $\mathbf{Q}_1$,$\mathbf{Q}_2$ and $\mathbf{Q}_3$ be the vectors, shown in Fig. 6-1, connecting the origin of reciprocal space and the centers of three of the edges of the hexagon, and let $\mathbf{a}_1$,$\mathbf{a}_2$ and $\mathbf{a}_3$ be unit vectors parallel to the three edges. Let $\phi_{\pm l}(\mathbf{q})$, for $l = 1,2,3$ be six real scalar fields defined for values of $\mathbf{q}$ which are measured from $\pm\mathbf{Q}_l$ and which satisfy $0 \leq |\mathbf{q}| \leq \Lambda$.

The Hamiltonian for the model is given by

$$\beta H = \beta H_0 + \beta H_I \tag{6.02}$$

where βH_0 is quadratic in the order parameter, and the interaction term βH_I is a sum of all the fourth-order invariants which can be formed by multiplying four fields.

The quadratic part of the LGW Hamiltonian is given by

$$\beta H_0 = \int_{\mathbf{q}} \sum_{l=1}^{3} \chi_l^{-1}(\mathbf{q})\, \phi_l(\mathbf{q})\, \phi_{-l}(\mathbf{q}) \tag{6.03}$$

where the integral is performed over the wave-vectors in the hypersphere $0 \leq |\mathbf{q}| \leq \Lambda$ and for $l = 1,2,3$ the inverse bare susceptibility, $\chi_l^{-1}(\mathbf{q})$, is given by

$$\chi_l^{-1}(\mathbf{q}) = r + q^2 - (\mathbf{q}\cdot\mathbf{a}_l)^2 + a(\mathbf{q}\cdot\mathbf{a}_l)^{2m} \tag{6.04}$$

For $a = 0$ the minimum of $\chi_l^{-1}(\mathbf{q})$ is obtained along the sides of the edges of the hexagon, and thus the hexagon constitutes the desired minimum-energy surface. The term $a(\mathbf{q}\cdot\mathbf{a}_l)^{2m}$ which breaks the degeneracy along the sides of the hexagon is added, following Mukamel and Hornreich, for computational reasons which will

be discussed later. The calculation is performed assuming that $a \neq 0$ and the degeneracy of the hexagon is restored at the end of the calculation by taking the limit of $m \to \infty$.

The interaction term, βH_I, of the Hamiltonian is given by

$$\beta H_I = \int_{\mathbf{q}_1}\int_{\mathbf{q}_2}\int_{\mathbf{q}_3}\int_{\mathbf{q}_4} \beta\,(H_1 + H_2 + H_3)\,\delta\,(\mathbf{q}_1 + \mathbf{q}_2 + \mathbf{q}_3 + \mathbf{q}_4) \tag{6.05}$$

where βH_1, βH_2, βH_3 are the fourth-order invariants. These invariants are found by requiring that the sum of the four wave-vectors associated with the four fields is equal to zero or to a reciprocal lattice vector. For example, the term

$$\phi_1(\mathbf{q}_1)\phi_{-1}(\mathbf{q}_2)\phi_1(\mathbf{q}_3)\phi_{-1}(\mathbf{q}_4) \tag{6.06}$$

is associated with the wave-vector

$$(\mathbf{Q}_1 + \mathbf{q}_1) + (-\mathbf{Q}_1 + \mathbf{q}_2) + (\mathbf{Q}_1 + \mathbf{q}_3) + (-\mathbf{Q}_1 + \mathbf{q}_4)$$

which is equal to zero due to the δ-function in Eq.(6.05). One also demands that each of the fourth-order terms should be invariant under C_6 rotations around the z axis and therefore the fourth-order invariant which includes the term given in Eq. (6.06) must also include two more similar terms in which the index $l = 1$ is replaced by $l = 2$ and $l = 3$. Thus the fourth-order invariants are given by

$$\begin{aligned}
\beta H_1 &= u_1 \sum_{l=1}^{3} \phi_l\phi_{-l}\phi_l\phi_{-l} \\
\beta H_2 &= u_2\,(\phi_1\phi_{-1}\phi_2\phi_{-2} + \phi_2\phi_{-2}\phi_3\phi_{-3} + \phi_3\phi_{-3}\phi_1\phi_{-1}) \\
\beta H_3 &= u_3 \sum_{l=1}^{3} (\phi_l\phi_l\phi_l\phi_l + \phi_{-l}\phi_{-l}\phi_{-l}\phi_{-l})
\end{aligned} \tag{6.07}$$

where the wave-vectors arguments have been suppressed, i.e., for example,

$$\phi_1\phi_{-1}\phi_2\phi_{-2} \equiv \phi_1(\mathbf{q}_1)\phi_{-1}(\mathbf{q}_2)\phi_2(\mathbf{q}_3)\phi_{-2}(\mathbf{q}_4)$$

For βH_1 and βH_2 the sum of the four wave-vectors associated with the four fields in each of the terms is equal to zero. For βH_3 the sum of the four wave-vectors associated with the four fields is given by the vectors $4\mathbf{Q}_l$, for $l = 1, 2, 3$. These wave-vectors are equal to reciprocal lattice vectors and therefore βH_3 is the term which is included in the calculation due to the periodicity of the hcp lattice.

6.4 Renormalization group calculation

The renormalization group calculations are performed using Wilson's momentum shell method [35]. The calculation consists of generating recursion relations by integrating over the field variables $\phi_{\pm l}(q)$ for wave-vectors $\mathbf{q}$ lying in the momentum shells $\Lambda/b < |q| < \Lambda$, rescaling the fields $\phi_{\pm l}(\mathbf{q}) = \varsigma\phi'_{\pm l}(\mathbf{q})$ where $\varsigma^2 = b^{2+d-\eta}$ and rescaling the wave-vectors $q' = bq$.

The first step in the calculation involves separating βH_0 into a part $\beta H_0^<$, which includes the low frequency modes, and a part $\beta H_0^>$, which includes the high frequency modes. Thus

$$\beta H_0 = \beta H_0^< + \beta H_0^> \tag{6.08}$$

where $\beta H_0^<$ and $\beta H_0^>$ are given by

$$\beta H_0^< = \int_{\mathbf{q}}^{<} \sum_{l=1}^{3} \chi_l^{-1}(\mathbf{q})\,\phi_l(\mathbf{q})\,\phi_{-l}(\mathbf{q}) \tag{6.09}$$

$$\beta H_0^> = \int_{\mathbf{q}}^{>} \sum_{l=1}^{3} \chi_l^{-1}(\mathbf{q})\,\phi_l(\mathbf{q})\,\phi_{-l}(\mathbf{q}) \tag{6.10}$$

and $\int_{\mathbf{q}}^{<}$ and $\int_{\mathbf{q}}^{>}$ are defined by

$$\int_{\mathbf{q}}^{<} \equiv \int_{0\leq|\mathbf{q}|\leq\frac{\Lambda}{b}} \frac{d^d q}{(2\pi)^d} \qquad \text{and} \qquad \int_{\mathbf{q}}^{>} \equiv \int_{\frac{\Lambda}{b}\leq|\mathbf{q}|\leq\Lambda} \frac{d^d q}{(2\pi)^d}$$

Next one defines an effective Hamiltonian $\beta H'(\phi)$, which depends only on the low frequency modes, by integrating over the fields which correspond to the high energy modes. Thus the partition function

$$Z = \prod_{l=1}^{3} \int d[\phi_l] e^{-\beta H_0 - \beta H_I} \tag{6.11}$$

can be written as

$$Z = \prod_{l=1}^{3} \int^{<} d[\phi_l] e^{-\beta H'(\phi)} \tag{6.12}$$

where the functional integration $\int^{<} d[\phi_l]$ is performed only over the fields $\phi_l(\mathbf{q})$ for which $\mathbf{q}$ satisfies $0 \leq |q| \leq \Lambda/b$, and

$$e^{-\beta H'(\phi)} \equiv e^{-\beta H_0^{<}} \prod_{l=1}^{3} \int^{>} d[\phi_l] e^{-\beta H_0^{>} - \beta H_I} \tag{6.13}$$

where in this case the functional integration $\int^{>} d[\phi_l]$ is performed over the fields $\phi_{\pm l}$ associated with wave-vectors in the shell $\Lambda/b \leq |q| \leq \Lambda$.

Defining

$$Z_I = \prod_{l=1}^{3} \int^{>} d[\phi_l] e^{-\beta H_0^{>}} \tag{6.14}$$

and defining the average of an operator O with respect to the 'partition function' Z_I by

$$\langle O \rangle_I = Z_I^{-1} \prod_{l=1}^{3} \int^{>} d[\phi_l] O e^{-\beta H_0^{>}} \tag{6.15}$$

the expression for the effective Hamiltonian Eq (6.13) can be written as

$$e^{-\beta H'} = Z_I \left\langle e^{-\beta H_I} \right\rangle_I e^{-\beta H_0^<} \tag{6.16}$$

The average $\left\langle e^{-\beta H_I} \right\rangle_I$ can be calculated to second order in $(-\beta H_I)$ by using the cumulant expansion which is given by

$$\left\langle e^{\lambda V} \right\rangle = \exp\left(\sum_{n=1}^{\infty} \frac{\lambda^n}{n!} c_n \right)$$

where

$$c_1 = < V > \qquad \text{and} \qquad c_2 = \frac{1}{2}\left[< V^2 > - < V >^2 \right] \tag{6.17}$$

In performing a cumulant expansion in powers of βH_I one is assuming that the fixed points u_1^*, u_2^*, and u_3^* are at least of the order of the small expansion parameter $\epsilon = d_u - d$. In this way one obtains an effective Hamiltonian given by

$$-\beta H' = \ln Z_I - \beta H_0^< + \langle (-\beta H_I) \rangle + \frac{1}{2}\left[\langle (-\beta H_I)^2 \rangle - \langle (-\beta H_I) \rangle^2 \right] \tag{6.18}$$

So far the effective Hamiltonian $\beta H'$, is a function of the fields $\phi_{\pm l}(\mathbf{q})$ for wavevectors which satisfy $0 \leq |q| \leq \Lambda$. The renormalized Hamiltonian $\beta H'(\phi_l'(\mathbf{q}'))$ is obtained from the effective Hamiltonian $\beta H\,(\phi_l(\mathbf{q}))$, by substituting $\mathbf{q}' = b\mathbf{q}$ and $\phi_{\pm l}(\mathbf{q}) = \varsigma \phi'_{\pm l}(\mathbf{q})$.

Using the standard diagrammatic methods to calculate $< (-\beta H) >_I$ and $< (-\beta H)^2 >_I$, and then using standard approximations, one can rewrite the renormalized Hamiltonian in a form which is identical to the form of the original Hamiltonian βH, but with renormalized coupling constants r', u_1', u_2', u_3', a' and with the coefficient $\varsigma^2 b^{-2-d}$ multiplying q'^2 in χ'^{-1}. In order to restore the value of this coefficient to unity one choses ς to be given by $\varsigma^2 = b^{2+d}$. However, from Eq. (2.05),

it follows that, ς^2 is also related to the critical exponent η through $\varsigma^2 = b^{2+d-\eta}$ and therefore one obtains $\eta = 0$ to order ϵ.

In this way the values of the renormalized coupling constants are given in terms of the bare coupling constants by the following renormalization group transformations

$$\begin{aligned} r' &= b^2 \left[r + (4u_1 + 2u_2) I_0(r)\right] \\ u_1' &= b^{4-d} \left[u_1 - (10u_1^2 - u_2^2 - 72u_3^2) I_1(r)\right] \\ u_2' &= b^{4-d} \left[u_2 - (8u_1u_2 - u_2^2) I_1(r) - 2u_2 I_2(r)\right] \\ u_3' &= b^{4-d} \left[u_3 - 12u_1u_3 I_1(r)\right] \\ a' &= b^{-2(m-1)} a \end{aligned} \tag{6.19}$$

where

$$\begin{aligned} I_0(r) &= \int_{\mathbf{q}}^{>} \chi_l(q) \\ I_1(r) &= \int_{\mathbf{q}}^{>} \chi_l^2(q) \\ I_2(r) &= \int_{\mathbf{q}}^{>} \chi_l(q)\chi_{l'}(q) \qquad l \neq l' \end{aligned} \tag{6.20}$$

From the recursion relation for a it follows that the variable a is an irrelevant variable and therefore one might be tempted to substitute $a = 0$ in the LGW Hamiltonian. However the integral $I_1(r)$ for $r = 0$ diverges as $a^{(d-5)/2}$ as $a \to 0$ and therefore the term multiplying a must be included in the LGW Hamiltonian. Such an irrelevant variable is called a 'dangerous irrelevant variable'. Following Aharony and Bruce [45], one deals with dangerous irrelevant variables by defining rescaled coupling constants given by

$$\tilde{u}_i = a^{(d-5)/2} u_i \tag{6.16}$$

for $i = 1, 2, 3$. In terms of the rescaled coupling constants the recursion relations, Eq. (6.19) are given by

$$\begin{aligned}
\tilde{u}_1' &= b^{4-d}\left[\tilde{u}_1 - (10\tilde{u}_1^2 - \tilde{u}_2^2 - 72\tilde{u}_3^2)\tilde{I}_1(r)\right] \\
\tilde{u}_2' &= b^{4-d}\left[\tilde{u}_2 - (8\tilde{u}_1\tilde{u}_2 - \tilde{u}_2^2)\tilde{I}_1(r) - 2\tilde{u}_2\tilde{I}_2(r)\right] \\
\tilde{u}_3' &= b^{4-d}\left[\tilde{u}_3 - 12\tilde{u}_1\tilde{u}_3\tilde{I}_1(r)\right]
\end{aligned} \tag{6.22}$$

where $\epsilon = 5 - m^{-1} - d$ and for $i = 1, 2$ $\tilde{I}_i(r) = a^{-(d-5)/2} I_i(r)$. The recursion relation for r' has been omitted, because to order ϵ it plays no role in determining the values of the fixed points, u_1^*, u_2^*, u_3^*, and their stability.

Having written the recursion relations in terms of the rescaled coupling constants, one can deal with the dangerous irrelevant variable a, in the usual way, by evaluating the integrals $\tilde{I}_1(r = 0)$ and $\tilde{I}_2(r = 0)$ for $a = 0$ and for $\epsilon = 0$. One then obtains

$$\begin{aligned}
\tilde{I}_1(a = 0, r = 0) &= K \ln b \\
\tilde{I}_2(a = 0, r = 0) &= 0
\end{aligned} \tag{6.23}$$

Assuming that the fixed points are given for values of u_i which are of order ϵ and using the definitions

$$x_i = \frac{K}{m\epsilon u_i} \tag{6.24}$$

for $i = 1, 2, 3$, the following recursion relations are obtained in terms of the x_i

$$\begin{aligned}
x_1' &= x_1 + (x_1 - 10x_1^2 - x_2^2 - 72x_3^2)\,\epsilon m \ln b \\
x_2' &= x_2 + (x_2 - 8x_1x_2 - x_2^2)\,\epsilon m \ln b \\
x_3' &= x_3 + (x_3 - 12x_1x_3)\,\epsilon m \ln b
\end{aligned} \tag{6.25}$$

The fixed points for the recursion relations are given by the solutions to the following equations

$$\begin{aligned} x_1 &= 10x_1^2 + x_2^2 + 72x_3^2 \\ x_2 &= 8x_1x + x_2^2 \\ x_3 &= 12x_1x_3 \end{aligned} \tag{6.26}$$

These equations have eight solutions, of which four are real and are given by

$$a)\ x_1^* = 0, \quad x_2^* = 0, \quad x_3^* = 0$$

$$b)\ x_1^* = 1/10, \quad x_2^* = 0, \quad x_3^* = 0$$

$$c)\ x_1^* = 1/12, \quad x_2^* = 0, \quad x_3^* = 1/72$$

$$d)\ x_1^* = 1/12, \quad x_2^* = 0, \quad x_3^* = -1/72$$

The stability of these fixed points is determined by calculating for each fixed point, the eigenvalues of the linearized renormalization group transformations. In our case these eigenvalues are determined from the matrix

$$\frac{\partial x_i'}{\partial x_j} = \begin{pmatrix} 1 + E(1 - 20x_1) & -2Ex_2 & -144Ex_3 \\ -8Ex_2 & 1 + E(1 - 8x_1 - 2x_2) & 0 \\ -12Ex_3 & 0 & 1 + E(1 - 12x_1) \end{pmatrix} \tag{6.27}$$

where $E = \epsilon m \ln b$. Evaluating the eigenvalues of the matrix given by Eq. (6.27) one finds that for each fixed point there exists at least one eigenvalue which is positive. Therefore the LGW Hamiltonian, analyzed in this section, does not contain a stable fixed point.

6.5 Conclusions and discussion.

In this Chapter an LGW Hamiltonian, which is assumed to describe the phase transition between the paramagnetic and the modulated phases of the JD model, was analyzed using a renormalization group calculation. In this Section the choice of the LGW Hamiltonian and the result of the calculation are discussed.

The LGW Hamiltonian was chosen such that its quadratic term contains, in the limit of $m \to \infty$, a minimum-energy surface which consists of a hexagon. This choice is motivated by the fact that for a specific value of κ, i.e., $\kappa = 1$, the JD model contains a minimum-energy surface which also consists of a hexagon. The choice is also motivated by the fact that for models which contain minimum-energy surfaces on polygons one can use the method of Mukamel and Hornreich to perform a renormalization group analysis. The fourth-order invariants of the LGW Hamiltonian include terms which were not included in previous analysis of LGW Hamiltonians which contain minimum-energy surfaces. These terms are included here because the JD model is defined on a lattice.

These considerations motivate the assumption that the phase transition for this LGW Hamiltonian, and the paramagnetic-modulated phase transition of the JD model, belong to the same universality class. The calculation revealed that the LGW Hamiltonian does not contain a stable fixed point and therefore one concludes that both the LGW Hamiltonian and the JD model exhibit a fluctuation-induced first-order transition.

The result of the calculation shows that this LGW Hamiltonian exhibits the same type of behaviour as the other LGW Hamiltonians which were previously analyzed for other models containing minimum-energy surfaces. This adds weight to the assumption that for these models the first-order nature of the transition is due to the existence of the minimum-energy surface. The shape of the surface or the type of the fourth-order invariants does not play a role in determinig the order of the transition. In particular one can apply this assumed universality to

the JD model, for the cases where $\kappa \neq 1$. For these cases the minimum-energy surface is not a hexagon and therefore the calculation in this Chapter does not strictly apply. However these results strongly suggest that for all values of κ the paramagnetic-modulated transition is first-order.

The results of this Chapter were obtained using an ϵ expansion from the upper critical dimensionality $d_u = 5$. Therefore one should be skeptical about their validity at $d = 3$, where the small expansion parameter ϵ is equal to two. However, these results gain some credibility from the fact that, at $d = 3$, the nematic to smectic-C phase transition is observed to be a first-order transition, and the LGW Hamiltonian which is assumed to describe the nematic to smectic-C transition also exhibits a first-order transition near the upper critical dimensionality $d_u = 5$.

CHAPTER 7

Conclusions

In this thesis both the high temperature (the order-disorder line) and the low temperature regions of the (κ, t) phase diagram of the JD model were investigated. The study was performed using different methods from which, in some cases, contradictory conclusions emerged. Therefore, in this Chapter, the results of the different studies are reviewed and compared. These results are also compared to results from previous studies of the JD model [8,9].

As in other models with competing interactions, the ground states of the JD model are found to include states which correspond to a phase without domain walls (the $< F >$ phase), states which correspond to a phase containing the maximum possible amount of domain walls (the $< AF >$ phase), and a highly degenerate point separating the $< F >$ states from the $< AF >$ states. At the degenerate point, an infinite number of spin configurations are degenerate with the ground states of the $< F >$ and the $< AF >$ phases. These include ordered configurations which can serve as ground states for phases with long range order. Such phases are expected to be located in a region of the phase diagram between the $< F >$ and the $< AF >$ phases.

Mean-field theory and low temperature expansions were used to determine which of the states which are degenerate at $\kappa = 1/2$ are stabilized at non-zero temperatures. From both methods it follows that the $< 2 >$ phase is stable in a region between the $< F >$ and the $< AF >$ phases. Furthermore, to order x,

where $x = e^{-2/t}$, both methods yield the same expressions, given by Eq. (5.18) and Eq. (5.19), for the phase boundaries of the $< 2 >$ phase. It follows that the width of the $< 2 >$ phase, along the κ direction, is of order x.

The predictions from mean-field theory and from the low temperature expansions concerning the stability of the $< 3 >$ phase are in contradiction. Both methods predict that the phase diagram contains a region where the $< 3 >$ phase is stable. However, mean-field theory predicts that the $< 3 >$ phase is not stable at an arbitrary low temperature but becomes stable at a branching point, which occurs at a finite temperature, while the low temperature expansions predict that the $< 3 >$ phase is stable for arbitrarily small values of t. The low temperature expansion also predicts that the width of the $< 3 >$ phase is of order x^2.

Mean-field theory is an approximate theory whereas the low-temperature expansions are expected to become exact in the low temperature limit. Therefore it follows that the prediction from the low temperature expansions that the $< 3 >$ phase is stable in the vicinity of the multiphase point is correct and, correspondingly, that mean-field theory gives a qualitatively incorrect picture of the phase diagram near the multiphase point.

An interesting unsolved question, raised by the stability of the $< 3 >$ phase, is whether the rest of the $< n >$ phases are stable at an arbitrary low temperature. From the low temperature expansions, it follows that to order x^2 these phases coexist with the $< F >$ and the $< 3 >$ phases along the possible phase boundary, given by Eq. (5.49), between the $< F >$ and the $< 3 >$ phases. From the fact that the widths of the $< 2 >$ and the $< 3 >$ phases are of the order of x and x^2 respectively, one might guess that the widths of the $< n >$ phases are of order x^{n-1}. Therefore, in order to decide whether the rest of the $< n >$ phases are stable for arbitrarily low temperature, one would have to extend the low temperature expansions to arbitrary order in x. This would require performing an inductive calculation of the type used by Selke and Fisher [14] for the three-dimensional ANNNI model. Such

a calculation might be difficult to perform because of the necessity of summing an infinite numbers of clusters, for each order in the expansion of the free energy in powers of x. Since mean-field theory fails to predict the region of stability of the $< 3 >$ phases correctly, it is impossible to use mean-field theory for the purpose of deciding if the $< n >$ phases, for $n \geq 4$, are stable in the vicinity of the multiphase point.

In spite of the fact that the question concerning the stability of the $< n >$ phases has been left unanswered, the expression which was obtained for the phase boundary between the $< F >$ and the $< 3 >$ phases is expected to be the correct expression, to order x^2, for the phase boundary between the ferromagnetic and the modulated phases. This follows from the fact that the low temperature expansion included all terms which contribute to the free energy to order x^2. Therefore even if the rest of the $< n >$ phases occupy a region of the phase diagram between the $< F >$ and the $< 3 >$ phase, their combined width is expected to be at most of order x^3. Thus the expression to order x^2 for the ferromagnetic-modulated phase boundary will remain unchanged.

A Monte Carlo simulation of the JD model showed that the Domany line and the phase boundary of the ferromagnetic phase are very close one to the other. Therefore Domany and Gubernatis suggested that both lines might coincide. A comparison between the asymptotic expression for the Domany line near the multiphase point and the the expression for the ferromagnetic-modulated phase boundary which was obtained using the low temperature expansions, showed that to order x^2 both expressions are identical. Domany postulated that the critical point of the two-dimensional kinetic Ising model on the honeycomb lattice maps onto a point on the Domany line which is a Lifshitz point. It follows that the Domany line and the phase boundary for the ferromagnetic phase meet at the Lifshiz point and approach each other asymptotically near the multiphase point. These facts strongly support the conjecture that both lines coincide.

It should be noted that in the Monte Carlo simulation the modulated phase, which is expected to coincide with the paramagnetic and the ferromagnetic phases at the Lifshitz point, is not observed. Instead the paramagnetic phase seemed to extend to temperatures which are lower than the temperature where the Lifshitz point is located. Therefore the line which Domany and Gubernatis found to be close to the Domany line is not the phase boundary between the ferromagnetic and the modulated phase, but the phase boundary between the paramagnetic phase and the ferromagnetic phase. The Monte Carlo simulation was performed in the vicinity of the Lifshitz point and was not extended to lower temperatures. Therefore it is possible that the modulated phases, described in this thesis, will be found at lower temperatures.

For $\kappa \geq 1/2$ both mean-field theory and the low temperature expansions predict the existence of the $< AF >$ phase. A phase transition from the paramagnetic phase into this phase has been observed in the Monte Carlo simulation. Mean-field theory also predicts that the $< 21^j >$ phases, for $j \geq 1$, are stable at arbitrarily low temperatures. To order x, in the low temperature expansion, these phases are found to coexist with the $< 2 >$ and with the $< AF >$ phases along their phase boundary. However, to order x^2, the expression for the free energy of the $< 21^j >$ phases was found to be divergent. These results, for the $< 21^j >$ phases of the JD model, resemble the results which are obtained for the Ising model on the triangular lattice with antiferromagnetic interactions. For both models possible phases which were found stable using mean-field theory are found to posses divergent low temperature expansions. The fact that the antiferromagnetic Ising model is disordered suggests that the $< 21^j >$ phases of the JD model are not stable.

In this thesis the phase transition between the paramagnetic and the modulated phases has also been studied. From minimizing the Hamiltonian it follows that the critical modes of the JD model, for $\kappa \geq 1/3$, lie on continuous lines in

reciprocal space. This raises the possibility that, as in other models which contain minimum-energy surfaces, the JD model also exhibits a fluctuation-induced first-order transition. An LGW Hamiltonian which describes the transition and which includes fourth-order invariants which are due to the lattice, was analyzed and found not to possess a stable fixed point. This result strongly suggests that the JD model exhibits a fluctuation-induced first-order transition into the modulated phase. The Monte Carlo simulation did not show a paramagnetic-modulated phase transition, and therefore the prediction that this transition is first-order was not tested. However, the simulation showed that the structure factor, calculated for few points in the paramagnetic phase, attains its maximum on a continuous surface in reciprocal space. This is in agreement with the fact that the JD model contains continuous minimum-energy surfaces.

The Monte Carlo simulation also showed that, for temperatures which are lower than the temperature at which the Lifshitz point is located, instead of observing a first-order transition between the paramagnetic and the modulated phases followed by a transition from the modulated phase to the ferromagnetic phase, a direct first-order transition between the paramagnetic and the ferromagnetic phases occurs. This result could be explained if one assumes that the κ dependent transition temperature for the transition between the paramagnetic and the modulated phases is very close to the transition temperature for the transition between the modulated phase and the ferromagnetic phase, or in other words the modulated phase is only stable for a very narrow range of temperature. Then it is possible that in the Monte Carlo simulation the narrow modulated phase is not observed. Also one would expect that near the Lifshitz point the modulated phases are of very long-wave lengths. Therefore it might be the case that the lattices used in the Monte Carlo simulation were not big enough to observe the modulated phases. If indeed the Monte Carlo simulation missed the modulated phases, it is also possible that the paramagnetic to ferromagnetic transition was observed to be first-order due to

the fact that, as predicted in this thesis, the transition between the paramagnetic and the modulated phases is first-order.

BIBLIOGRAPHY

1. R. J. Baxter, *Exactly Solved Models in Statistical Mechanics* (Academic Press, 1982).
2. E. Ising, Z. Phys. **21**, 613 (1925).
3. L. Onsager, Phys. Rev. **76**, 1232 (1944).
4. B. M. McCoy and T. T. Wu *The Two-Dimensional Ising Model* (Harvard University press, 1982).
5. P. Rujan, J. Stat. Phys. **29**, 231 (1982).
6. I. G. Enting, J. Phys. A **11**, 2001 (1978).
7. T. R. Welbery and G. H. Miller, Acta Crystallogr. A **34**, 120 (1978).
8. E. Domany, Phys. Rev. Lett. **52**, 871 (1984); Err. Phys. Rev. Lett **52**, 1731 (1984).
9. E. Domany and J. E. Gubernatis, Phys. Rev. B **32**, 3354 (1985).
10. For few examples, see the papers of M. E. Fisher and J. Yeomans in *Multicritical Phenomena* Series B, No. 106 of the Nato Advanced Study Institute Series, edited by R. Pynn and A. Skjeltrop (Plenum, New York, 1983).
11. R. J. Elliot, Phys. Rev. **124**, 346 (1961).
12. For reviews, see P. Bak, Rep. Prog. Phys. **45**, 587 (1982); M. E. Fisher and D. A. Huse, in *Melting Localization and Chaos*, edited by R. K. Kalia and P. Vashista (Elsevier, New York, 1982); W. Selke, in *Modulated Structure Materials* Series E, No. 83 of the Nato Advanced Study Institute Series, edited by T. Tsakalakos (Nijhoff, The Hague, 1984).
13. S. Redner and H. E. Stanley, J. Phys. C **10**, 4765 (1977); S. Redner and H. E. Stanley, Phys. Rev. B **16**, 4901 (1977).
14. M. E. Fisher and W. Selke , Phys. Rev. Lett. **44**, 1502 (1980); M. E. Fisher and W. Selke, Philos. Trans. Roy. Soc. London **302**, 1 (1981).

15. P. Bak and J. von Bohm, Phys. Rev. B **21**, 5297 (1980).

16. J. Villan and M. B. Gordon, J. Phys. C **13**, 3117, (1980).

17. P. Bak, Phys. Rev. Lett. **13**, 791 (1980); M. H. Jensen and P. Bak, Phys. Rev. B **27**, 6853 (1983).

18. P. M. Duxbury and W. Selke, J. Phys. A **16**, L741 (1983); W. Selke and P. M. Duxbury, Z. Phys. B **57**, 49 (1984).

19. J. H. Taylor and J. S. Desjardins, Phys. Rev. B **30**, 5203 (1984).

20. T. DeSimone and R. M. Stratt, Phys. Rev. B **32**, 1537 (1985).

21. W. Selke and M. E. Fisher, Phys. Rev. B **20**, 257 (1979).

22. K. Kaski and W. Selke, Phys. Rev. B **31**, 3128 (1985).

23. S. A. Brazovskii, Sov. Phys. JETP **41**, 85 (1975). [Zh. Eksp. Teor. Fiz **68**, 175 (1975).]

24. J. Swift, Phys. Rev. A **14**, 2274 (1976).

25. J. Swift and P. C. Hohenberg, Phys. Rev. A **15**, 319 (1979).

26. J. Swift and P. Leitner, Phys. Rev. B **16**, 4137 (1977).

27. D. Mukamel and R. M. Hornreich, J. Phys. C **13**, 161 (1980).

28. D. D. Ling, B. Friman and G. Grinstein, Phys. Rev. B **24**, 2718 (1981).

29. D. S. Zimmerman, Phys. Rev. B **33**, 6451 (1986).

30. P. Bak, S. Krinsky, and D. Mukamel, Phys. Rev. Lett. **36**, 52 (1976).

31. D. Mukamel and S. Krinsky Phys. Rev. B **13**, 5065 (1976); D. Mukamel and S. Krinsky Phys. Rev. B **13**, 5078 (1976); D. Mukamel and S. Krinsky Phys. Rev. B **13**, 5086 (1976); D. Mukamel and S. Krinsky J. Phys. C **8**, L496 (1975).

32. For reviews of critical phenomena see M. E. Fisher in *Critical Phenomena* edited by F. J. W. Hahne (Springer-Verlag Berlin Heildelgerg 1983); S. K. Ma *Modern Theory of Critical Phenomena* (Benjamin, Reading, 1976).

33. See articles in *Phase Transitions and Critical Phenomena Vo. 6*, edited by M. S. Green and C. Domb (Academic press, 1976).

34. See article by Aharony in Ref 33.

35. K. G. Wilson and J. Kogut, Phys. Rep. **12**, C (1974).

36. For an introduction see A. Aharony in *Critical Phenomena* edited by F. J. W. Hahne (Springer-Verlag Berlin Heildelberg 1983).

37. For a review see I. D. Lawrie and S. Sarbach in *Phase Transitions and Critical Phenomena*, edited by C. Domb and J. L. Lebowitz (Academic Press, 1984).

38. R. M. Hornreich, M. Luban, and S. Shtrikman Phys. Rev. Lett. **35**, 1678 (1975).

39. For review, see R. M. Hornreich, J. Magn. Magn. Mat. **15-18**, 387 (1980).

40. A. Aharony, E. Domany, R. M. Hornreich, T. Schneider and M. Zanneti, Phys. Rev. B **32**, 3358 (1985).

41. R. Dengler, Phys. Lett. **108A**, 269 (1985).

42. R. J. Glauber, J. Math. Phys. **4** 294 (1963).

43. G. H. Wannier, Rev. Mod. Phys. **17**, 50 (1945).

44. K. A. Muller, W. Berlinger, J. Y. Buzaré, and J. C. Fayet, Phys. Rev. B **21**, 1763 (1980).

45. A. Aharony and A. Bruce, Phys. Rev. Lett **42**, 462 (1979).

46. G. H. Wannier, Phys. Rev. **79**, 357 (1950).

47. M. Schick, Prog. in Sur. Sci. **11**, 245 (1981).

48. T. D. Schultz, Nuevo Cimento **8**, 943 (1958).

49. M. Burley, Proc. Phys. Soc. London **85**, 1163 (1965).

50. C. Domb, Adv. Phys. **9**, 149 (1960).

51. N. D. Mackenzie and A. P. Young, J. Phys. C **14**, 3927 (1981).

52. P. G. deGennes, Mol. Cryst. Liq. Cryst. **21**, 49 (1973).

53. P. G. deGennes, *The Physics of Liquid Crystals*, (Oxford University press, 1974).

54. W. L. McMillan, Phys. Rev. A **8**, 328 (1973).

APPENDIX 1

CALCULATION OF THE DOUBLE SUM

In this Appendix the double sum

$$\frac{9}{2}\sum_{m=2}^{\infty}\sum_{l_1=2}^{m}\frac{1}{4^m}\left(\frac{8}{7}\right)^{l_1}\frac{(2m-l_1-2)!}{(m-1)!(m-l_1)!}(l_1-1) \tag{A.1}$$

is calculated. This expression follows from Eq. (5.36)-Eq. (5.42) using $y = 1 - x$. For the $< 21^j >$ phases a similar double sum is obtained by using $y = 1 + x$. This suggests the need to study the more general expression

$$S(A) = 9\frac{2A+6}{16}\sum_{m=2}^{\infty}\sum_{l_1=2}^{m}\left(\frac{4}{2A+6}\right)^{2m}\left(\frac{2A+6}{2A+5}\right)^{l_1}\frac{(2m-l_1-2)!}{(m-1)!(m-l_1)!}(l_1-1) \tag{A.2}$$

corresponding to $y = 1 - Ax$. Changing the limits and the order of the sums one obtains

$$S(A) = \frac{9}{2A+5}\sum_{n=1}^{\infty}\left[\frac{16}{(2A+5)(2A+6)}\right]^n nR(n,z) \tag{A.3}$$

where

$$R(n,z) = \sum_{m=0}^{\infty} z^{2m}\frac{1}{4^m}\frac{(2m+n-1)!}{(m+n)!m!} \tag{A.4}$$

and

$$z = \frac{8}{2A+6} \tag{A.5}$$

Using the identity

$$(2m+n-1)! = \int_0^\infty e^{-t} t^{2m+n-1} dt \tag{A.6}$$

changing the order of the sum and the integral and using the representation of the modified Bessel function $I_n(\alpha)$

$$I_n(\alpha) = \sum_{m=0}^{\infty} \frac{1}{m!(m+n)!} \left(\frac{\alpha}{2}\right)^{n+2m} \tag{A.7}$$

one obtains

$$R(n,z) = \left(\frac{2}{z}\right)^n \int_0^\infty e^{-t} t^{-1} I_n(tz) dt \tag{A.8}$$

Using the recursion relation

$$\frac{I_n(y)}{y} = \frac{I_{n-1}(y) - I_{n+1}(y)}{2n} \tag{A.9}$$

and changing variables one obtains

$$R(n,z) = \left(\frac{2}{z}\right)^n \int_0^\infty e^{-y/z} \frac{I_{n-1}(y) - I_{n+1}(y)}{2n} dy \tag{A.10}$$

Using

$$\int_0^\infty e^{-\alpha y} I_n(y) dy = \frac{1}{\sqrt{\alpha^2-1}\left(\alpha + \sqrt{\alpha^2-1}\right)^n} \tag{A.11}$$

it follows that

$$R(n,z) = \frac{1}{n} \frac{2^n}{\left[1+\sqrt{1-z^2}\right]^n} \tag{A.12}$$

The expression in Eq. (A.12) is only valid for $z \leq 1$. This result follows from the fact that for $z \geq 1$ the sum in Eq. (A.4) is divergent. For the $< 21^j >$ phases

$A = -1$ and therefore $z = 2$. It follows that for the $< 21^j >$ phases the double sum in Eq. (A.2) is divergent.

For $A = 1$ one obtains $R(n,1) = 2^n/n$ and therefore the sum in Eq. (A.1) is given by

$$S(1) = \frac{9}{7}\sum_{n=1}^{\infty}\left(\frac{2}{7}\right)nR(n,1) = \frac{9}{7}\sum_{n=1}^{\infty}\left(\frac{4}{7}\right)^n = \frac{12}{7} \qquad (A.13)$$